2005

Effect of Bond Thickness on Lifetime of Adhesive Joints

Ehab Mohammed El-Said El-Refaai Shehab

EFFECT OF BOND THICKNESS ON LIFETIME OF ADHESIVE JOINTS

Thesis submitted to the Deanship of Graduate Studies of

United Arab Emirates University

in partial fulfillment of the requirements for the degree of

Master of Science

in

Materials Science and Engineering

by

Ehab Mohammed El-Said El-Refaai Shehab

2005

SUPERVISION COMMITTEE MEMBERS

Advisor

Dr. Abdullah Al-Khanbashi

Chemical and Petroleum Engineering Department

U.A.E. University

ES/F11

United Arab Emirates University
Graduate Studies
M.S.c. Program in Materials Science and Engineering

THESIS EXAMINATION REPORT

Student ID : 200250406
Student Name : Ehab Mohammed El-Said

Title of The Thesis : Effect of Bond Thickness on Lifetime of Adhesive Joints.

The Thesis Examination as A Partial Fulfillment of M. Sc. Degree in Materilas Science and Engineering Was conducted ..... Based on Examining the Thesis and the Students Presentation and the Subsequent Discussion, The Commi Recommends:

☐ Thesis is Satisfactory as is.

☑ Thesis is Satisfactory After Minor Modifications.

☐ Thesis should be Re-Evaluated After Major Modifications.

☐ Thesis is Rejected.

Examining Committee Members:

Thesis Supervisor: Name: Dr. Al-Khanbashi ..... Signature: ..... Date: 5/1/2

Thesis Co-Advisor: Name: ..... Signature: ..... Date:

Member : Name: Kristofer Gamstedt ... Signature: ..... Date: 5/1/

Name: Adel Hammami. Signature: ..... Date: 5/1/

Approval of Program Coordinator:

Dr. Yousef Haik ..... Date : 6/1/2005

APPROVAL:
Dean of Graduate Studies ..... Date :.....

Dean of Graduate Studies
U.A.E. UNIVERSITY

EFFECT OF BOND THICKNESS ON LIFETIME OF ADHESIVE JOINTS

ABSTRACT

The aim of this research was to study the effect of bond thickness on the fracture energy and the lifetime of an adhesively bonded system and develop a model to predict the lifetime of adhesive joints. An approach based on fracture mechanics was employed to assess aluminum/epoxy bond lifetime. An experimental investigation was carried out using double cantilever beam (DCB) specimens with various bond thicknesses under mode I.

This study describes an approach to predict the rate of crack propagation using Paris' power law. The approach used elevated temperatures to accelerate the crack propagation under constant loads. The elevated temperatures were kept below the glass transition of the adhesive. The general idea was to apply a constant load below the critical value to allow for measurable slow crack propagation. The fracture energy of the bonded joints was evaluated using both simple beam and beam on elastic foundation analyses. A simple model was proposed to predict the variation of the two kinetic parameters of Paris' law as a function of bond thickness. A model was developed, which would enable crack propagation to be modeled and hence the lifetime of adhesive joints to be predicted.

ACKNOWLEDGEMENTS

I owe my sincere appreciation to my family who have supported and encouraged me over the years.

I wish to express my sincere appreciation to my advisor, Dr. Abdullah Al-Khanbashi, for his valuable time, advice, guidance, and support throughout my research and for his patience, understanding, and encouragement over the last two years.

I would like to gratefully thank Prof. Abdelsamie Moet and Associate Prof. Alaa Eldin Hamdy for their advice during my research. My sincere appreciation is extended to Dr. Adel Hammami for his presence in my defense. Thanks are also extended to Mr. Essam Shaaban and Mr. Ramy Hamdan for useful discussions and their help in this work, as well as to Mr. Stephen Aston for his help in checking the manuscript.

TABLE OF CONTENTS

LIST OF FIGURES

LIST OF TABLES

1. Introduction

1.1 Background

The potential number of applications of adhesives for bonding structural components is rising rapidly. Adhesive bonding of components is becoming more common in industry as well as in advanced technology, including mechanical, civil and electrical engineering, the automotive and aircraft industries and electronics. Adhesive joints offer many advantages over conventional fasteners, such as rivets and bolts, including lower weight, ability to bond dissimilar materials, electrical and thermal insulation, lower manufacturing costs, and increased design flexibility.

Adhesive joints can fail after prolonged periods of time at loads below the fracture loads by crack propagation. The initiation and propagation of cracks in a bonded joint are directly related to the service conditions to which the joint is exposed. Static loads and elevated temperatures are some of the principal conditions, which cause the initiation and propagation of cracks in an adhesive joint. Therefore, any study involving adhesive joints should include a detailed assessment of the lifetime of the bond system in the service conditions of that particular application. However, the full potential of the technology has not been exploited because an understanding of the mechanisms of adhesion failure is incomplete [1]. Without a thorough understanding of adhesion failure, the quantitative prediction of the lifetime of adhesive joints has not been possible.

The slow progress in the development of adhesion science may be due to the fact that the science encompasses various disciplines. These include surface chemistry, polymer

chemistry, and fracture mechanics. In the past, most research was limited to testing joint strength and joint durability after exposure to a variety of harsh environmental conditions. Recent advances in the analysis of adhesive joints, such as the topography of the adherend surface and the mode of failure of adhesively bonded system, are enabling researchers to study fundamental interactions occurring in the adhesive bonding process. These advances in the understanding of the adhesion, together with a more thorough study of fracture mechanics, should allow better approximations of the lifetime of adhesive joints under service conditions. Design engineers could then confidently expand the use of adhesive bonding to capitalize on the advantages of this joining technology.

The lifetime of adhesive joints is a major concern when components are designed utilizing classic or newly developed materials. The lifetime of adhesive joints depends on many factors and their combinations (e.g. adhesive, adherend, curing, etc). The fracture behavior of adhesive joints is extremely complex and they present the designer with a challenging task if they are to be employed with maximum efficiency. A growing number of applications of adhesive joints require improved methods of testing and control to evaluate their behaviors. A great variety of test geometries and specimens are used to determine adhesive properties and the strength of adhesive joints.

In the present study, a fracture mechanics-based approach utilizing a double cantilever beam (DCB) specimen was used to predict adhesive joint lifetime. The DCB fracture test specimen is one of the most well-defined specimens for the evaluation of the material properties of adhesives. Experimental investigation was carried out under mode I using constant loads. The rate of crack propagation was accelerated by means of elevated temperatures, which were kept below the glass transition of the adhesive. The fracture energy of the DCB specimens was evaluated using both simple beam and beam on elastic foundation

analyses. Subsequently, accelerated rate of crack propagation studies were carried out to establish an equation of state usable for lifetime prediction.

1.2 Research Objectives

The present research attempts to establish a general approach for obtaining quantitatively predictions for the lifetime of adhesive joints. Comparisons between the predictions and the experimental results of lifetime were used to validate the analytical technique. The present study was carried out with the following objectives:

(i) Gain an understanding of the effect of bond thickness on the lifetime of adhesive joints.

(ii) Study the effect of service conditions, such as temperature and applied loads on the lifetime of adhesive joints.

(iii) Enable the joint lifetime to be predicted.

These objectives were fulfilled through a lifetime assessment carried out by determining the time required for a dominant crack to become unstable and causing fracture. A linear elastic fracture mechanics approach was used to determine the crack propagation rate and hence predict the lifetime of the adhesive joints. However, the development of a suitable analysis to predict the lifetime of adhesive joints still remains incomplete because of the complications caused by the interaction between different conditions, such as specimen geometry, bond thickness, application of loads, and temperature.

1.3 Overview of the Study

This study is divided into five sections. Chapter 1 includes a general introduction and the objectives of the present research. Chapter 2 gives a review of the principles related to this study, including adhesives, the theories of adhesion, aluminum surface pretreatment, fracture mechanics, the double cantilever beam test, and finally, a review of some bond thickness and lifetime studies involving adhesive joints. Chapter 3 discusses the experiments (materials, specimen geometry, and test procedures). Chapter 4 is divided into three parts that analyze and discuss the experimental results under various service conditions, such as different temperatures and applied loads. Chapter 5 summarizes the conclusions drawn from chapter 4 as well as other suggestions for future work.

2. Literature Review

This chapter is a review of the background related to this study, including adhesives, the mechanisms of adhesion, aluminum surface pretreatment, fracture mechanics, and the double cantilever beam test. A literature review of bond thickness and lifetime studies involving adhesive joints is presented.

2.1 Adhesives & Adhesion

An adhesive is described as a material which when applied to the surfaces of materials (adherends) can join them together and resist separation or a substance that bonds materials together by surface attachment [2]. Adhesives have existed for thousands of years but have become much more important in the past few decades. The use of adhesives has increased because of the growing availability of new and improved adhesives and due to significant advances in bonding technology. Modern applications of adhesives are found in the aircraft and automobile industries and civil structures because of the ability of the adhesive to carry static and fatigue loads over the service life of the bonded joint. Adhesive joints have many advantages compared with other joining methods [3]. These include weight saving, lower fabrication costs, and uniform stress distribution. One of the main disadvantages of adhesive bonding is that surface preparation of the adherends is essential for the production of durable bonds. However, it is difficult to analyze, design, and optimize adhesive joints.

Adhesion refers to the attraction between an adhesive and the substrate. When an adhesive and adherend are brought into contact, the result is an adhesive joint. The system

comprises an adhesive, adherends, and appropriate surface pretreatment of the adherends. It is essential to understand how each of the above components reacts to external applied loads, either mechanical or environmental. The performance of an adhesive joint depends on other criteria as well, such as the material properties of the adhesive and adherends and the geometry of the bonded joint. In order to obtain good adhesion and optimal bond performance for a specific application, it is important to evaluate all the above factors for a given adhesive/adherend combination and then proceed to design a bonded joint.

In the absence of a rule-based design code for predicting the lifetime of adhesive joints it is necessary to utilize an analytic approach [4]. This, in common with other engineering structures, can be approached either by comparing the stress in the materials, i.e. the adhesive and the adherends to some limit value, or by studying the initiation and propagation of cracks, which lead to the failure of the bond. In order to understand the joint being investigated, the mode of failure must be characterized. There are three failure modes of an adhesive joint [5]:

1. Cohesive Failure : This is characterized by failure of the adhesive itself, as shown in Fig.2.1
2. Adhesive Failure: This is characterized by failure of the joint at the adhesive/adherend interface, which is caused by inadequate surface preparation, as shown in Fig.2.1
3. Substrate Failure: A substrate failure occurs when the adherend fails instead of the adhesive. In metals, this occurs when the adherend yields.

In general, interfacial failure is difficult to predict because of the problem of calculating stresses at the adhesive/adherend interface. Therefore, designers usually assume that a well made joint will not fail interfacially and therefore concentrate their efforts on predicting the failure of either adherend or adhesive.

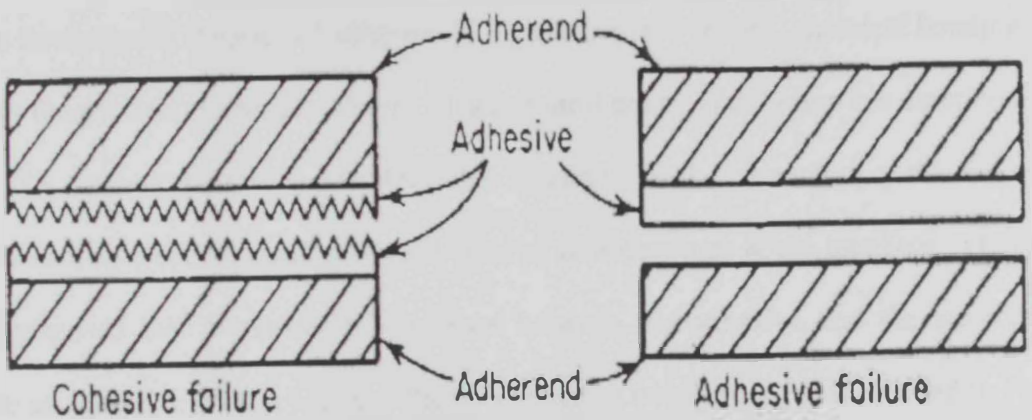

Figure 2.1: Cohesive and adhesive failures of adhesive joints [5]

2.2 Adhesion Theories

Adhesion science is a multidisciplinary field and an area of research that presents many challenges. Over the years, the scientific community has put forth several theories in an attempt to provide an explanation for the phenomenon of adhesion [6]. The interaction that occurs between the adhesive and the substrate directly influences joint strength. Interactions occurring across an interface vary in nature, ranging from weak forces to covalent and ionic bonding. In addition, surface roughness can contribute to joint strength. The type of interaction occurring depends on the topography and chemistry of the adherend surface. There are four fundamental theories of adhesion [7,8]: electrostatic theory, chemical bonding theory, diffusion theory, and mechanical theory. These four theories of adhesion are described below.

The electrostatic theory postulates that as a result of the interaction of the adhesive and the adherend, an electrostatically charged layer of ions develops at the interface. Derjaguin et al. [9] proposed that a transfer of electrons between the adhesive and the adherends can generate an attractive charge between the two resulting in adhesion, as illustrated in Fig. 2.2a. Work is required to separate the charges to break the bond between them. This induces a potential that increases until the substrate and adhesive are separated. The chemical bonding theory has been investigated by Fowkes [10]. This theory of adhesion is based on the concept that adhesion occurs as a result of intermolecular forces at the interface provided that contact between adhesive and adherend is established, as illustrated in Fig. 2.2b. This theory is currently the most widely accepted in adhesion science. The forces at the adhesive/adherend interface may be generally grouped into two categories: primary forces, including (ionic, covalent, and metallic bonds), and secondary forces, including van der Waals forces.

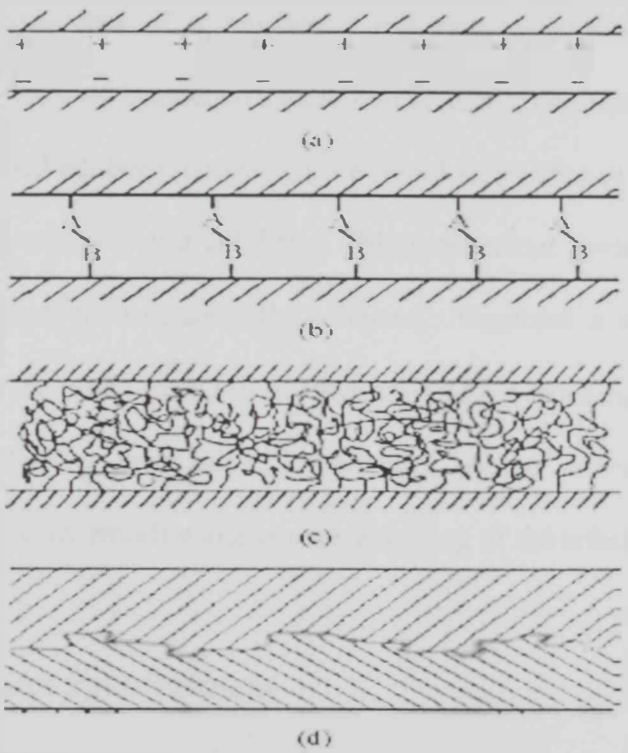

Figure 2.2: Mechanisms of bonding [8]: (a) Bond formed by electrostatic attraction, (b) Chemical bond formed between two groups, (c) Diffusion bond, and (d) Mechanical bond formed when a liquid polymer wets a rough solid surface.

The diffusion theory has been proposed by Voyutskii [11]. He stated that the phenomenon of adhesion could be explained by the diffusion of chains of one polymer into a second polymer and vice versa, as illustrated in Fig. 2.2c. The diffusion of polymer molecules across an interface has two requirements: the chain segments must possess adequate mobility and the polymer must be soluble. This mechanism can occur when the adhesive is significantly soluble in the substrate, and the kinetics of diffusion allow enough flow before the adhesive solidifies. The mechanical theory asserts that adhesion is a result of an adhesive interlocking into the irregularities of a roughened substrate, as illustrated in Fig. 2.2d. According to this theory, increased interfacial area of contact improves adhesion. McBain and Hopkins [12] stated that good adhesion occurs when a liquid adhesive can flow into the pores on the surface of a solid substrate and solidify. This mechanical anchoring prevents the adhesive from being pulled off the surface of the adherend. Venables et al. [13] have shown that some pretreatments of aluminum result in the formation of a porous surface region which promotes adhesion by allowing mechanical interlocking of the adhesive. In general, roughening the surface of the adherends enhances the spreading of the adhesive.

2.3 Aluminum Surface Pretreatment

The importance of bonded aluminum is reflected in its widespread use in the aerospace, transport, and general engineering industries. Aluminum alloys are extremely valuable in the aerospace industry, on account of their light weight and high strength. The adhesive bonding of aluminum has many advantages over other methods of fastening [14]. These include weight saving, uniform stress distribution, no holes are drilled in the adherends, and the reduced risk of corrosion. These advantages have attracted attention to adhesive

bonding as a possible alternative to mechanical fasteners. By roughening the surface, surface pretreatments may increase the surface area of an adherend thereby increasing the interlocking between the adhesive and the adherend. Surface preparation of the adherends of adhesive joints is essential for the production of durable bonds.

The pretreatment of aluminum has been the subject of intensive research in order to obtain a strong bond between the aluminum and the adhesive. Zhang et al. [15,16] investigated the effect of surface roughness of substrates on the fracture resistance of epoxy/aluminum double cantilever beam (DCB) specimens. The experimental results showed that increasing surface roughness enhances the fracture resistance of the joints. The strength of an adhesive joint depends on the adhesive and on the metal and its surface pretreatment [17]. Therefore, surface pretreatment is an important factor and plays a critical role in the development and evaluation of adhesive joints. Many types of pretreatment have been designed to modify the surface of aluminum to enhance bond durability [18]. Prior to adhesive bonding, it is sufficient to remove surface contamination to ensure initially strong joints because metals are normally contaminated with a surface layer having properties widely different from those of the metal itself [19]. The pretreatment procedures which have been used for aluminum alloys prior to adhesive bonding fall into several categories, namely mechanical treatment, alkaline etching, chemical etching by chromic acid, and acid anodizing.

Mechanical treatment of aluminum has been found to give low initial bond strength. The original oxide is removed during the process and a new oxide layer will form on exposure to air. The environmental resistance will be low unless subsequent chemical treatment is used. In alkaline etching, various alkaline cleaners can be used to etch the aluminum. These alkaline cleaners are generally a mixture of salts, such as sodium carbonate and sodium hydroxide. Alkaline etching results in moderately high bond strength. The longest established

effective surface pretreatment of aluminum prior to adhesive bonding is chemical etching by chromic acid. The solution of a chromic acid bath must be carefully controlled. Other etchants for the surface preparation of aluminum for adhesive bonding are used, such as etchants based on phosphoric acid. In acid anodizing, a wide variety of electrolytes is capable of providing anodic coatings on aluminum, such as sulfuric, chromic, and phosphoric acids, which produce a porous oxide film. The most successful and widely used treatment in the aerospace industry is phosphoric or chromic acid anodizing [20]. For automotive applications, simpler, cheaper and more environmentally sound processes are required. The choice of a surface pretreatment is crucial in realizing the required bond strength and durability of adhesive joints. The type of pretreatment selected for an aluminum piece is dependent upon the end use. For structural adhesive joints, particularly in the aerospace industry, anodization is the preferred treatment. However, for less critical applications, and for the adhesion of paints and coatings, where high bond strength is not a requirement, less expensive pretreatment methods can be used.

2.4 Fracture Testing

In the last twenty years, structural adhesives have become common and hence a great number of tests for adhesive joint strength and durability have been developed. Testing of an adhesively bonded system is a complex issue as the system consists of adherends, adhesive, and the interface between the adherends and the adhesive. This makes the interpretation of results a very difficult issue [21]. Great care and caution must be needed in the process of designing, testing, and analyzing data that deals with adhesive joints. Also, the use of non-ideal testing geometries significantly complicates the analysis of the data. Factors such as

bond thickness and plastic zone size have to be considered in order to gain a detailed understanding of joint performance. Testing of adhesives and their bonded joints serves as a tool for quality control besides aiding in other processes, such as adhesive formulation, development, and selection. It must be noted that the testing conditions, testing geometries, and testing loads should closely mimic the service conditions.

There are basically two different approaches for analyzing adhesive joints, specifically with respect to joint design and failure prediction. The first approach considers the nature and magnitude of the stresses found in certain types of joint designs and test methods. This approach permits quantitative joint design studies and failure predictions based on parameters, such as adhesive properties, geometry, test rate, and temperature [22]. An advantage of using the above approach is that it enables many aspects of the mechanical behavior of adhesive joints to be easily understood and predicted. However, a drawback to this method is that stress states calculated for a particular specimen are indeed very specific to that particular test geometry and in order to determine failure loads for different loading geometries, additional techniques are required. The second approach for analyzing adhesive joints is called fracture mechanics and is described in the following section.

2.4.1 Review of Fracture Mechanics

The fracture mechanics approach recognizes that all materials contain flaws and that adhesive joints usually fail due to the initiation and propagation of flaws of a critical size within the adhesive layer. The sources of flaws in adhesives are bubbles, dust particles, or unbonded areas [23]. These flaws are either present in a critical size or develop to the critical size during the fracture test. Fracture mechanics attempts to link these processes with

predictions of the joint strength under various loading conditions by analyzing the stress state within the joint. The approach has been widely applied to metallic materials and considerable effort has been made to apply the approach to polymers and adhesive joints. The fracture mechanics approach has proved useful for identifying mechanisms of failure, predicting the crack propagation rate, and estimating the service life of flawed components, which may have been generated during manufacture or appeared in service.

There are two main approaches for the study of fracture mechanics. The first one is based on the work of Griffith [24]. He assumes that fracture occurs when sufficient energy is released by the propagation of the crack to supply the energy required for the formation of new surfaces. This approach provides for a measure of the energy required to extend a crack over a unit surface area, and this energy is referred to as the fracture energy or the strain energy release rate. The second approach is based on the work of Irwin [25]. He states that the stress field around a crack could be described by a parameter called the stress intensity factor, K, and the fracture occurs when the value of K exceeds a critical value, K_c. While K is a stress field parameter independent of the material, K_c is a material property usually referred to as the fracture toughness.

Griffith's [24] describes crack propagation in terms of the work done by external forces, W_d, the elastic energy stored in the bulk specimen, U, and the surface energy, γ_m, as:

$$\frac{\partial(W_d - U)}{\partial a} \geq 2\gamma_m \frac{\partial A}{\partial a} \tag{2.1}$$

In the above equation, ∂A is the increase in surface area with crack propagation of ∂a. For a crack propagating in a thickness, b, the above equation becomes:

$$\frac{1}{b}\frac{\partial(W_d - U)}{\partial a} \geq 2\gamma_m \tag{2.2}$$

It is found in metals that the energy required for crack propagation is far greater than twice the surface free energy. However, most fracture processes result in localized viscoelastic and/or plastic energy dissipation at regions of high strain within the material. Therefore, if the assumption is made that energy dissipation around the crack tip occurs in a manner independent of applied loads and test geometry, then the term $2\gamma_m$ can be replaced by the critical energy release rate, G_c, which encompasses all the energy losses incurred around the crack tip, and the above equation further modifies to:

$$\frac{1}{b}\frac{\partial(W_d - U)}{\partial a} \geq G_c \tag{2.3}$$

If a sharp crack is present in the material and uniformly stressed, infinite, and linear elastic fracture mechanics are assumed, then stress function solution relating the local stress concentration of stresses at the crack tip to the applied far field stress, σ_o, has been developed. For regions close to the crack tip, the solution is given by:

$$\sigma_{ij} = \sigma_o \left(\frac{a}{2r}\right)^{1/2} f_{ij}(\theta) \tag{2.4}$$

where σ_{ij} are the components of the stress tensor at a point and r,θ are the polar coordinates of the point. Irwin [25] modified the above equation to include the parameter, K, which relates the magnitude of the stress intensity near the crack to the applied load and structure geometry. The modified equation takes the form:

$$\sigma_{ij} = \sigma_o \frac{K}{(2\pi r)^{1/2}} f_{ij}(\theta) \tag{2.5}$$

Adhesive joints in general can be loaded in three different modes, mode I or tensile mode, mode II or shear mode, and mode III or tearing mode. Mode I failures are the most

common with respect to adhesive joints in service conditions. From the above equation, one can see that as r tends to zero, the stress σ_{ij} tends to infinity and hence stress by itself does not make a reasonable local fracture criterion. Since the stress intensity factor defines the stress field around the crack, Irwin [25] postulated the following fracture condition for mode I:

$$K_I \geq K_{IC} \tag{2.6}$$

where the stress intensity factor, K_I, can be expressed as:

$$K_I = Y\sigma_o a^{1/2} \tag{2.7}$$

and the critical stress intensity factor, K_{IC}, is given by:

$$K_{IC} = Y\sigma_c a^{1/2} \tag{2.8}$$

In the above equation, σ_c is the applied stress at the onset of crack propagation and Y is the geometry factor, which can be determined experimentally.

In conclusion, it must be mentioned that there is very little experimental data available to validate the above fracture criteria, and these criteria do not adequately predict the fracture behavior of adhesive joints with cracks at an interface. It must also be mentioned that, at present, researchers commonly adopt the energy approach when studying crack propagation in adhesive joints. In linear elastic fracture mechanics, values of strain energy release rate, G, and stress intensity factor, K are expressed as:

$$G = \frac{K^2}{E} \tag{2.9}$$

For a crack propagates in the adhesive layer, the above expressions are still valid and by using an appropriate value of the adhesive modulus, E_a, one can correlate G_{joint} and K_{joint} through the following expression:

$$G_{IC} = \frac{K_{IC}^2}{E_a} \tag{2.10}$$

In the case of a crack at the interface, there is no clearly established relationship but the appropriate value of the modulus should be some weighted average of the moduli of the materials forming the interface. G_{IC} and K_{IC} may be related as:

$$G_{IC} = K_{IC}^2 \frac{1}{2}\left(\frac{1}{E_a} + \frac{1}{E_s}\right)\left(\frac{2\alpha - 1}{\alpha^2}\right) \qquad (2.11)$$

where α is a function of the moduli and Poisson's ratio of the materials forming the interface.

2.4.2 Adhesive Joint Tests

This section focuses on joint test methods for characterizing strength of adhesion between polymeric adhesives and substrates. The strength of adhesive joints depends on many factors, including material properties of adhesive and adherends, mode of loading, and surface properties of the substrates. The preparation of test specimens is well recognized as having a critical role in the accuracy and reproducibility of test data. Adhesive joints are expected to perform satisfactorily under service conditions that include applied loads and exposure to hostile environments, such as water, high temperature, humidity, or a combination of these conditions. Therefore, a great number of tests for adhesive joint strength have been developed. When considering a test method for establishing adhesive strength, there are some basic requirements that should be considered. An appropriate test method should provide quantitative test data that are suitable for design calculations, involve straightforward specimen preparation, involve robust test procedures, be cost effective, and be accepted by users (e.g. through the use of standards).

The field of adhesive joint analysis may be divided into two major areas of emphasis [26]. The first one is a stress-based approach. This approach focuses on determining the distribution of stresses within the adhesive layer. Failure is assumed to occur when these

stresses reach a critical value. This analysis permits quantitative joint design studies and failure predictions based on parameters, such as adhesive properties and joint geometry [27]. A second parallel approach to the examination of adhesive joints based on the principles of fracture mechanics has emerged. However, the use of linear elastic fracture mechanics and its energy-based approach has gained general recognition as the most appropriate way of predicting failure if the adherends remain elastic [28, 29].

The use of fracture mechanics for bond analysis was first proposed by Ripling et al. [30]. They proposed the use of the more fundamental strain energy release rate, G, to replace the stress intensity factor, K, in describing fracture of adhesive joints, because the use of K solutions depends on the full development of a plastic zone ahead of the crack tip and the plastic zone in the case of adhesive joints is often restricted by the adherends.

The following sections will present a brief review of the different tests that have been used in evaluating the strength of adhesive joints, such as the wedge test, the end notched flexure test, the mixed mode bending test, and the double cantilever beam test.

2.4.2.1 Wedge Test

The wedge test is commonly referred to as the Boeing wedge test. The test [31, 32] uses the introduction of a wedge between two surfaces to force the adherends apart, as shown in Fig.2.3. The Boeing wedge test is a commonly utilized method to test the durability of adhesive joints when exposed to different environments. This test has been incorporated into a testing standard as ASTM D3762. The test consists of creating an initial crack by inserting a wedge and then following the propagation of the crack with time.

Crack length is monitored with time often using ruled scales attached to the adherends. The fracture energy, G, can be calculated from:

$$G = \frac{3Ed^2h^3}{16a^4} \tag{2.12}$$

where E is the modulus of elasticity of the adherend, d is the thickness of the wedge, h is the adherend thickness, and a is the crack length.

The wedge test is simple and cheap to perform. An important assumption in this test is that adherends should not deform plastically. Commonly a crack propagation limit is reached within several days, making this test attractive for rapidly assessing durability. This test is considered a reliable method for assessing the environmental durability of adherend surface preparations. The test is widely utilized when comparing different surface pretreatments [33]. One of the disadvantages of the wedge test is that the specimen must be removed from the test environment to make crack length measurements.

2.4.2.2 End Notched Flexure Test (ENF)

This test has been developed to evaluate the fracture energy of adhesive joints under mode II. The end notch flexure specimen is essentially the double cantilever beam specimen loaded in flexure [34]. Double cantilever beam (DCB) test geometry can be used by applying a three-point bending load instead of opposing end loads (mode I), as shown in Fig.2.4. The strain energy release rate, G_{II}, can be calculated from:

$$G_{II} = \frac{9P^2a^2}{16Eb^2h^3} \tag{2.13}$$

where P is the applied load, a is the crack length, E is the modulus of elasticity of the adherend, b is the specimen width, and h is the adherend thickness.

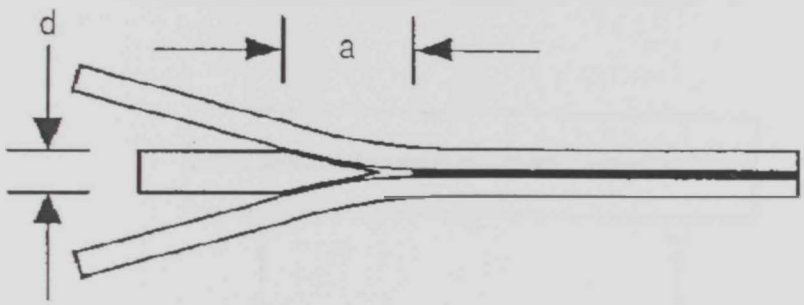

Figure 2.3: Wedge test [19]

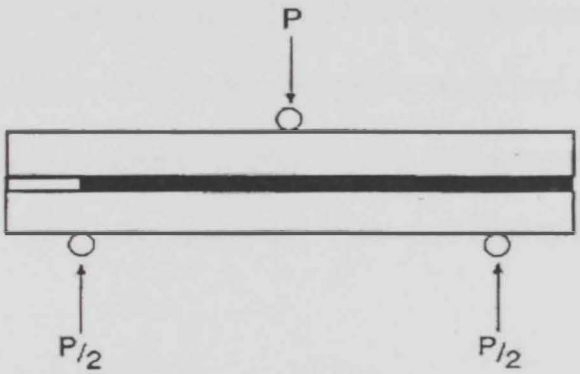

Figure 2.4: End notch flexure specimen

Only elastically deforming adherends are considered in the calculation of fracture energy. When plasticity occurs, additional complications arise not only from the coupling effects between the fracture process and plasticity in adherends but also from the geometric non linearity caused by large deformations and rotations of the specimens [35].

2.4.2.3 Mixed Mode Bending Test (MMB)

The mixed mode bending (MMB) specimen shown in Fig.2.5 is similar to the end notch flexure (ENF) specimen except that at one end, the load is applied to the upper arm only thus providing crack opening as well as shear. The MMB test combines mode I (DCB) and mode II (ENF) tests. This is achieved by adding an opening mode load to a mid span loaded ENF specimen but this approach requires a complex loading system to control the two applied loads simultaneously [36]. The relative magnitude of the two applied loads determines the mixed mode ratio.

2.4.2.4 Double Cantilever Beam Test (DCB)

This popular test is used to obtain the fracture energy of adhesive joints under mode I. The fracture energy, G_{IC}, of an adhesive joint is a measure of the fracture toughness of the adhesive in the presence of flaws. The double cantilever beam (DCB) test as shown in Fig.2.6 was found to be useful in evaluating the energy release rate [37]. Ripling et al. [38] developed a test method to measure the fracture energy of structural bonds between metallic substrates under mode I using a DCB specimen. This work led to the publication of an ASTM standard to deduce the values of G_{IC} from adhesively bonded double cantilever beam (DCB) test specimens.

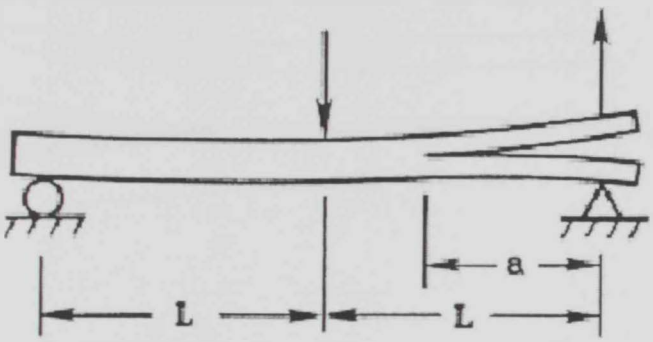

Figure 2.5: Mixed mode bending specimen [34]

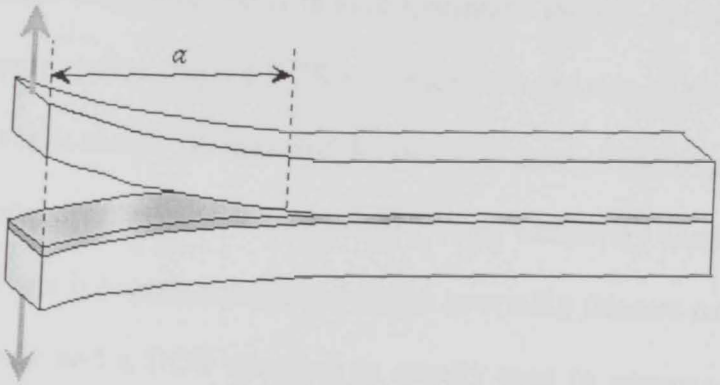

Figure 2.6: Double cantilever beam specimen

Each arm separated from its mate by a crack, is treated as a cantilever beam. Later, because of high stresses at the crack tip, each half of the DCB was modeled as a beam that is partly free and partly supported by an elastic foundation. Recently, a DCB specimen has been used to study the effects of fatigue loads and the environment on the strength and durability of adhesive joints [39-42].

Ripling et al. [39] used a tapered double cantilever beam (TDCB) specimen to study aluminum/epoxy bond durability. Yan et al. [40] used a DCB specimen to study the fracture behavior of rubber-toughened epoxy in bulk specimen. Pirondi and Nicoletto [41] studied the fatigue crack propagation using a DCB specimen with the aim of characterizing an adhesive for structural applications. Pereira and Morais [42] used a DCB specimen to measure the critical strain energy release rate under mode I of an adhesively bonded stainless steel joint. Energy release rate is commonly selected as the governing fracture parameter in the analysis of adhesive joints and a DCB specimen is usually used to generate mode I fracture data. Several methods can be used to calculate the energy release rate [43], including those based on simple beam theory, those based on beam on elastic foundation, and finite element-based methods. The fracture energy, G_{IC}, can be calculated from [44]:

$$G_{IC} = \frac{12 P^2 a_f^2}{E b^2 h^3} \tag{2.14}$$

where P is the load, a_f is the crack length at which the specimen failed, E is the modulus of elasticity of the adherend, b is the width of the specimen, and h is the adherend thickness.

Wang et al. [45, 46] used TDCB to introduce a solution for a tapered beam on elastic foundation. The advantage of using a DCB specimen is that under displacement control. The energy release rate decreases with increasing crack length; therefore, a crack may be arrested without complete fracture of the specimen and several measurements are possible from a

single specimen. Double cantilever beam (DCB) specimens are widely used in mode I fracture toughness and fatigue tests of polymers and composites. The specimen is very simple, inexpensive to fabricate, and good for screening adherend surface quality.

2.5 Review of Bond Thickness Studies on Adhesive Joints

In many structures where adhesive joints are used, knowledge of the effect of bond thickness on the structure's service life (strength, fatigue, and creep) is very limited [47]. An important parameter in adhesive joint design is bond thickness. Many studies have been conducted to investigate the effect of the bond thickness of the adhesive on the fracture energy of toughened adhesive joints [48-60]. These studies have demonstrated the dependence of the fracture energy of adhesive joints on bond thickness. References [52, 53] presented the general trend of experimental results that showed the relation between fracture energy and bond thickness. References [52, 53] showed a pronounced effect of bond thickness on fracture energy and showed that there was an optimum thickness at which maximum fracture energy was obtained.

Kinloch et al. [48, 49] studied fracture energy over a range of temperatures and loading rates in bulk and in adhesive joints using a tapered double cantilever beam (TDCB) and compact tension (CT) specimens. It was found that the adhesive fracture energy of joints consisting of steel substrates bonded with an epoxy is a strong function of adhesive bond thickness. They showed that for a rubber-toughened adhesive, the relation between the fracture energy and the bond thickness is complex. The complex behavior of tough adhesives was attributed to the extensive plasticity that occurs at the crack tip. Due to the presence of relatively thin adhesive layers and high yield strength substrates, there are restrictions imposed

on the full development of the plastic zone ahead of the crack tip. Since the fracture energy is largely derived from the dissipated energy in forming the plastic zone, the fracture energy will decrease as the bond thickness is reduced below a certain value. They explained this behavior in terms of the plastic zone size imposed by the adherends.

Ben Ouezdou et al. [50, 51] showed that the bond thickness of an adhesive affects the total energy release rate and the contribution of the adhesive layer increases as its thickness increases. They introduced a model to evaluate the energy release rate of the adhesives under mode I using a double cantilever beam (DCB) specimen and taking into account the adhesive bond thickness and its material properties. Since the adhesive bond is usually softer and thinner than the adherend, they considered the adherend as a beam that is partly free and partly supported by an elastic foundation, and the adhesive bond as a thin strip under prescribed displacement. Thus, the system of each arm of the adherend and the adhesive bond can be modeled as a beam on an elastic foundation. The fracture energy can be presented as:

$$G_{IC} = G_{IC}^{(1)}[\Phi^2 + \alpha\Psi^2] \tag{2.15}$$

where $G_{IC}^{(1)}$ is similar to G_{IC} in Eq.2.14 and other terms can be calculated from:

$$\Phi = [\frac{\mathrm{Sinh}^2\beta L + \sin^2\beta L}{\mathrm{Sinh}^2\beta L - \sin^2\beta L}] + \frac{1}{\beta a}[\frac{\mathrm{Sinh}\beta L * \mathrm{Cosh}\beta L - \sin\beta L * \cos\beta L}{\mathrm{Sinh}^2\beta L - \sin^2\beta L}] \tag{2.16}$$

and

$$\Psi = \sin\beta L\mathrm{Sinh}\,\beta L - \frac{1}{\beta a}(\frac{\xi - 1}{2})\sin\beta L * \mathrm{Cosh}\,\beta L$$

$$+ \Phi\cos\beta L * \mathrm{Cosh}\beta L - \frac{1}{\beta a}(\frac{\xi + 1}{2})\cos\beta L * \mathrm{Sinh}\beta L \tag{2.17}$$

and

$$\xi = [\frac{\text{Sinh}^{2}\beta L + \sin^{2}\beta L}{\text{Sinh}^{2}\beta L - \sin^{2}\beta L}] + 2\beta a[\frac{\text{Sinh}\,\beta L * \text{Cosh}\,\beta L + \sin\beta L * \cos\beta L}{\text{Sinh}^{2}\beta L - \sin^{2}\beta L}] \quad (2.18)$$

and

$$\alpha = \frac{(1 - \upsilon_{\text{Adhesive}})}{(1 + \upsilon_{\text{Adhesive}})(1 - 2\upsilon_{\text{Adhesive}})} \quad (2.19)$$

and

$$\beta = [\frac{3E_{\text{Adhesive}} / E_{\text{Adherend}}}{t_a h^3}]^{1/4} \quad (2.20)$$

where L = W-a, W is the total specimen length, t_a is the half-thickness of the adhesive, and υ is Poisson's ratio.

Bascom et al. [52] studied the fracture behavior of an elastomer-modified epoxy using TDCB. The fracture energy of the elastomer-modified epoxy exhibited a strong dependence on the bond thickness; there was a maximum of fracture energy when the bond thickness was approximately equal to the plastic zone size. They explained that the reduction in the fracture energy as the bond thickness was reduced below this maximum was caused by a restraint in the development of the plastic zone.

Hunston et al. [53] described the failure of adhesive bond specimens over a wide range of temperatures and loading rates using TDCB. The measurement of fracture energy of an adhesive showed an increase in G_{IC} as the temperature increases or the loading rate decreases, the high G_{IC} being related to the large crack tip deformation zone. The optimum condition was obtained when the bond thickness was approximately equal to the plastic zone size. Increasing temperature or decreasing loading rate increase the zone size and therefore the optimum bond thickness.

Abou-Hamda et al. [54] presented an experimentation method for estimating fatigue crack propagation of a DCB specimen. A series of fatigue crack propagation tests were conducted under tensile loading conditions for three different bond thicknesses at room temperature. They concluded that the greater the thickness, the higher the fracture resistance. Furthermore, the plastic zone created around the crack tip was small enough so that it does not to have any effect on the fracture property measured.

Daghyani et al. [55, 56] investigated the fracture behavior of a compact tension (CT) specimen with a rubber-modified epoxy with various bond thicknesses. There was a direct relationship between the fracture energy of adhesive joints and the plastic zone size that is controlled by the bond thickness. As the bond thickness is increased, the constraint at the crack tip is reduced, which increases the crack tip plastic zone size. As the constraint at the crack tip is reduced, the fracture energy of the adhesive joint is increased towards that of the bulk adhesive material.

Yan et al. [57, 58] investigated the effect of bond thickness on fracture behavior in an adhesive joint based on experimental investigation and finite element analysis using DCB and CT specimens with different bond thickness. For both specimens, the fracture energy increased with bond thickness then decreased with a further increase in bond thickness. They found that thick bonds allow more plastic deformation at the crack tip before fracture.

Krenk et al. [59] studied the fatigue resistance of a single-lap joint using finite element analysis and crack propagation experiments. The fatigue tests with a cyclic load did not show any significant influence of adhesive bond thickness. The experiments showed nearly constant rate crack propagation until failure with no appreciable crack initiation period. There was no systematic influence of bond thickness on fatigue life.

Mall and Ramamurthy [60] investigated bonded joints experimentally to study the effect of bond thickness on critical strain energy release rate under cyclic loading. They used a DCB specimen with different bond thicknesses and the tested specimens were found to have almost the same critical strain energy release rate, G_{IC}, value at a relatively low bond thickness while G_{IC} increased by 50 % in the case of high bond thickness.

However, no simple relationship was found between the bond thickness and the fracture energy of adhesive joints. In fact, the fracture energy of an adhesive joint is dependent on bond thickness, the material properties of the adhesive and adherends, as well as testing procedures and methods of analyzing the results.

2.6 Review of Lifetime Studies on Adhesive Joints

Creep is a time-dependent deformation that results from the application of a constant load. As a specimen is subjected to a constant load, the strain of the specimen is measured as a function of time. Creep behavior can be divided into three stages of deformation when depicted on a plot of strain versus time, as shown in Fig.2.7. The first stage is known as primary creep and is characterized by a strain rate that begins at a relatively high value but soon decreases to a much lower and almost constant value. This point marks the end of primary creep and the beginning of steady state creep. The end of the second stage is often identified by a deviation from linearity of the strain rate. The third stage is referred to as tertiary creep and ultimately leads to fracture. A great deal of work has been dedicated to the area of steady state creep behavior because the majority of a component's creep life is spent in this stage.

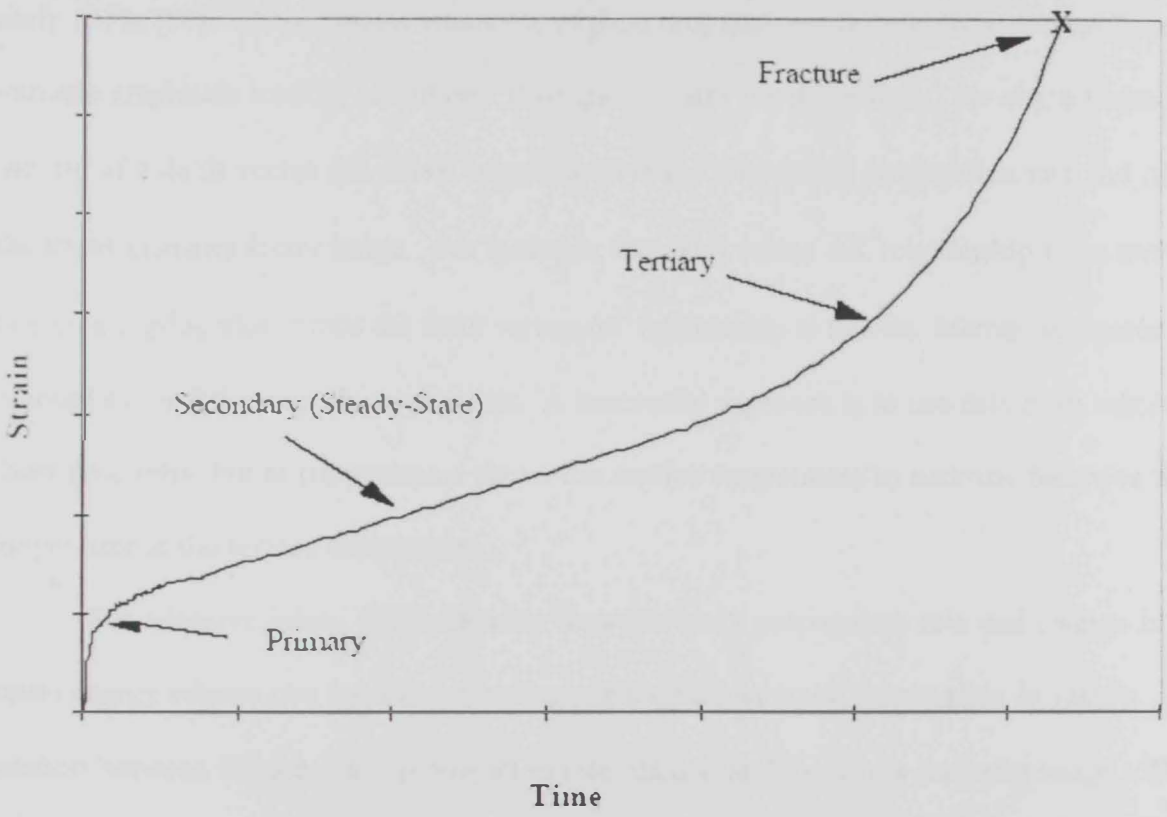

Figure 2.7: Schematic of a typical creep curve

In crack propagation during a static load, the crack propagation rate can be estimated based on fracture mechanics, in a manner similar to the procedures for fatigue crack propagation. The crack propagation concept developed in the 1950s and 1960s has enjoyed wide acceptance, since cracks are directly related to failure and since modern technology has provided tools, which enable measurement of very small cracks. Several fatigue crack propagation models based on linear elastic fracture mechanics concepts were developed in the early 1970s [61]. These models attempt to explain propagation resulting from overloads under variable amplitude loading conditions. Propagation rates for the material are characterized by the use of a da/dt versus ΔK curve, where da/dt is the time-based propagation rate and ΔK is the stress intensity factor range. For example, the da/dt versus ΔK relationship fits a straight line on a log-log plot. Once the da/dt versus ΔK relationship is known, lifetime estimates can proceed as for fatigue crack propagation. A successful approach is to use data from relatively short time tests, but at temperatures above the service temperature to estimate behavior for a longer time at the service temperature.

For adhesive joints, the correlation between crack propagation rate and change in the strain energy release rate has the same shape as the fatigue crack propagation in metals. The relation between fatigue crack propagation rate, da/dN, and the stress intensity range, ΔK, is shown in Fig.2.8. There have been many attempts to model the relation between the fatigue crack propagation rate and the stress intensity range. Paris and Erdogan [62] gave the relation most commonly found in the literature:

$$\frac{da}{dN} = A(\Delta K)^m \tag{2.21}$$

where A and m are material dependent constants. This equation is valid only in region II of the crack propagation rate.

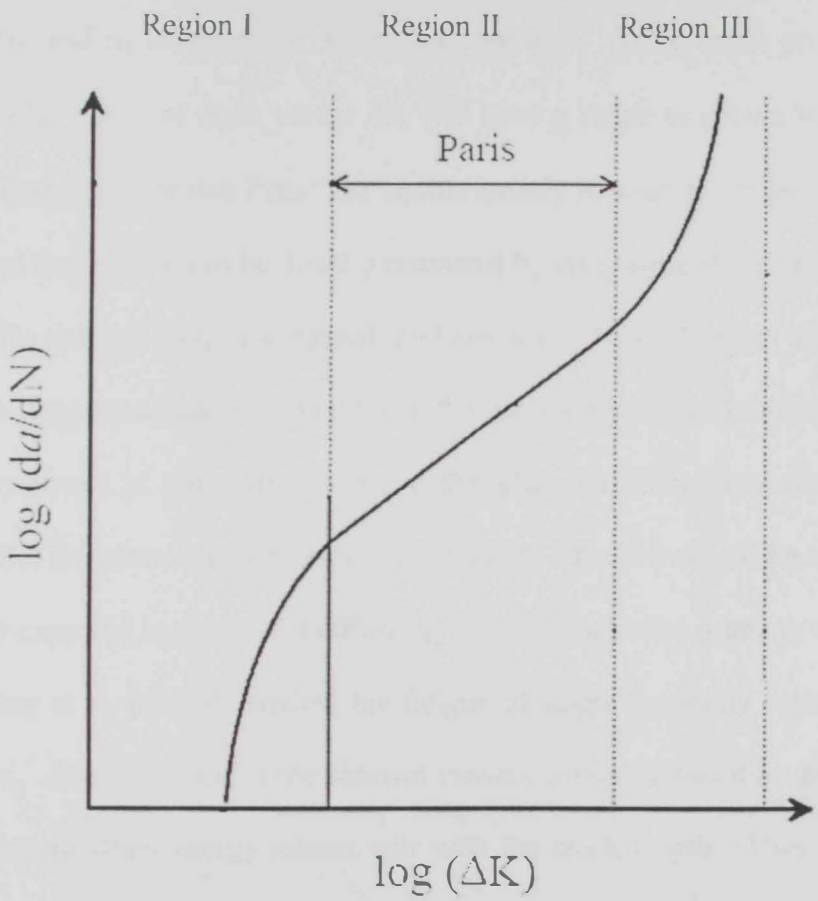

Figure 2.8: Schematic of a typical fatigue crack propagation behavior

Ewalds and Wanhill [63] postulated the following equation that models the complete crack propagation rate curve:

$$\frac{da}{dN} = C(\Delta K)^m \frac{C(\Delta K)^m}{(1-R)K_c - \Delta K}\left[\frac{1-(\frac{\Delta K_{th}}{\Delta K})^{n_1}}{1-(\frac{K_{max}}{K_c})^{n_2}}\right]^{n_3} \qquad (2.22)$$

where n_1, n_2, and n_3 are material dependent constants. If the crack propagation is studied experimentally, a plot of da/dt versus ΔK will have a shape as shown in Fig.2.7. It can be concluded from this plot that Paris' law should mainly be used to model crack propagation in region II and the lifetime can be directly estimated by integrating Paris' law.

Harris and Fay [64] investigated the behavior of two adhesives using single-lap joints over a wide temperature range. They found that the fatigue life of joints for both adhesives is significantly lower at temperatures above the glass transition temperatures. The results suggested that the glass transition temperature of the adhesive should be above the maximum temperature expected in service for efficiently designed adhesive joints in applications.

Curley et al. [65, 66] studied the fatigue of single-lap joints experimentally in a wet environment. Analytical and finite element models were developed to describe the variation of the maximum strain energy release rate with the crack length. They used finite element analysis to calculate G_{max} for different crack lengths and obtained a relationship between G_{max} and crack length by fitting a power law curve to the finite element data. The resulting expression was given by:

$$N_f = \int_{a_o}^{a_f} \frac{1}{da/dN}da = \int_{a_o}^{a_f}\left(\frac{1-(G_{max}/G_c)^{n_2}}{DG^{n}_{max}[1-(G_{th}/G_{max})^{n_1}]}\right)da \qquad (2.23)$$

where G_{th} is the fatigue threshold and G_c the fracture toughness. The constants n, n_1, n_2 can be obtained by fitting the above expression to experimental data.

Abdel Wahab et al. [67] proposed a numerical procedure using finite element analysis for the prediction of the fatigue lifetime of adhesive joints. The fatigue crack propagation behavior of adhesive joints was examined by Liechti et al. [68, 69] over a range of temperatures in air and saltwater. In air, the lowest crack propagation rates and highest threshold value were at room temperature. Higher temperatures in air gave rise to higher exponents and increased crack propagation rates. Saltwater led to a decrease in threshold values and an increase in crack propagation rates with increasing temperature.

Crocombe et al. [70] studied creep crack propagation in bulk specimens of an adhesive and in joints bonded with the same adhesive, and the creep crack propagation was analyzed. Extensive damage occurred ahead of the crack tip and the damage was associated with the elongated plastic zone, and the propagation of the damage zone caused a higher creep crack propagation velocity in the joints than in the bulk adhesive.

3. Experimental Procedures

This chapter deals with the materials selected for the present study and their properties, the geometry of the specimens used as well as the preparation and testing procedures.

3.1 Specimens Preparation

The experiments were carried out to investigate the effect of bond thickness on the lifetime of adhesive joints. The specimens were fabricated from aluminum beams (150x20x4 mm) as adherends and epoxy adhesive. The adhesive was diglycidyl ether of bisphenol A (DGEBA) epoxy resin. According to the manufacturer's data sheet (ITW Devcon, Danvers, MA, USA), this epoxy adhesive exhibits an adhesive tensile shear of 17.24 MPa according to ASTM D1002. Differential scanning calorimetric measurements, in our labs, showed that the glass transition temperature of this epoxy adhesive was 120°C.

The experiments were performed using double cantilever beam (DCB) geometry as shown in Fig.3.1. The specimens were prepared by fabricating the two halves of the DCB from commercial aluminum. The adherends were acquired in the form of rectangular bars (50x4 mm) and they were machined to appropriate dimensions for the set of experiments. Two aluminum end blocks, 20x20x10 mm, each containing a 5 mm loading hole, were bonded to each specimen using four screws 3 mm in diameter.

The mechanical properties of the bulk specimens of the adhesive and the aluminum used in this study were measured under tension at room temperature. Tensile tests were performed on a MTS universal testing machine with a load cell of 100 KN.

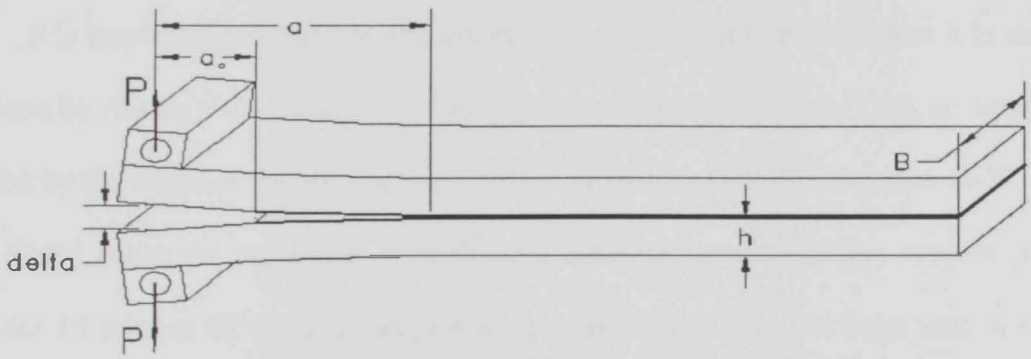

Figure 3.1: Test specimen configuration

Bulk specimens of adhesive were manufactured by injecting the mixed adhesive into closed aluminum moulds, which were coated to facilitate specimen removal. The filled moulds were left to cure at room temperature for 7 days. The load was applied at a constant cross-head speed of 0.1 mm/min at ambient temperature. The stress was calculated from the load divided by the cross-sectional area. The strain was measured using an extensometer with a gauge length of 50 mm which was attached to the middle of the specimen. The elastic properties of the adhesive were: Young's modulus E = 4.5 GPa and Poisson's ratio $\upsilon = 0.35$. The elastic properties of the adherends were: Young's modulus E = 69 GPa and Poisson's ratio $\upsilon = 0.3$. The reported properties represent the average of three tests.

It is important to clean the aluminum surface of any oil or dirt before it is used. This was done by rinsing with acetone and rubbing dry with a paper towel. Then the samples were handled by the edges or the top and were etched in 10% NaOH for 1.5 min at 60°C. Samples were rinsed under the tap and then in flowing distilled water. Finally, samples were oven dried for 15 min. at 60°C. The samples were stored inside the desiccator until it was used. The surface morphology of pretreated surface is shown by the scanning electron microscope (SEM) micrographs in Fig. 3.2. The surface characteristics of the aluminum samples were studied before and after the etching process. The results indicated that alkaline etching under the present conditions is promising as a simple, very rapid and environmentally friendly pretreatment for adhesive bonding. Once the surface had been prepared, the epoxy resin was mixed in accordance with the manufacturer's recommendations. The adhesive was supplied in twin packs of resin and hardener. The mixing was carried out in a container and was continued until the mixture had a uniform color.

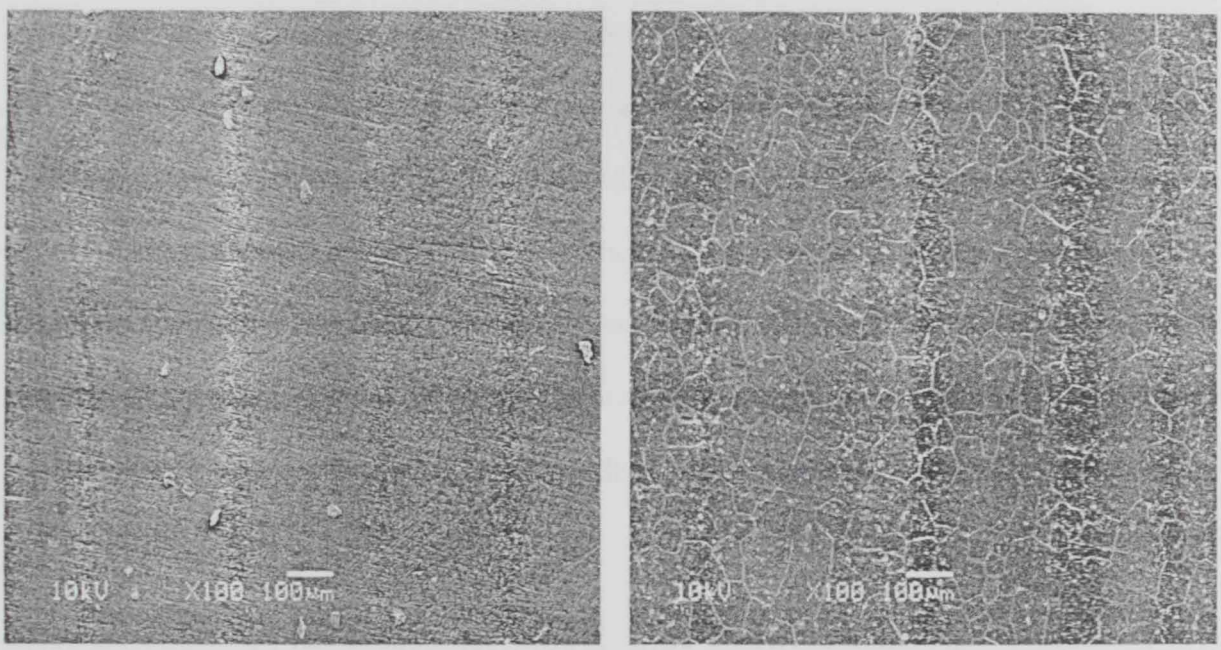

a b

Figure 3.2: SEM micrographs of aluminum alloy (a) before etching and (b) after etching.

Specimens were then bonded together with the adhesive by applying the epoxy to the aluminum surfaces separately and then bringing the two together. During hardening of the adhesive, certain uniform loads were applied to the surface of the aluminum in order to expel the excess epoxy resin to maintain the bond thickness and to ensure a good contact between the adhesive and the aluminum. The loads were maintained until the epoxy had fully cured. The samples were left for 7 days to cure at room temperature, which is the minimum time to fully develop their mechanical strength. When fully cured, any excess adhesive was removed by careful polishing of the specimen edges to leave the joint with smooth sides.

The joints were maintained in normal laboratory conditions for a minimum of twenty four hours prior to testing i.e. they were maintained at room temperature. The thickness of the adhesive should be carefully controlled. The bond thickness was controlled by polypropylene tape shims placed at the front and at the end of the beam. A series of different bond thicknesses were tested. A pre-crack was created in each specimen by extending a thin Teflon shim beyond the thickness spacer into the bonded area, and its length was 30 mm.

3.2 Testing Procedures

The rate of crack propagation was accelerated by means of elevated temperatures, which were kept below the glass transition of the epoxy, at constant loads. The constant load device was accommodated within a controlled temperature chamber as shown in Fig.3.3. A proportional controller equipped with a heat sensor was placed 2 mm from the specimen to adjust the temperature as desired. The loads were applied by using dead weights, which were allowed to engage gently within 3 seconds using a screw jack to avoid impact effects. The crack propagation length as a function of time was monitored through changes in the load-

point displacement of the two cantilevers of the specimen. Load-point displacement is related to crack opening displacement, from which crack length may be calculated. The load-point displacement and the temperature were continuously recorded by means of displacement and temperature transducers which were connected to a data acquisition system based on LabVIEW5 (National Instruments, Austin, Texas) as a text file.

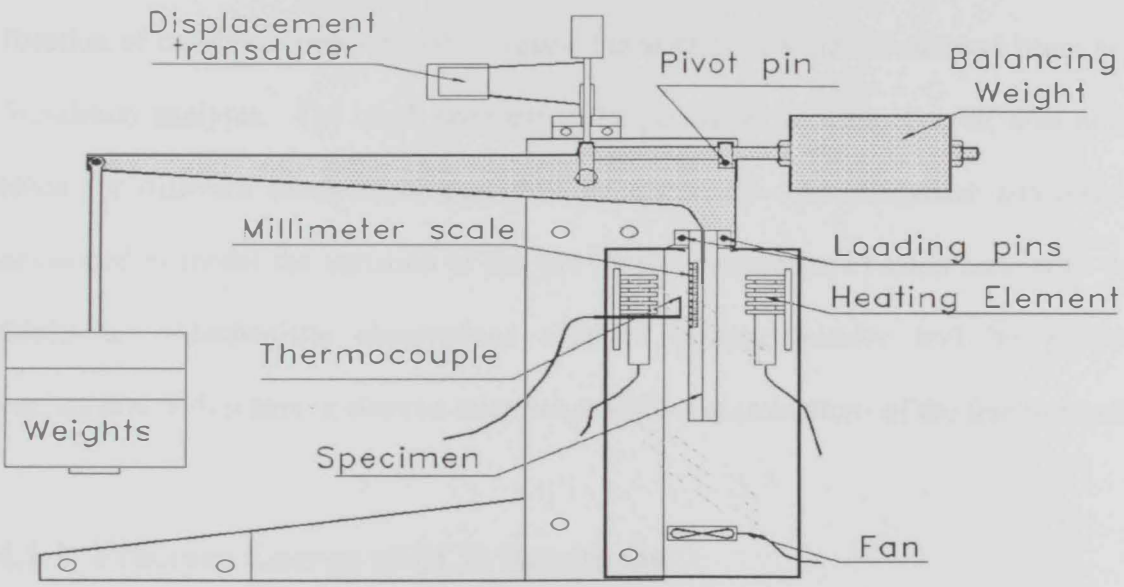

Figure 3.3: Experimental setup

4. Results & Discussion

Part I: Constant Loads at Constant Temperature

This part will present and discuss the results obtained from experimental measurement of DCB specimens under mode I at 50°C. The fracture energy of the adhesive joints as a function of bond thickness will be evaluated based on both simple beam and beam on elastic foundation analyses. The crack propagation length curves as a function of time at constant loads for different bond thicknesses will be discussed. An analytical analysis will be developed to model the variation of the two kinetic parameters of Paris' law with the bond thickness. Mechanistic observations obtained photographically will be presented in conjunction with scanning electron microscope (SEM) examinations of the fracture surfaces.

4.1.1 Fracture Energy of DCB Specimens

Fracture energy is commonly used to characterize the strength of adhesive joints. Ripling et al. [37] used a double cantilever beam (DCB) specimen to measure fracture energy in adhesive joints. A simple beam analysis was developed, which considered each arm of the DCB specimen as a cantilever beam built-in at one end, and only bending of the cantilever part was considered in the energy analysis. The expression for the fracture energy was presented in the literature review (Eq.2.14) but this equation does not account for the adhesive thickness, despite the experimentally observed dependency of the fracture energy on this parameter [52, 53].

However, even a thin layer of adhesive with a relatively small elastic modulus may contribute to the fracture energy of the adhesive joint. Ben Ouezdou et al. [50, 51] introduced a model to evaluate the fracture energy of adhesive joints under mode I using a DCB specimen. The system of each arm of the adherend and the adhesive bond can be modeled as a beam on elastic foundation. The expression for the fracture energy was presented in the literature review (Eq.2.15).

In order to determine the fracture energy of adhesive joints under mode I using a DCB specimen, different bond thicknesses were tested. The specimens were loaded to failure with constant loads at 50°C. The crack will propagate rapidly at a critical load, P_f, which corresponds to the load required to initiate rapid crack propagation. It is possible to determine the fracture energy or critical strain energy release rate, G_{IC}, by measuring P_f. The results obtained for G_{IC} as a function of bond thickness at 50°C are shown in Fig. 4.1 for both simple beam and beam on elastic foundation analyses. The two curves are similar in behavior but the values of G_{IC} for the beam on elastic foundation analysis are higher than those for the simple beam analysis.

The results show the significant effect of the adhesive bond thickness on the fracture energy; and the model built using simple beam analysis underestimates the fracture energy of the adhesive joints. Also, the data demonstrates that G_{IC} is relatively low at very low bond thicknesses. It increases with increasing thickness reaching a maximum value and then decreases. The maximum fracture energy is obtained at an optimum thickness. The optimum thickness is the same for the two methods of calculating the fracture energy.

The high constraint in thin bonds is expected to be the main reason for low fracture energy. The fracture energy increases initially with increasing bond thickness due to the relief

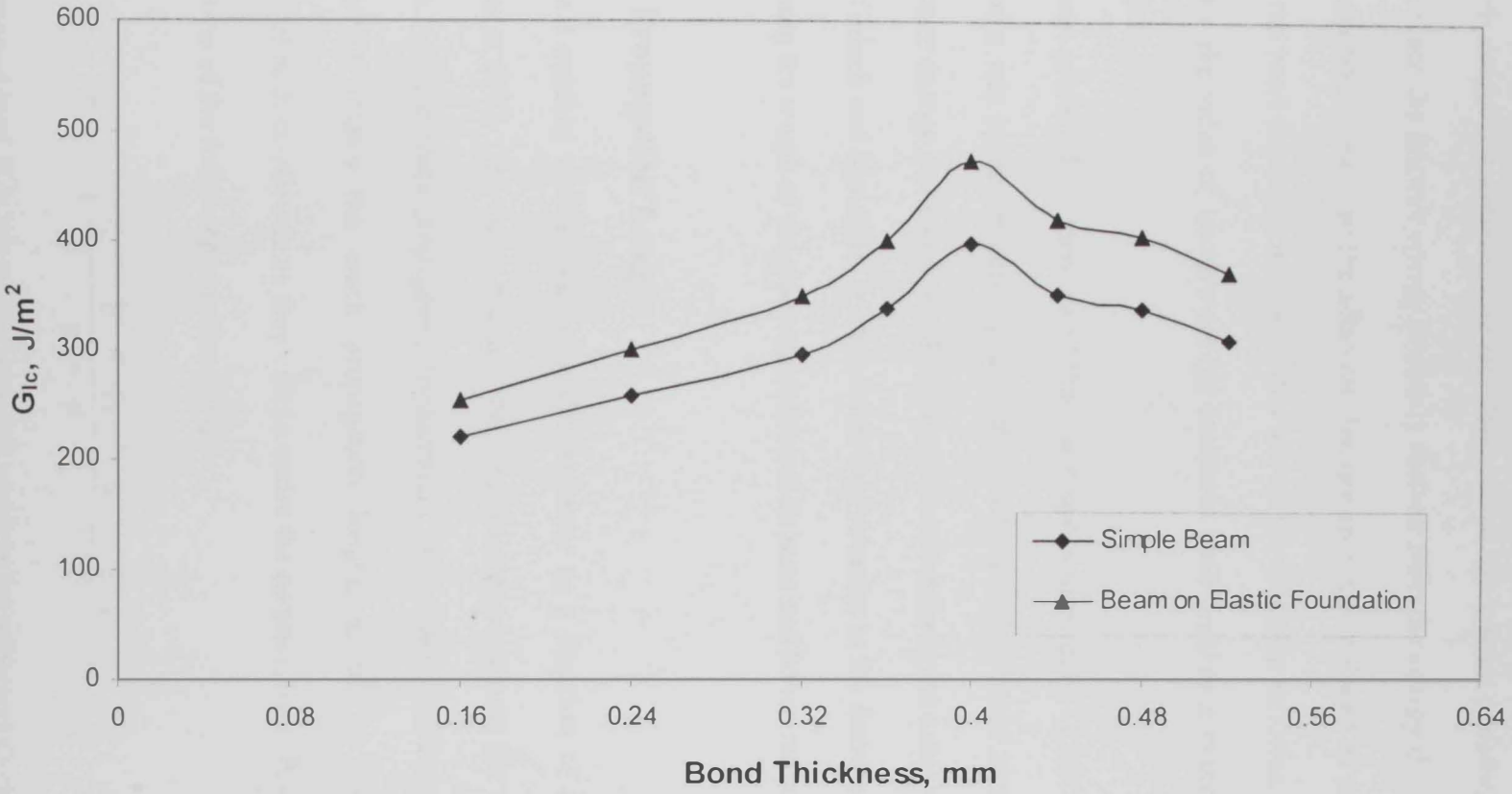

Figure 4.1: Fracture energy as a function of bond thickness under monotonic loads at 50°C

of constraint. It has been suggested that at small values of bond thicknesses and with the presence of high modulus substrates, the development of the crack-tip deformation zone was restricted [48]. Since the fracture energy is mainly derived from the energy dissipated in forming the crack-tip deformation zone, so the adhesive fracture energy is reduced as the bond thickness decreases. As the bond thickness increases, this allows the crack-tip deformation zone to grow and consequently the value of fracture energy increases until reaches a maximum value at an optimum thickness.

It has been previously demonstrated that there was a maximum of fracture energy when the bond thickness was approximately equal to the crack-tip deformation zone size [52]. The decrease in fracture energy at thicknesses higher than the optimum is not completely explained in the literature. Kinlock and Shaw [48] tried to relate this behavior to the decrease in the degree of constraint reducing the length of the crack-tip deformation zone and hence reducing its volume.

4.1.2 Crack Propagation Length

Figure 4.2 exhibits typical load-point displacement as a function of time for different bond thicknesses at 50°C. The curve displays the load-point displacement for the entire lifetime of the specimen. As the crack propagates, displacement of the two cantilever beams increases. Fracture mechanics relates the crack propagation length, a, to the load-point loading displacement, δ, of both cantilevers as they extend under the constant load, P, in mode I of DCB geometry by means of the following equation [71]:

$$a = \left(\frac{\delta * E * B * h^{3}}{8 * P} \right)^{1/3} \qquad (4.1)$$

where P is the applied load, B is the specimen width, and h is the adherend thickness.

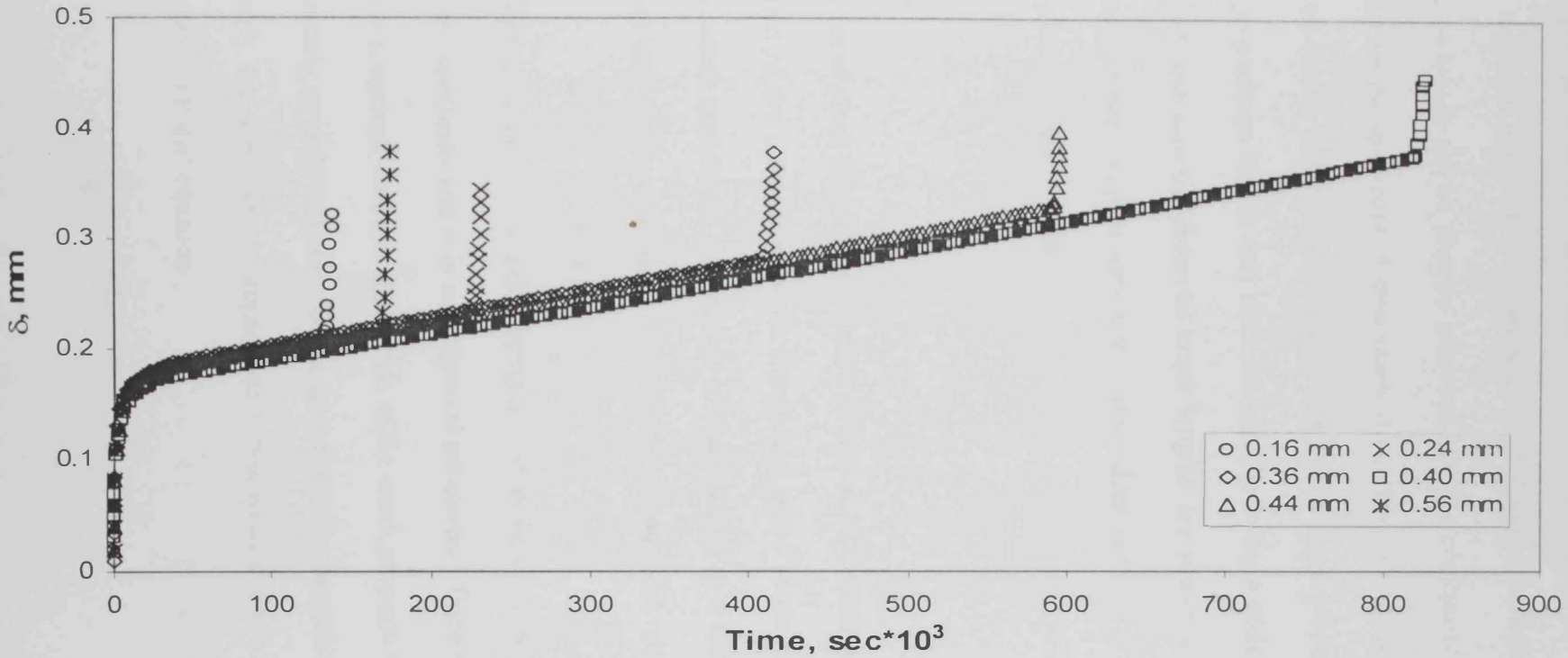

Figure 4.2: Typical load-point displacement curve as a function of time

Equation 2.15 adopts the beam on elastic foundation theory for G_{Ic} calculation, but the correction for the crack length is not explicitly expressed as a function of adherend thickness [72]. The crack propagation length can be directly observed but it is convenient to estimate the crack propagation length from the load-point displacement data. This is helpful for experiments continuing for a long time during which visual observations of the crack propagation front are impractical. The crack propagation length was recorded visually using a scale attached to the specimen side. Calculated and directly observed crack lengths are shown in Fig. 4.3. The measured and the calculated values compare well, which allow determination of the crack length for experiments requiring long periods of time.

4.1.3 Data Analysis

The typical behavior of crack length as a function of time at 50°C is shown in Fig. 4.4. At the beginning, propagation of the crack front starts slowly and speed increases with time as it approaches complete specimen separation. All curves of crack length as a function of time for different bond thicknesses look similar and can be described by an empirical relationship:

$$a(t) = a_i \left(1 - \frac{t}{t^*}\right)^n \qquad (4.2)$$

where a_i is the crack length at onset of the crack propagation, t^* is the time required to achieve a complete separation of the specimen and n is an empirical parameter. Equation 4.2 is used to obtain the rate of crack propagation, da/dt, as a function of the crack propagation length, a. The simplest and most commonly used formulation for the rate of crack propagation is Paris' power law equation. Accordingly, the rate of crack propagation is plotted as a function of strain energy release rate in accordance with Paris' equation:

$$\frac{da}{dt} = AG^m \qquad (4.3)$$

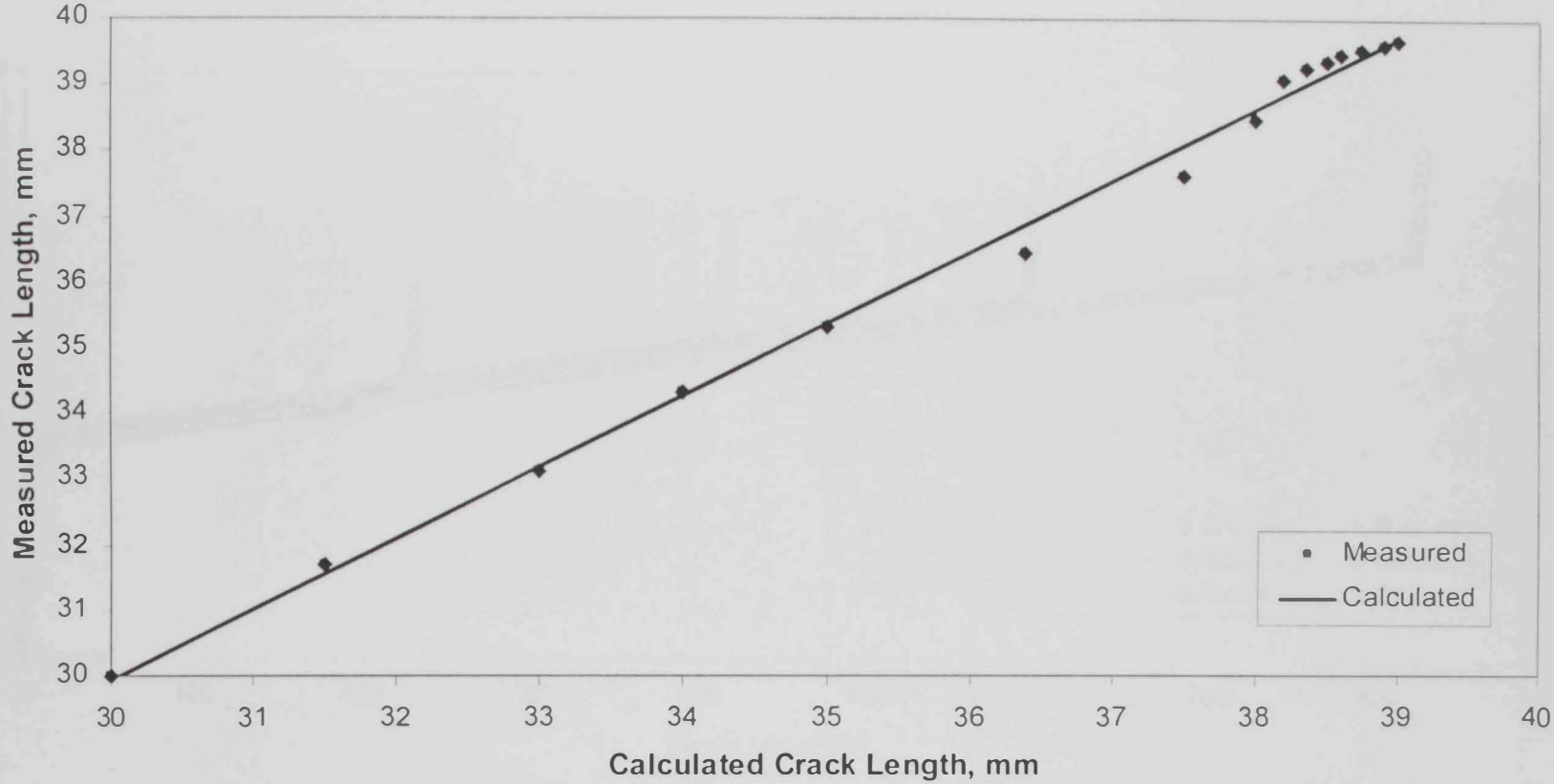

Figure 4.3: The calculated and the observed values of crack propagation length

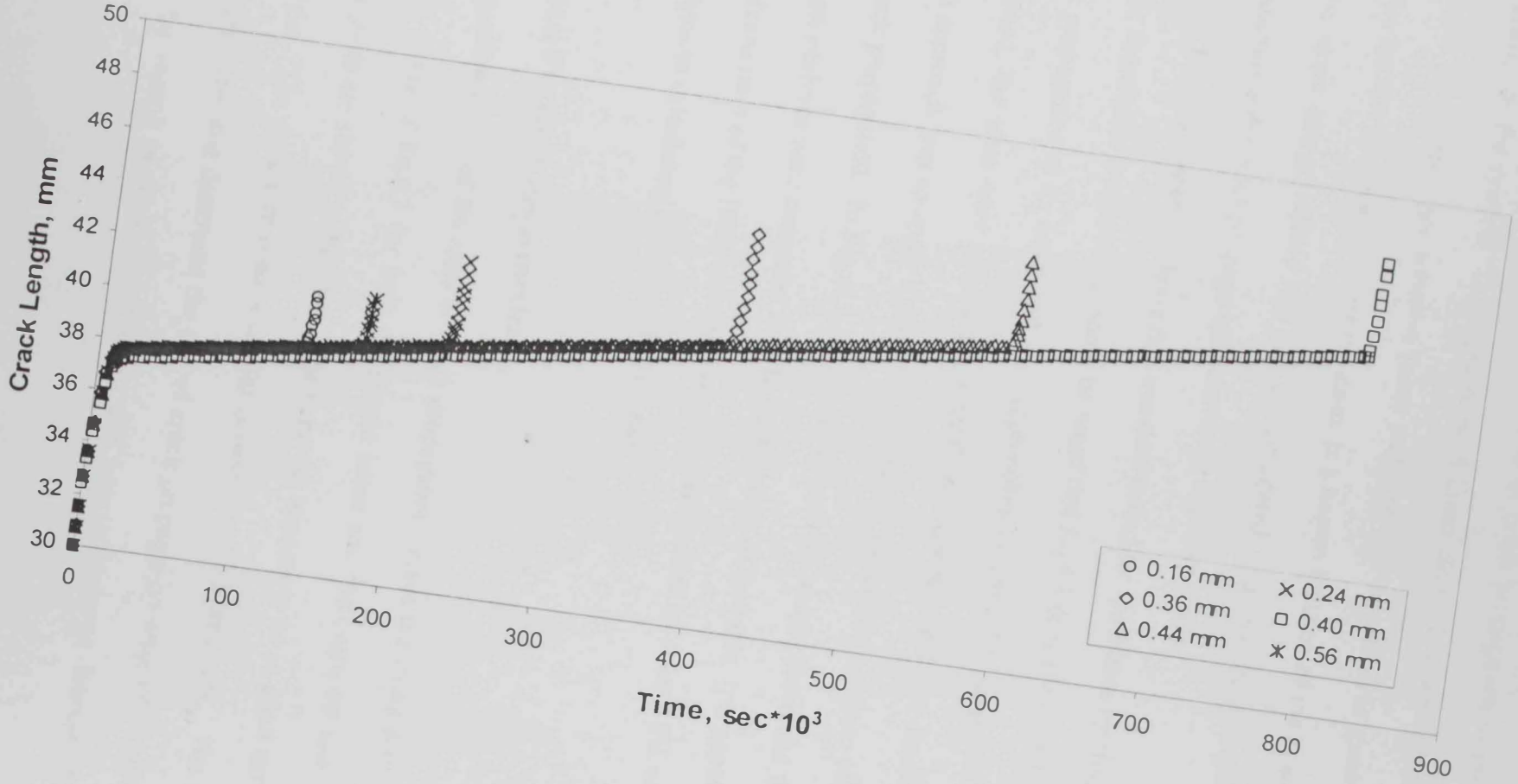

Figure 4.4: Typical crack propagation length as a function of time

Equation 4.3 relates the kinetics of crack propagation to the associated change in the energy of the system. The application of linear elastic fracture mechanics to predict the rate of crack propagation for adhesive joints under service conditions is generally based on the notion that the rate of crack propagation, da/dt, is a known function of the strain energy release rate, G. The strain energy release rate can be considered as a fracture parameter that can be used to characterize the crack propagation behavior in adhesive joints.

The strain energy release rate was determined for specimens by simple beam and beam on elastic foundation analyses. It should be noted that Eq.4.3 does not include the rise in the rate of crack propagation at its onset and as it approaches its critical propagation rate. As previously mentioned, the tests were conducted at 50°C in order to accelerate crack propagation. The general approach was to apply a constant load below the critical value to allow for measurable slow crack propagation. In Fig. 4.5, the results of both the simple beam and the beam on elastic foundation analyses were compared for a bond thickness of 0.40 mm. It is apparent that the strain energy release rates of the DCB specimen were underestimated by about 18% when using simple beam analysis in calculating the energy release rate.

4.1.4 Crack Propagation Kinetics

A logarithmic plot of the rates of crack propagation versus the strain energy release rate was plotted in terms of Eq.4.3 for both the simple beam and the beam on elastic foundation analyses. The plots are shown in Fig. 4.6. The behavior appears to be in good agreement with Paris' power law. The results showed a similar behavior in both analyses. The two kinetic parameters of Paris' law that determine the rate of crack propagation were determined for each bond thickness by means of both simple beam and beam on elastic foundation analyses.

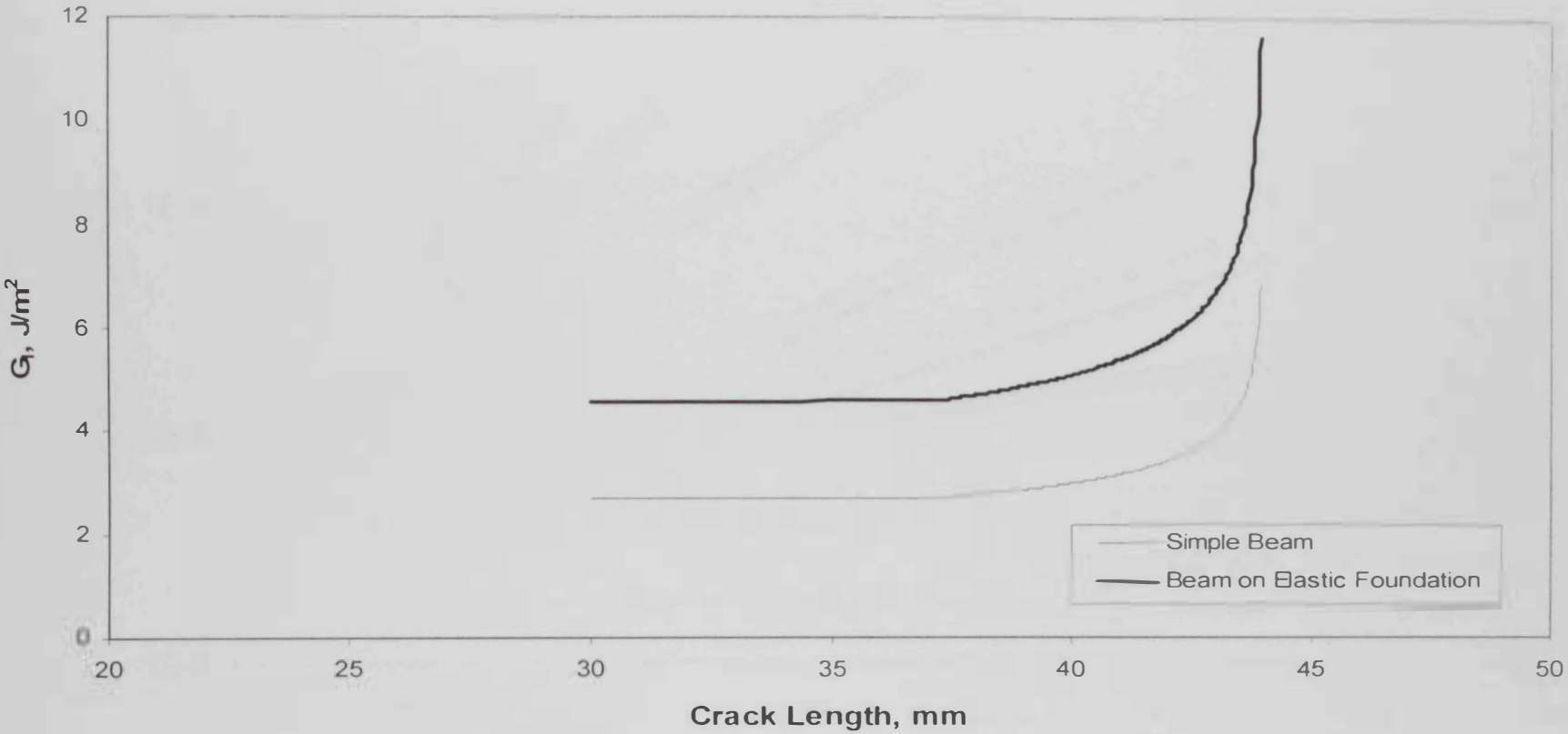

Figure 4.5: Energy release rates for DCB specimens

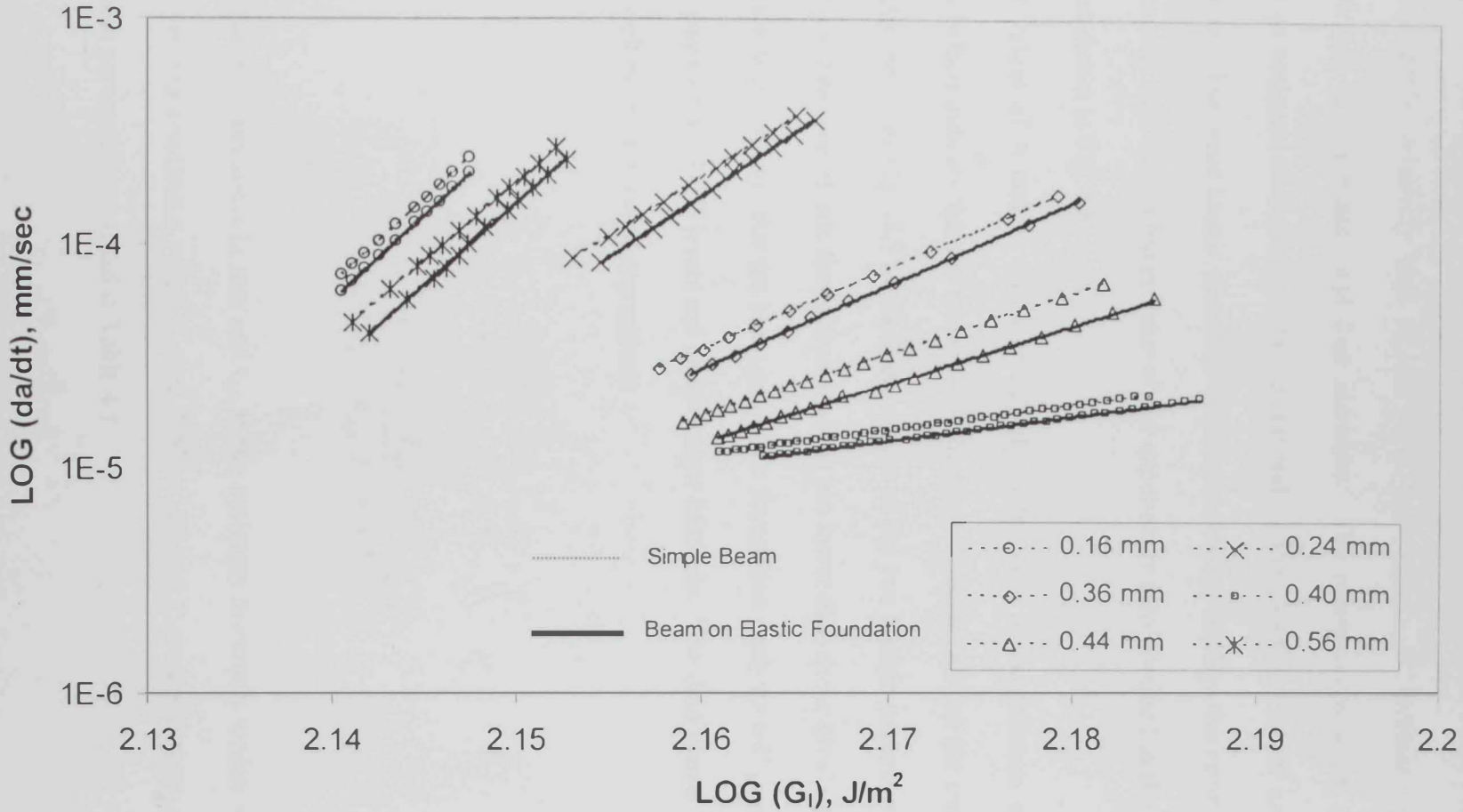

Figure 4.6: Paris plots for crack propagation at 50°C

A plot of the intercept, A, as a function of bond thickness, as shown in Fig. 4.7, indicates that the intercept is relatively high at low bond thicknesses. It decreases with increasing thickness falling to a minimum and then increases. The minimum value of the intercept is obtained at an optimum thickness and this corresponds to the idea that a lower intercept means a longer lifetime. The other kinetic parameter (the exponent), m, displays the same behavior of the intercept, namely that the minimum value of the exponent is also obtained at the same optimum thickness, as shown in Fig. 4.8.

The values of A and m vary significantly in the case of experiments at various bond thicknesses, which indicate that the variation of the bond thickness affects the crack propagation behavior. As shown in Figs. 4.7 and 4.8, the values of the two kinetic parameters of Paris' law obtained by the beam on elastic foundation analysis are lower than those obtained by the simple beam analysis, which means that the beam on elastic foundation analysis will predict lower rates of crack propagation for DCB joints and hence longer lifetimes. The data appear to be described reasonably well by the following expressions:

$$A = \frac{b(t_a - t_{opt})^2}{c(t_a - t_{opt})^2 + d} + f \qquad (4.4)$$

and

$$m = \frac{b'(t_a - t_{opt})^2}{c'(t_a - t_{opt})^2 + d'} + f' \qquad (4.5)$$

where t_a is the bond thickness in mm and t_{opt} is the optimum thickness, which equals 0.40 mm under the given test conditions, where b, c, d, f, b', c', d', and f' are the fitting parameters. The values of these parameters are listed in Table 4.1.

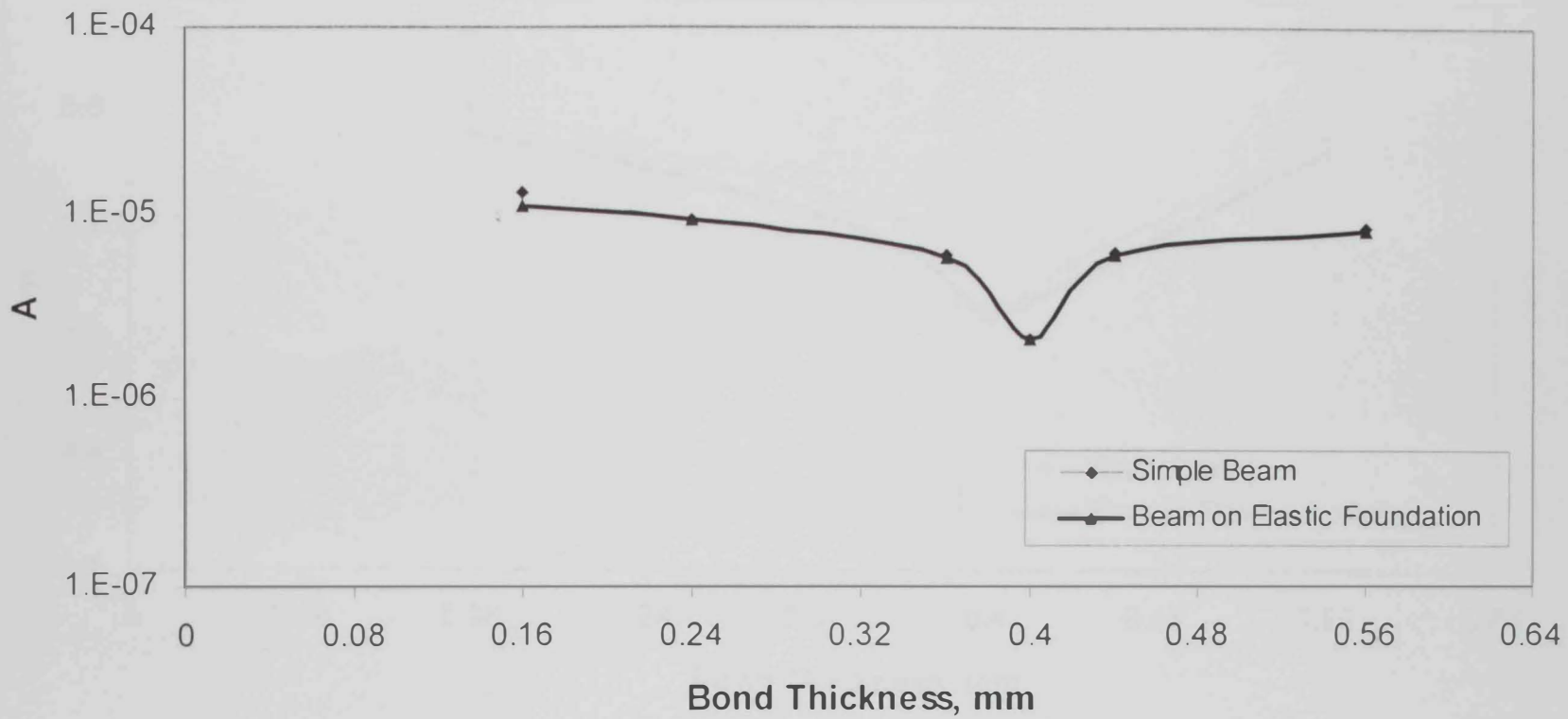

Figure 4.7: Paris kinetic parameter, A, as a function of bond thickness at 50°C

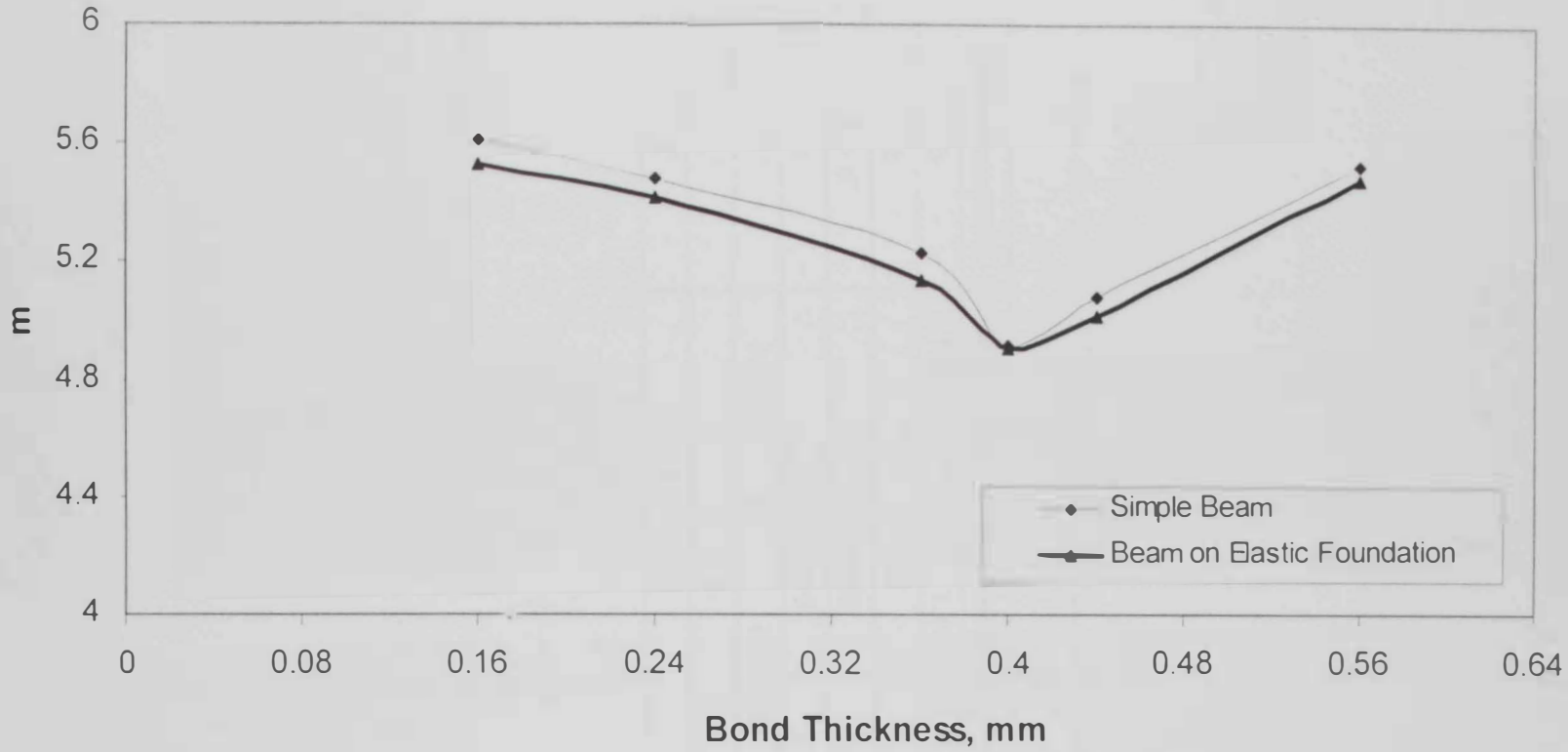

Figure 4.8: Paris kinetic parameter, m, as a function of bond thickness at 50°C

Table 4.1: Values of fitting parameters of Eqs.4.4 and 4.5

Fitting Parameters	Simple Beam	Beam on Elastic Foundation
b	1.16675×10^{-5}	1.16145×10^{-5}
c	1.3	
d = d'	0.0048	
f	2.13×10^{-5}	
b'	1.21415	1.21125
c'	1.0	
f'	4.91	

It should be noted that the values of the exponent, m, for polymeric adhesives are relatively high. Lifetime studies for fatigue crack propagation have revealed that the slopes of the crack propagation curves indicated by m for adhesives are much higher than those for metals [54]. This indicates that adhesive joints have a greater sensitivity to small changes in the applied strain energy release rate. It should be mentioned that higher values of A or m indicate that an adhesive joint is more susceptible to crack propagation. Also, a higher value of m is especially dangerous because it means that a slight change in loading conditions could cause a significant increase in the crack propagation rate, thus making the system highly unstable if cracking ever begins. The values of the two kinetic parameters determined within the stable propagation stage represent material characteristics of the adhesive joint which are specific to DCB specimen under mode I under the given test conditions. Eqs.4.4 and 4.5 seem to offer a reasonable description of the data and may be used to obtain the intercept and the exponent at the desired bond thickness.

4.1.5 Lifetime of DCB Specimens

The experimental and calculated results obtained for the lifetime of the DCB specimens as a function of bond thickness at 50°C are shown in Fig. 4.9. It shows that lifetime is relatively low at low bond thicknesses and it increases with increasing thickness reaching a maximum value and then decreases. The maximum lifetime is obtained at the optimum thickness. The maximum lifetime and maximum fracture energy occur at the same optimum thickness. As shown in Fig. 4.9, the lifetimes of DCB specimens obtained using the beam on elastic foundation analysis are higher than those obtained using the simple beam analysis. This indicates that the simple beam analysis is more conservative than the beam on elastic foundation analysis because it ignores the effect of bond thickness in the calculation of strain energy release rate for the DCB specimens.

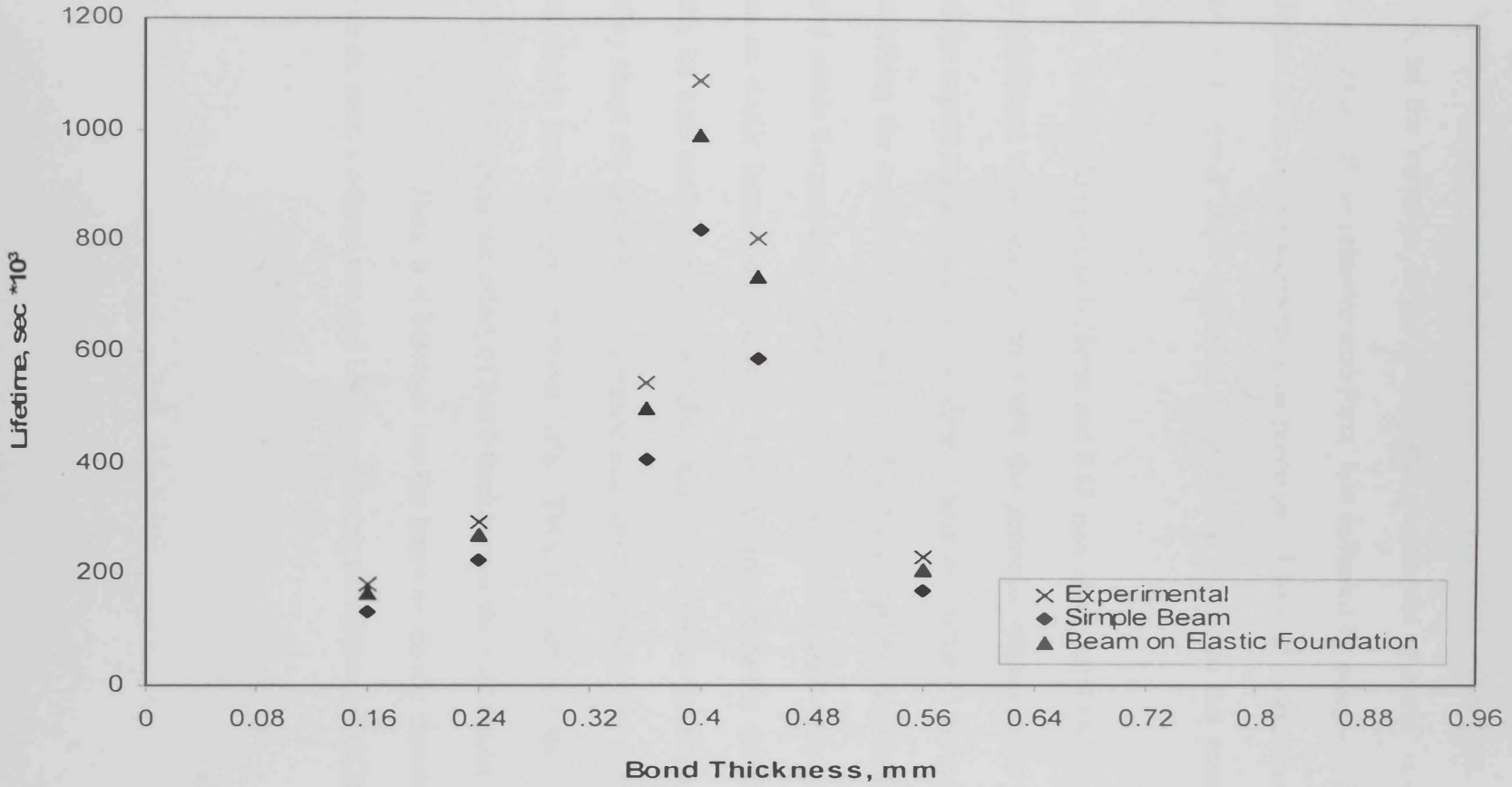

Figure 4.9: Lifetime as a function of bond thickness under constant load at 50°C

An analytical approach was developed which would enable crack propagation to be modeled and hence the lifetime of adhesive joints to be predicted. Therefore, Eqs.4.4 and 4.5 were used to model the variation of the two kinetic parameters of Paris' law with the bond thickness. Substitution of these relations into Paris' law followed by integration of this equation allowed the lifetime of the DCB specimens to be predicted. This analytical approach was used to predict lifetime of a typical DCB specimen subjected to the same test conditions but with different bond thicknesses.

Two other bond thicknesses of 0.28mm and 0.48 mm of a typical DCB joint subjected to the same test conditions were selected to verify the previous relations and to compare the predictions and the experimental results for lifetime. These two different bond thicknesses were not used in describing the analytical approach. Table 4.2 compares the lifetimes of the DCB joints determined within the propagation stage experimentally and analytically using both simple beam and beam on elastic foundation analyses. The agreement between the experimental and analytical results for both analyses was relatively good. It should be noted that the lifetime is underestimated by about 6% in the beam on elastic foundation analysis and this underestimation increases in the simple beam analysis to about 10%. Thus, the simple beam analysis is more conservative because it neglects the effect of bond thickness in the calculation of strain energy release rate for DCB joints. Thus, it is better to use the beam on elastic foundation analysis in calculating the strain energy release rate and hence predicting the lifetime of DCB joints.

Table 4.2: Experimental and analytical values of lifetimes of DCB specimens at 50°C

Bond Thickness (mm)	Lifetime (sec) (Experiment)	Lifetime (sec) (Simple Beam)	% Error	Lifetime (sec) (Beam on Elastic Foundation)	% Error
0.28	266557	239165	10.28	248648	6.72
0.48	438584	395687	9.78	413526	5.71

4.1.6 Fracture Surface Inspection

Mechanistic observations obtained photographically during the experiment were presented in conjunction with a scanning electron microscope (SEM) examination of the fracture surfaces after complete separation of the specimen. Observations of the specimens during the tests showed that the crack propagated cohesively through the adhesive layer for the fracture tests conducted using the DCB specimen under mode I although it was sometimes not located precisely in the middle of the adhesive layer. Figure 4.10 is a representative optical micrograph of the specimen after applying the load. The two cantilevers were deflected and the crack extends within the adhesive layer. Since the fracture path was cohesive, this suggests that the surface preparation of the aluminum was adequate for the conditions examined. The typical appearance of the propagating crack front is shown in Fig. 4.11. Examination of the crack front reveals that the propagation had assumed a curved shape that remained self-similar.

It has been previously demonstrated that the epoxy polymer exhibits deformation markings in the region of crack initiation [53]. Figures 4.12 and 4.13 show the variation of fractographic features for 0.16 mm and 0.40 mm bond thicknesses at the crack initiation. For the thinnest bond, the fracture surface shows the deformation marks appear at the crack initiation. With increasing bond thickness to 0.40 mm, more deformation marks appear at the crack initiation. Therefore, the amount of these deformation marks increases with further increase in bond thickness. A close examination of the fracture surface, as shown in Fig. 4.14, indicated that the fracture surface reveals some defects. It is quite likely that the high stress field ahead of the crack tip causes these defects to serve as initiation points for failure.

Figure 4.10: Photograph of the side view of the crack propagation in the DCB specimen

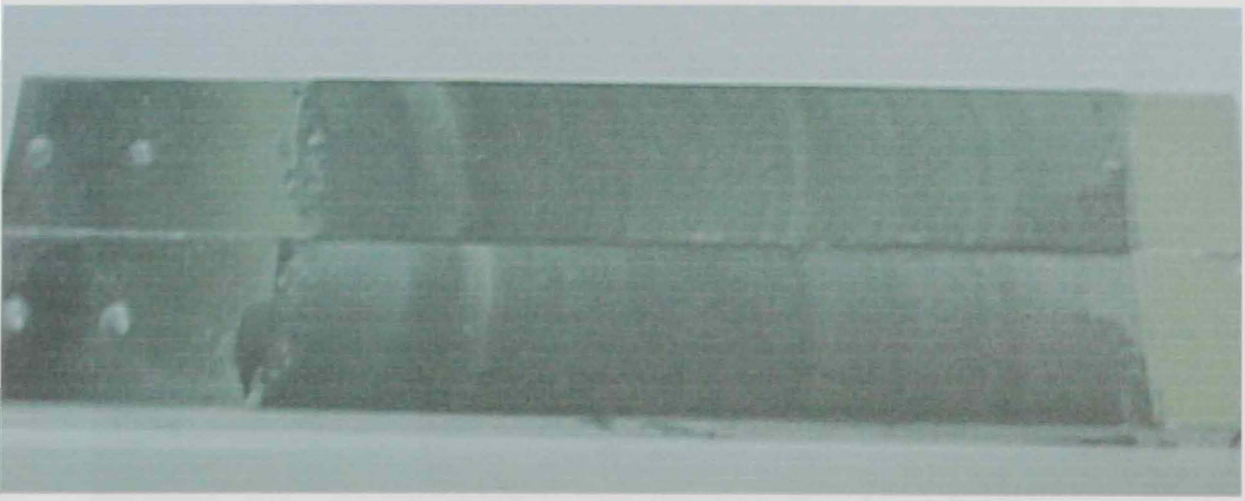

Figure 4.11: Photograph of typical appearance of fracture surface of DCB specimen

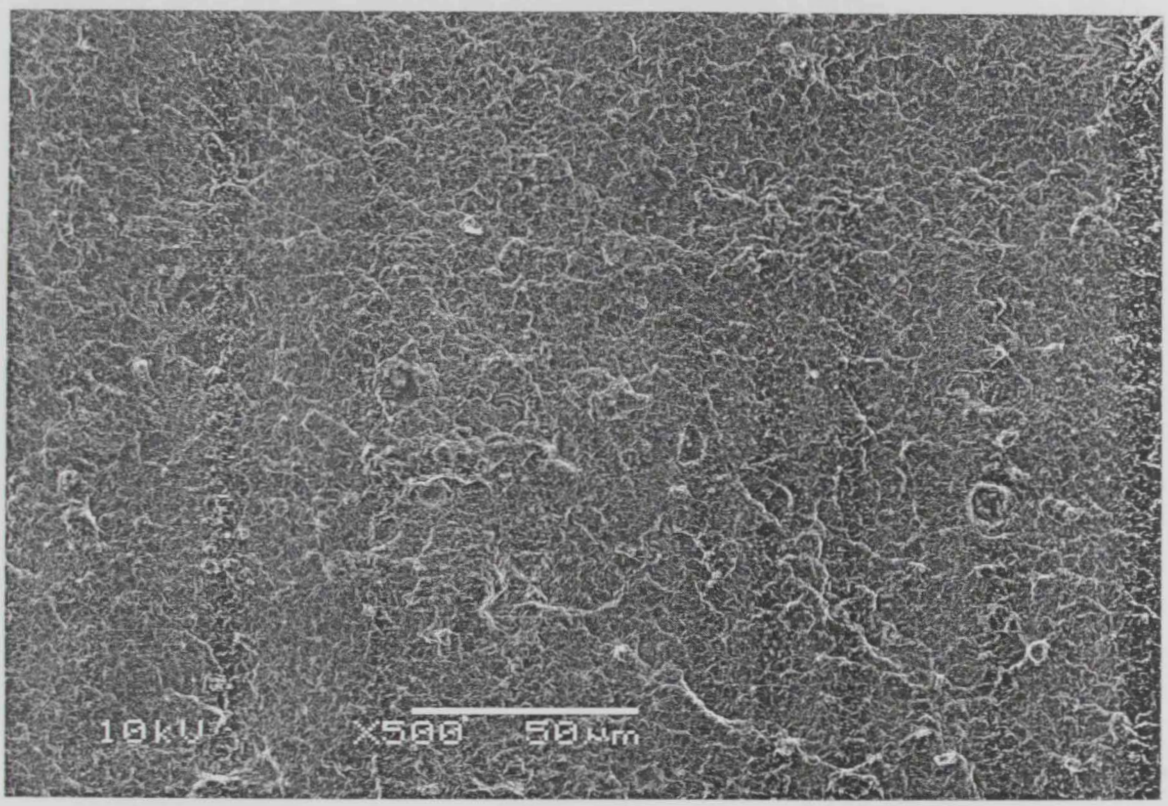

Figure 4.12: SEM picture of fracture surface for bond thickness (0.16 mm) at the initiation

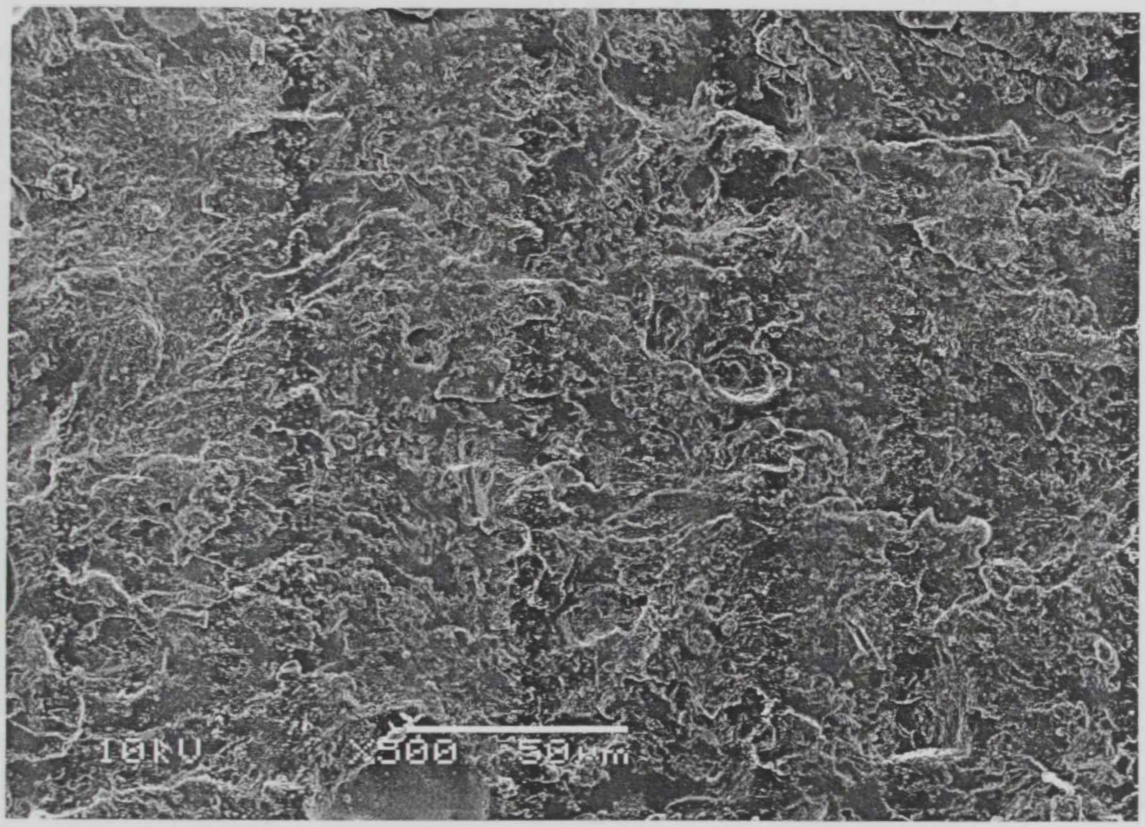

Figure 4.13: SEM picture of fracture surface for bond thickness (0.40 mm) at the initiation

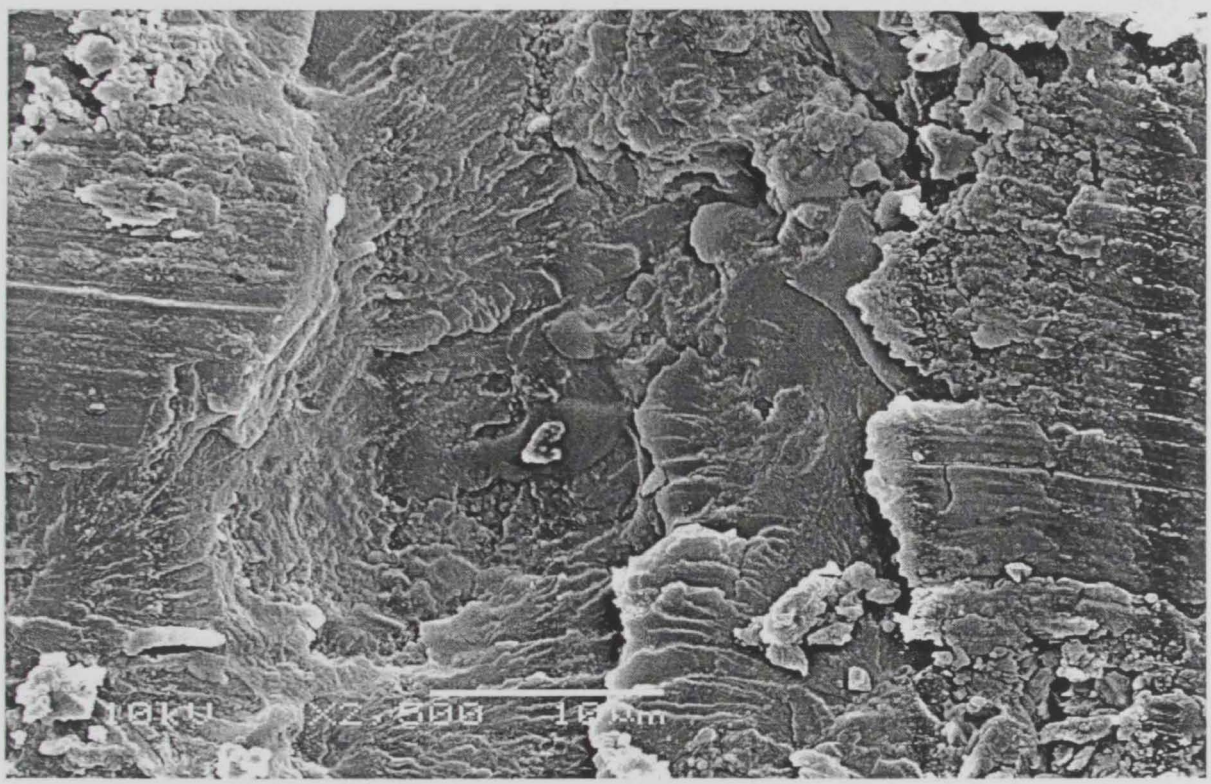

Figure 4.14: SEM picture of fracture surface at higher magnification

Results & Discussion

Part II: Constant Loads at Different Temperatures

This part will present and discuss the results obtained from experimental measurement of DCB specimens under mode I at three different temperatures (40°, 50°, and 60°C). The fracture energy of the joints as a function of bond thickness will be evaluated based on both simple beam and beam on elastic foundation analyses. The values of the two kinetic parameters of Paris' law that represent the crack propagation rate will be determined. An analytical approach will be developed to model the variation of the two kinetic parameters of Paris' law as a function of bond thickness and temperature. The analytical approach will be used to enable crack propagation to be modeled and hence the lifetime of adhesive joints to be predicted.

4.2.1 Fracture Energy of DCB Specimens

In order to determine the fracture energy of the DCB specimens under mode I, the specimens were loaded to failure with constant loads at 40°, 50°, and 60°C. The crack will propagate rapidly at a critical load, P_f, which corresponds to the load required to initiate rapid crack propagation. For each temperature, it is possible to determine the fracture energy or critical strain energy release rate, G_{IC}, by measuring P_f. The fracture energy of the DCB specimens was evaluated through both simple beam and for beam on elastic foundation analyses. The expression of fracture energy for both the simple beam and the beam on elastic foundation analyses was presented in the literature review by Eqs.2.14 and 2.15 respectively.

The results obtained for G_{IC} as a function of bond thickness at 40°, 50°, and 60°C are shown in Fig. 4.15 for both the simple beam and the beam on elastic foundation analyses. Both analyses show similar behavior but the values of G_{IC} in the beam on elastic foundation analysis are higher than those in the simple beam analysis that neglect the effect of bond thickness in evaluating the fracture energy of the DCB specimens. The results show the significant effect of adhesive bond thickness on fracture energy; and the model built using simple beam analysis underestimates the fracture energy of the adhesive joints.

All of the curves exhibit similar characteristics at the three different temperatures. For all temperatures, the data demonstrates that the fracture energy is relatively low at very low bond thicknesses. It increases with increasing thickness reaching a maximum value and then decreases. The maximum fracture energy is obtained at an optimum thickness.

The results show that the fracture energy of the DCB specimens is significantly lowered at the highest temperature. It is more useful to plot the fracture energy against temperature at the optimum thickness as shown in Fig. 4.16, which indicates that the fracture energy decreases with an increase in temperature for both simple beam and beam on elastic foundation analyses. It should be noticed that the optimum thickness corresponding to the maximum fracture energy increases with increasing temperature. This can be explained by considering that higher temperatures lower the yield strength of the adhesive and this gives rise to a large crack-tip deformation zone size because the size of this zone is inversely proportional to the yield strength of the adhesive. Also, it has been previously demonstrated that the ratio of the crack-tip deformation zone size to the bond thickness is an important factor for obtaining the maximum fracture energy for the adhesive joints [24]. As a result, the optimum thickness is increased. However, the optimum thickness is not a constant for all temperatures; it increases with increasing temperature, as shown in Fig. 4.17.

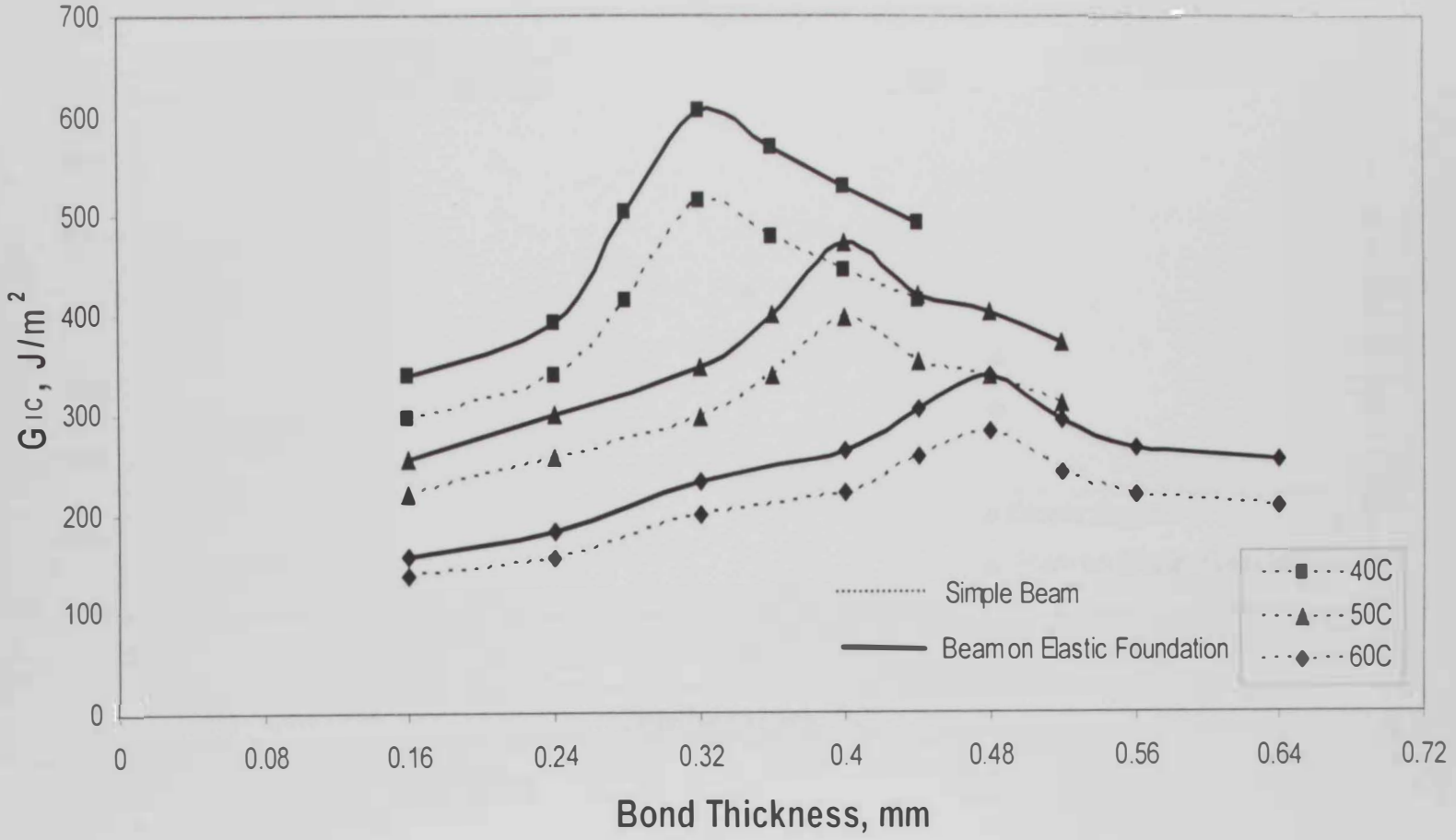

Figure 4.15: Fracture energy as a function of bond thickness under monotonic loads

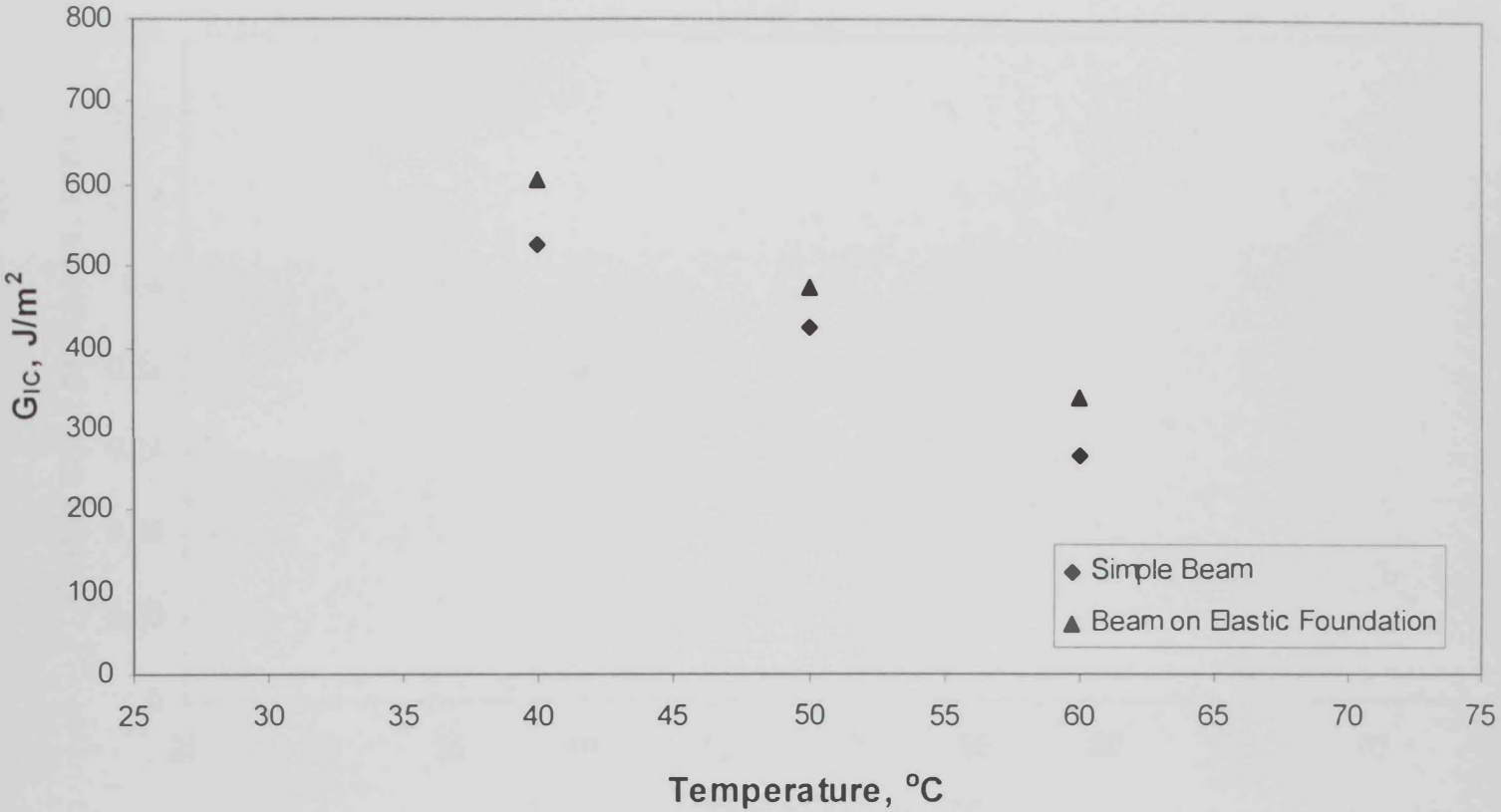

Figure 4.16: The relation between fracture energy and temperature for optimum thicknesses

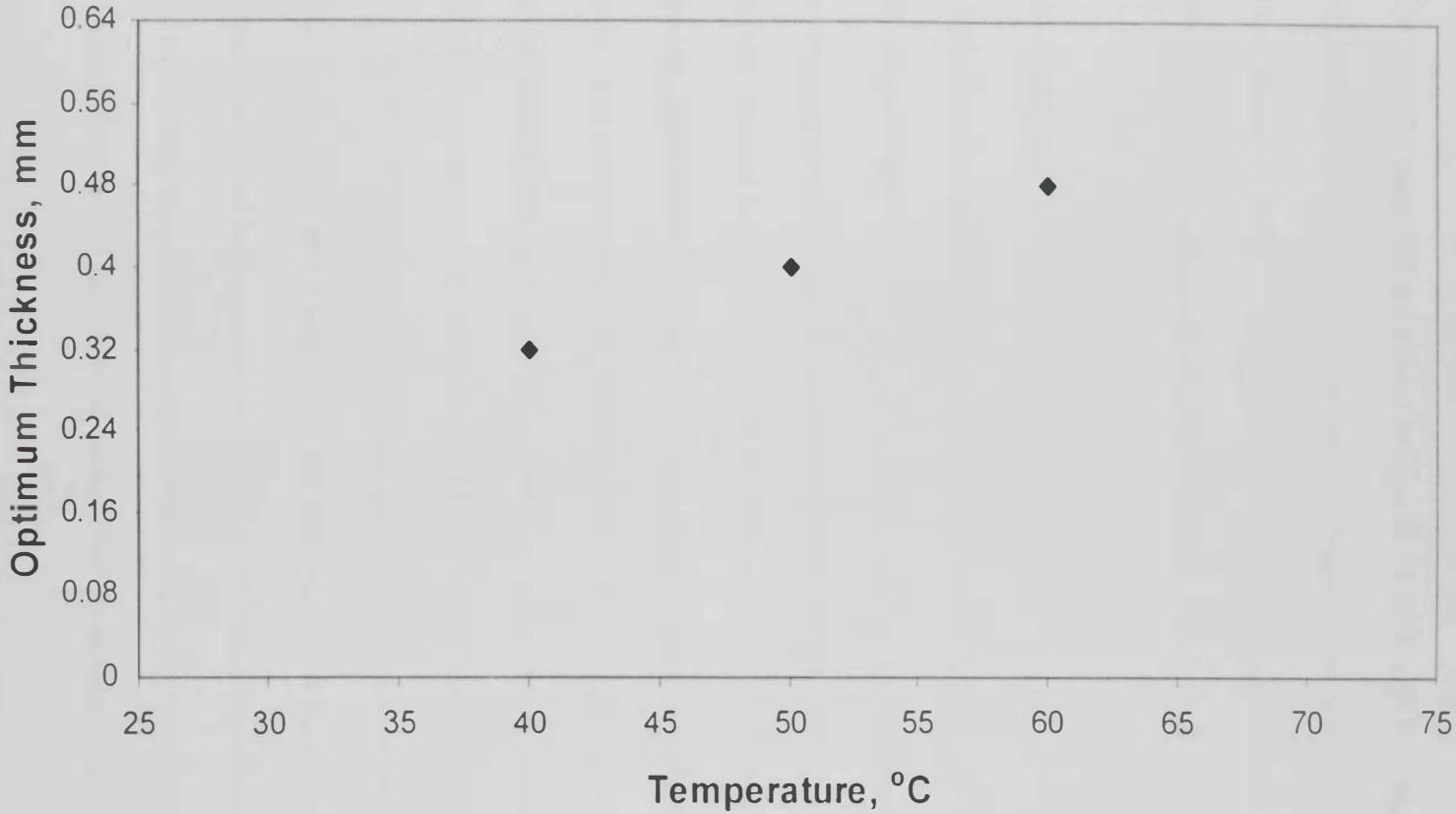

Figure 4.17: The relation between optimum thickness and temperature

4.2.2 Crack Propagation Length

The results of a typical load-point displacement as a function of time for different bond thicknesses at 40°, 50°, and 60°C are shown in Figs. 4.18, 4.19, and 4.20 respectively. The curves display the load-point displacement for the entire lifetime of the DCB specimens. As previously reported in the results of Part I of this study, the crack propagation length was determined as a function of the load-point displacement of both cantilevers using Eq.4.1.

4.2.3 Data Analysis

The typical behavior of crack length as a function of time at 40°, 50°, and 60°C is shown in Figs. 4.21, 4.22, and 4.23 respectively. Four distinctive zones can be distinguished in the curves of crack length. These zones may be a characteristic that is representative for all cases. The first zone starts after application of the constant load, and it may be represented by an instantaneous jump followed by the onse of time-dependent displacement. The instantaneous displacement corresponds to the elastic deflection of both cantilevers. The second zone starts with the onset of time-dependent displacement, and it reflects th beginning of the damage process at the crack tip leading to the initiation of crack propagation. The third zone corresponds to stable crack propagation, and it constitutes the greater part of the curve. The fourth zone shows asymptotic increase of the deflection, and it is indicative of unstable crack propagation. In th zone, the specimen was completely separated. All curves of crack length as a function of time for differe bond thicknesses at different temperatures look similar and can be described by an empirical relationship of the form of Eq.4.2 that was presented in the results of Part I of this study, and it was used to obtain the rate of crack propagation, da/dt, as a function of the crack propagation length, a.

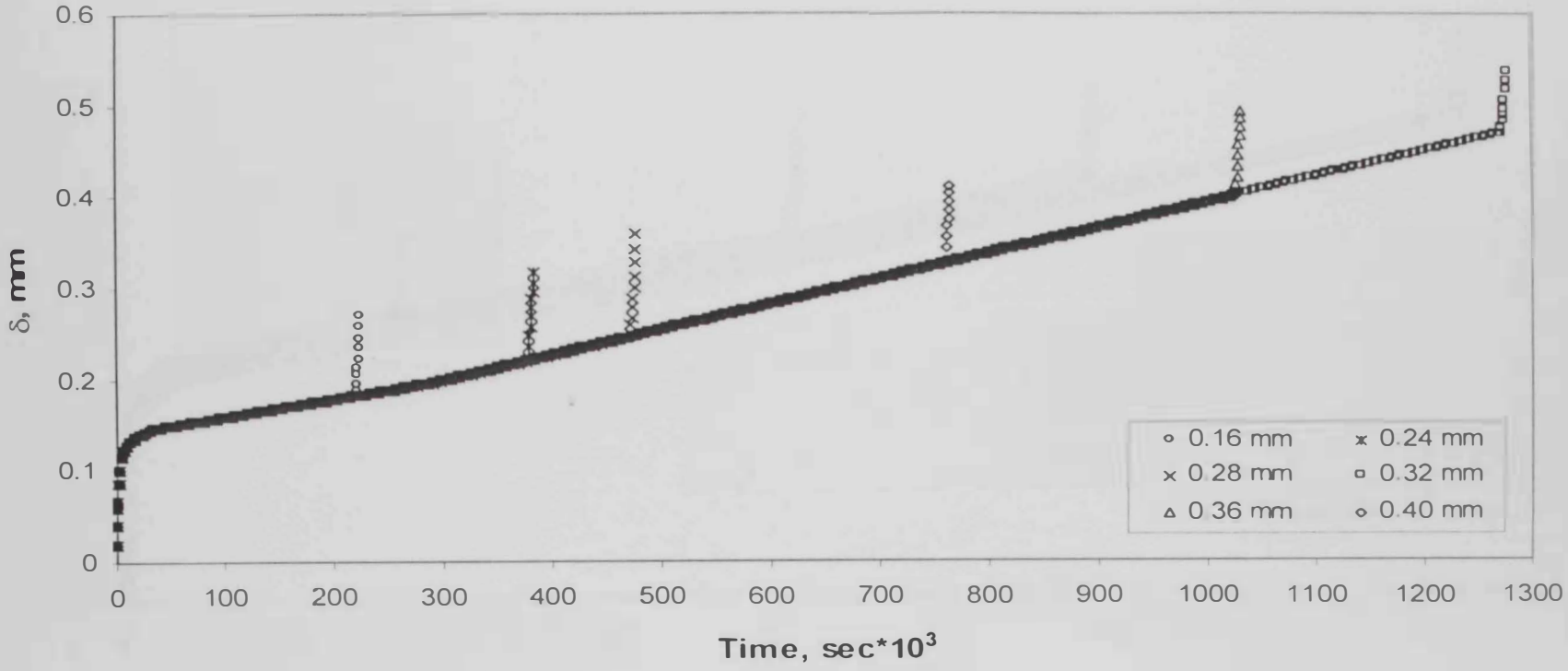

Figure 4.18: Typical load-point displacement curve as a function of time at 40°C

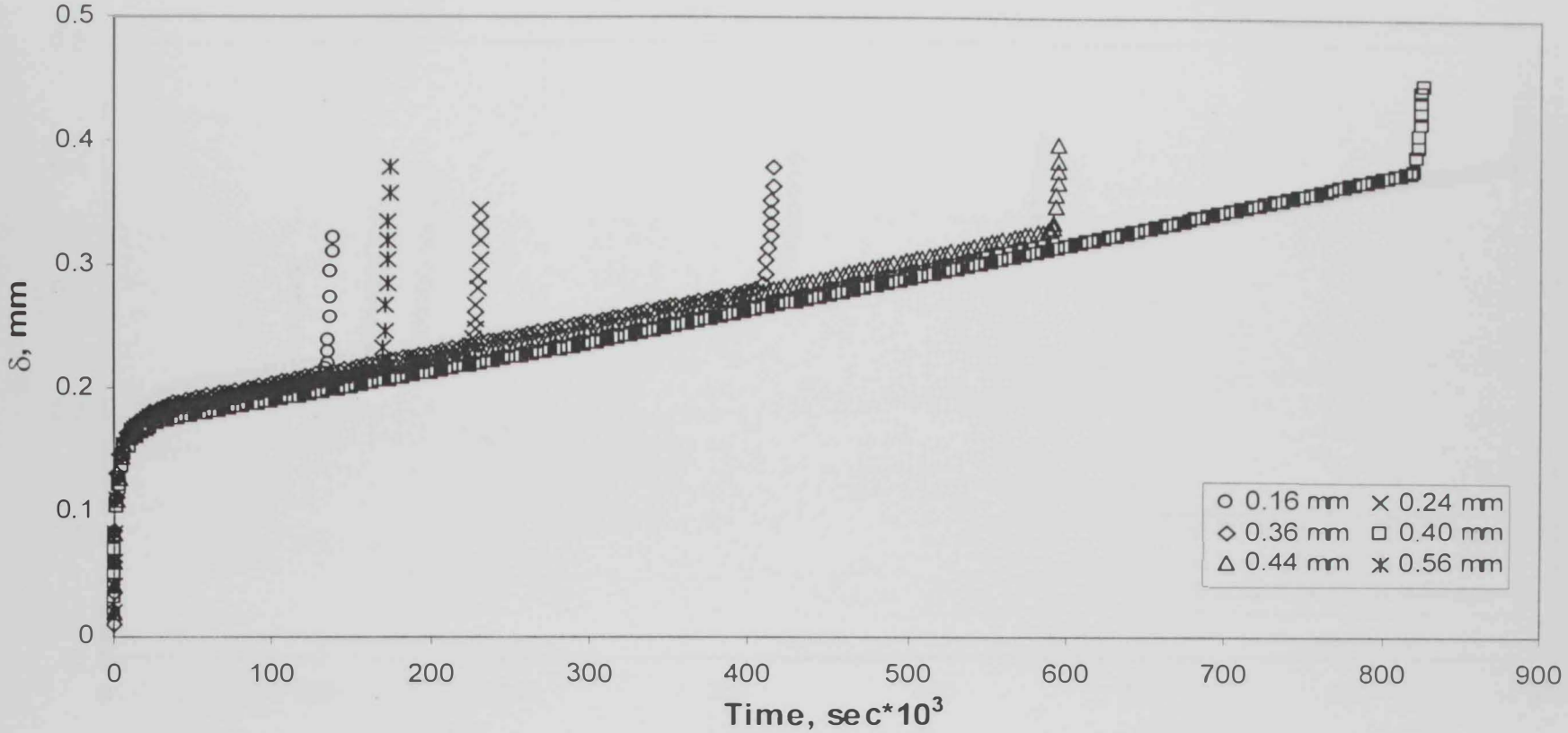

Figure 4.19: Typical load-point displacement curve as a function of time at 50°C

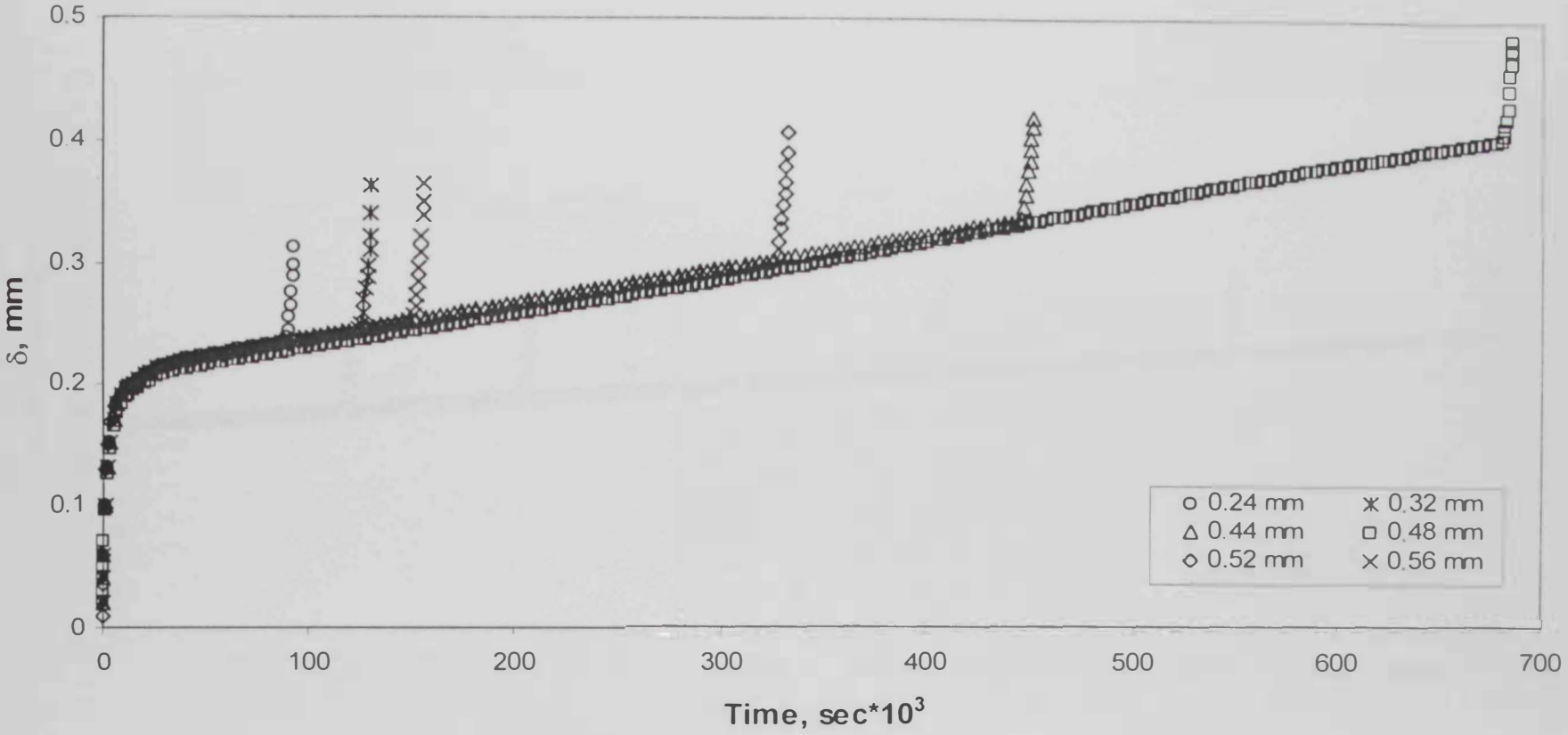

Figure 4.20: Typical load-point displacement curve as a function of time at 60°C

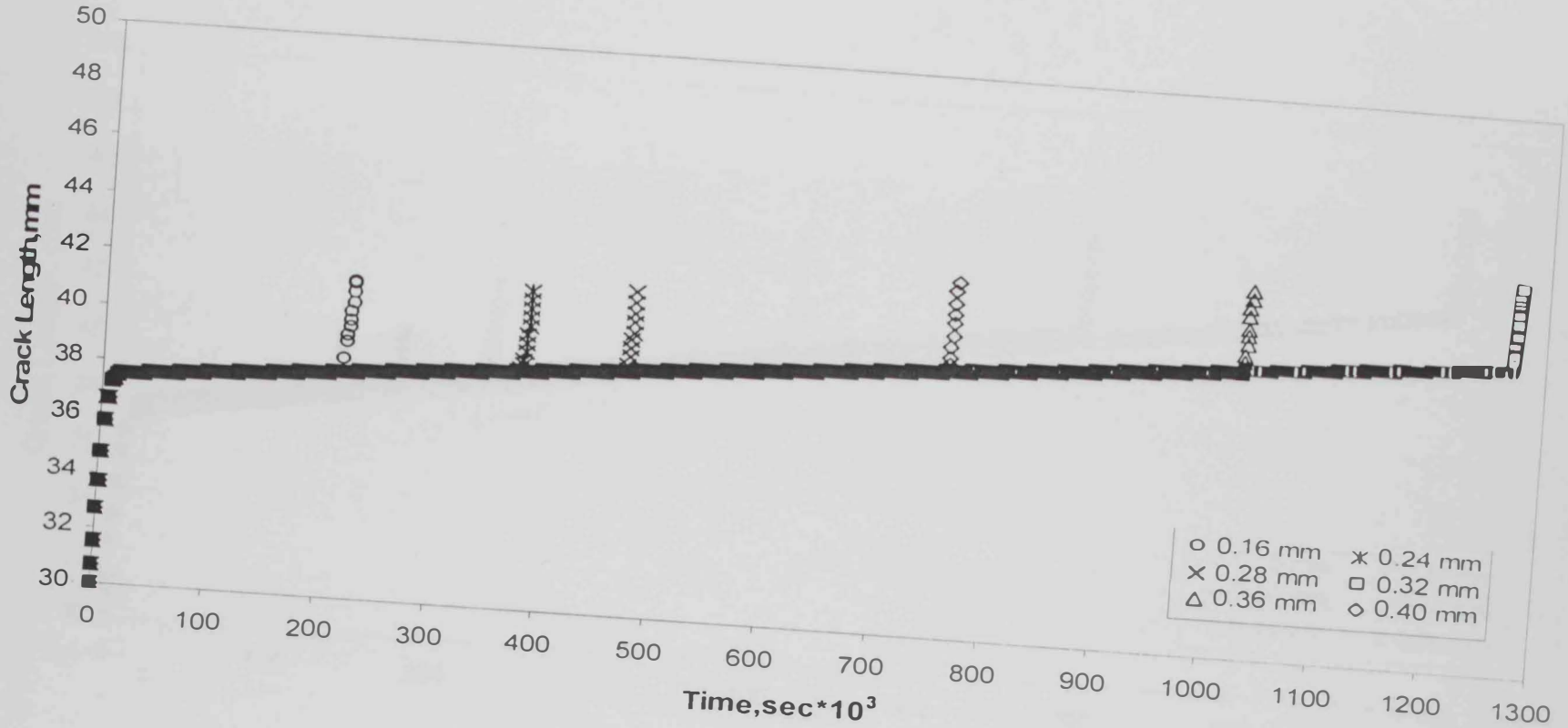

Figure 4.21: Typical crack propagation length as a function of time at 40°C

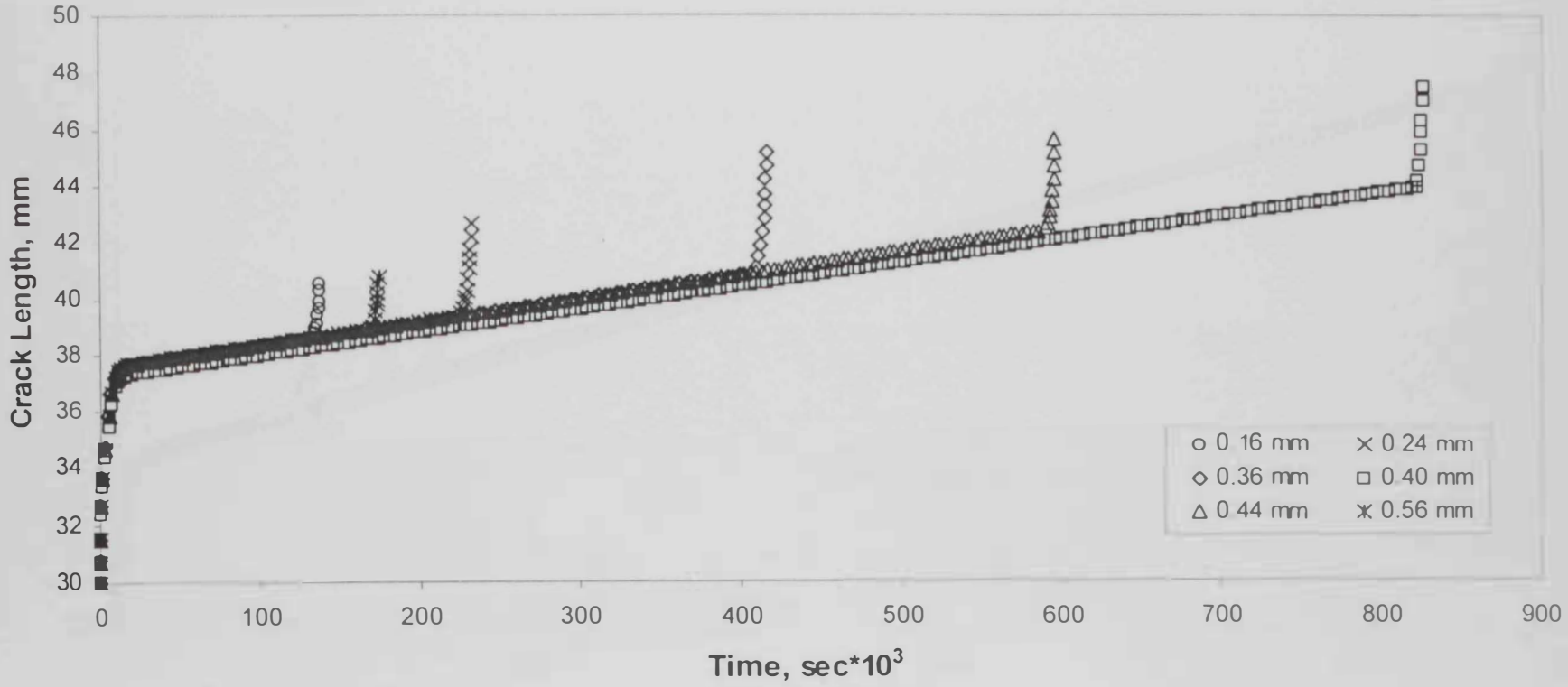

Figure 4.22: Typical crack propagation length as a function of time at 50°C

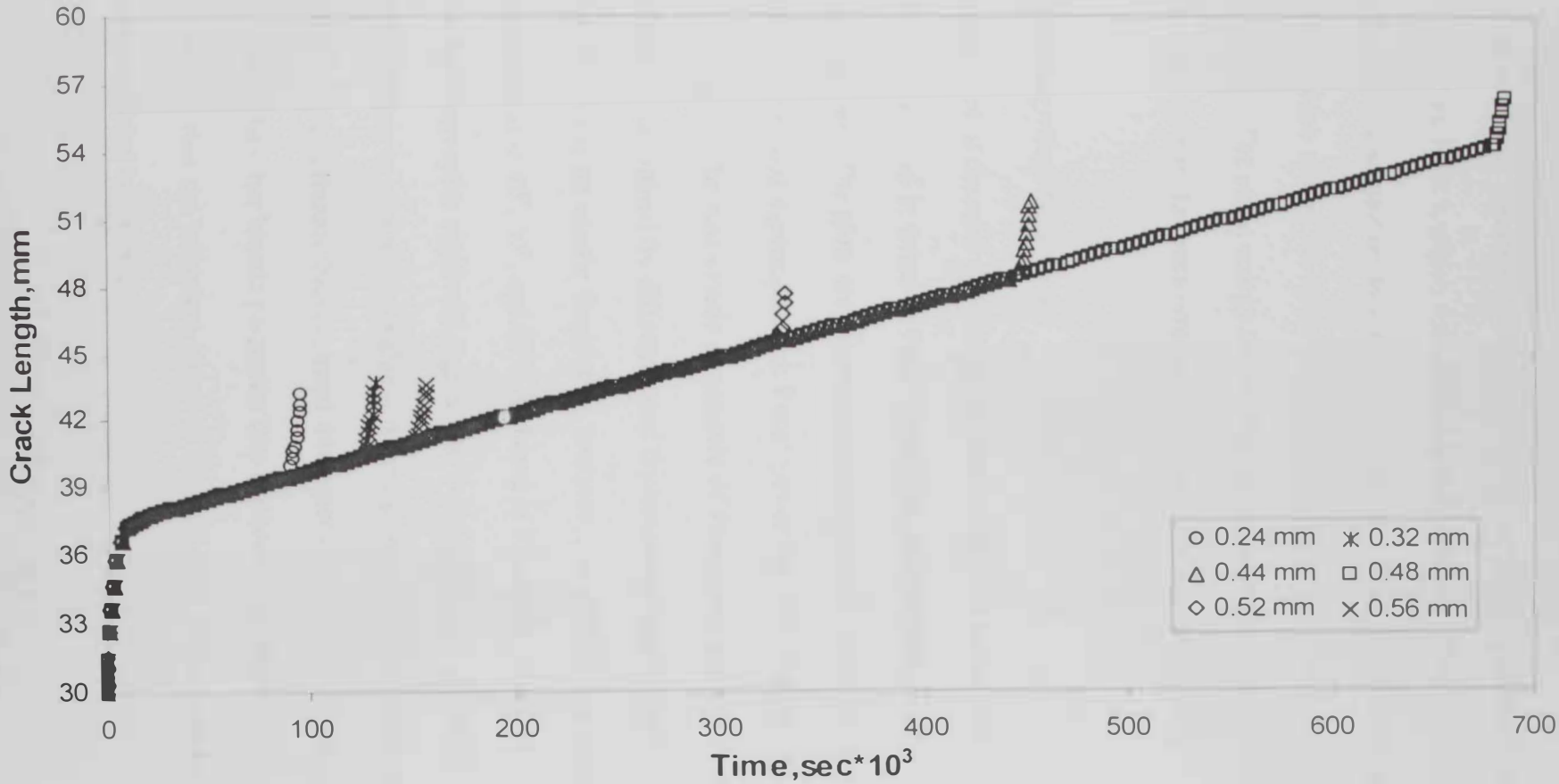

Figure 4.23: Typical crack propagation length as a function of time at 60°C

The simplest and most commonly used formulation for the rate of crack propagation is Paris' power law equation, Eq.4.3, which was presented in the results of Part I. Accordingly, the rate of crack propagation was plotted as a function of strain energy release rate in accordance with Paris' equation, which relates the kinetics of crack propagation to the associated change in the energy of the system. The strain energy release rate can be considered as a fracture parameter that can be used to characterize the crack propagation behavior in adhesive joints.

4.2.4 Crack Propagation Kinetics

A logarithmic plot of the rates of crack propagation versus the strain energy release rate at 40°, 50°, and 60°C was plotted in terms of Paris' power law in both simple beam and beam on elastic foundation analyses. The plots are shown in Figs. 4.24, 4.25, and 4.26 respectively. The behavior appears to be in good agreement with Paris' power law. The results showed a similar behavior in each analysis. The two kinetic parameters of Paris' law that determine the rate of crack propagation were determined for different bond thicknesses at each temperature in both the simple beam and the beam on elastic foundation analyses. A plot of the intercept, A, as a function of bond thickness at 40°, 50°, and 60°C is shown in Fig. 4.27. The plot indicates that at each temperature, the intercept is relatively high at low bond thickness. Then, it decreases with increasing thickness falling to a minimum value and then increases. The minimum value of the intercept is obtained at an optimum thickness and this agrees with the idea that lower intercept means longer lifetime. The other kinetic parameter (the exponent), m, displays the same behavior as the intercept, namely that the minimum value of the exponent is also obtained at the same optimum thickness as shown in Fig. 4.28.

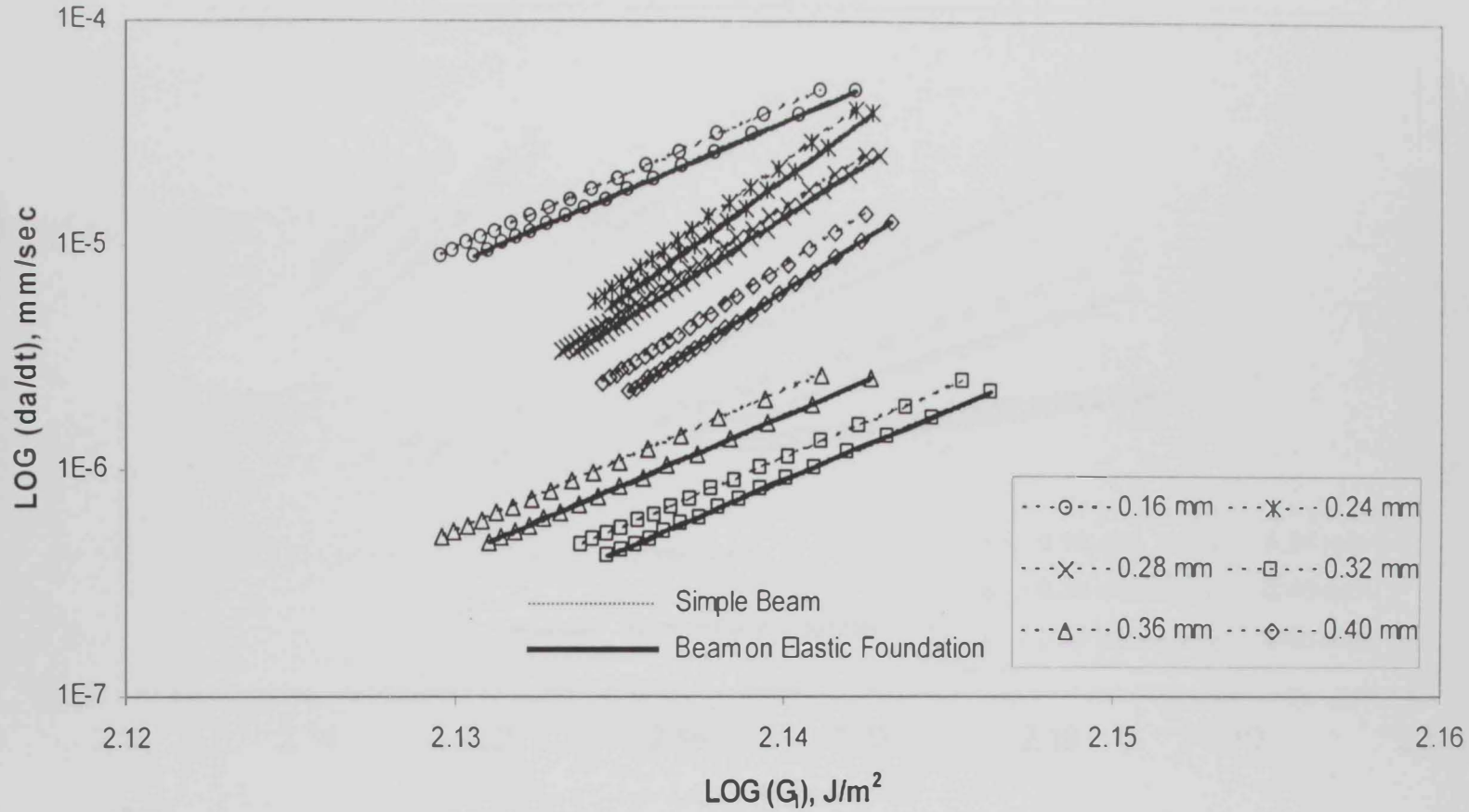

Figure 4.24: Paris plots for crack propagation at 40°C

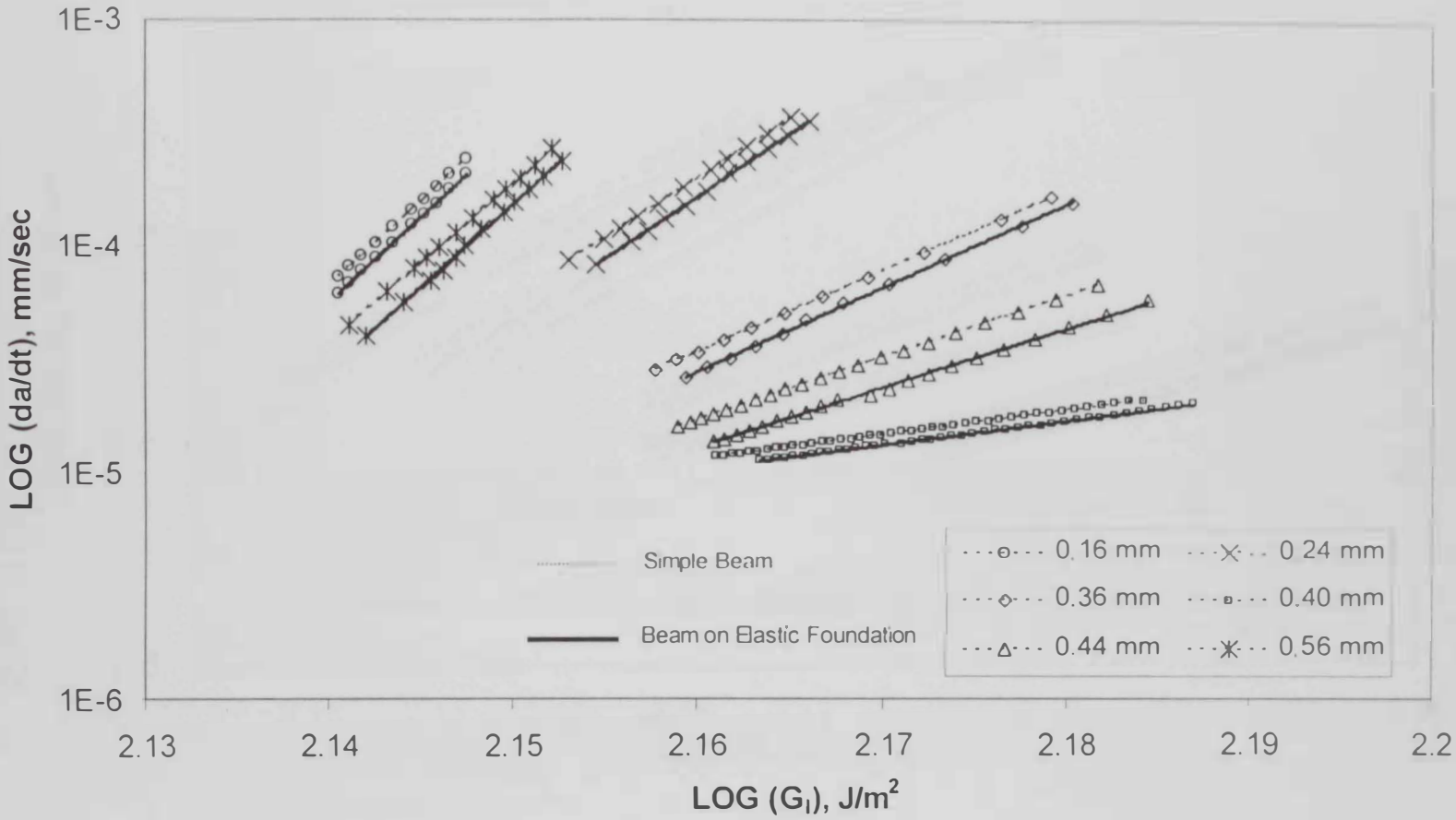

Figure 4.25: Paris plots for crack propagation at 50°C

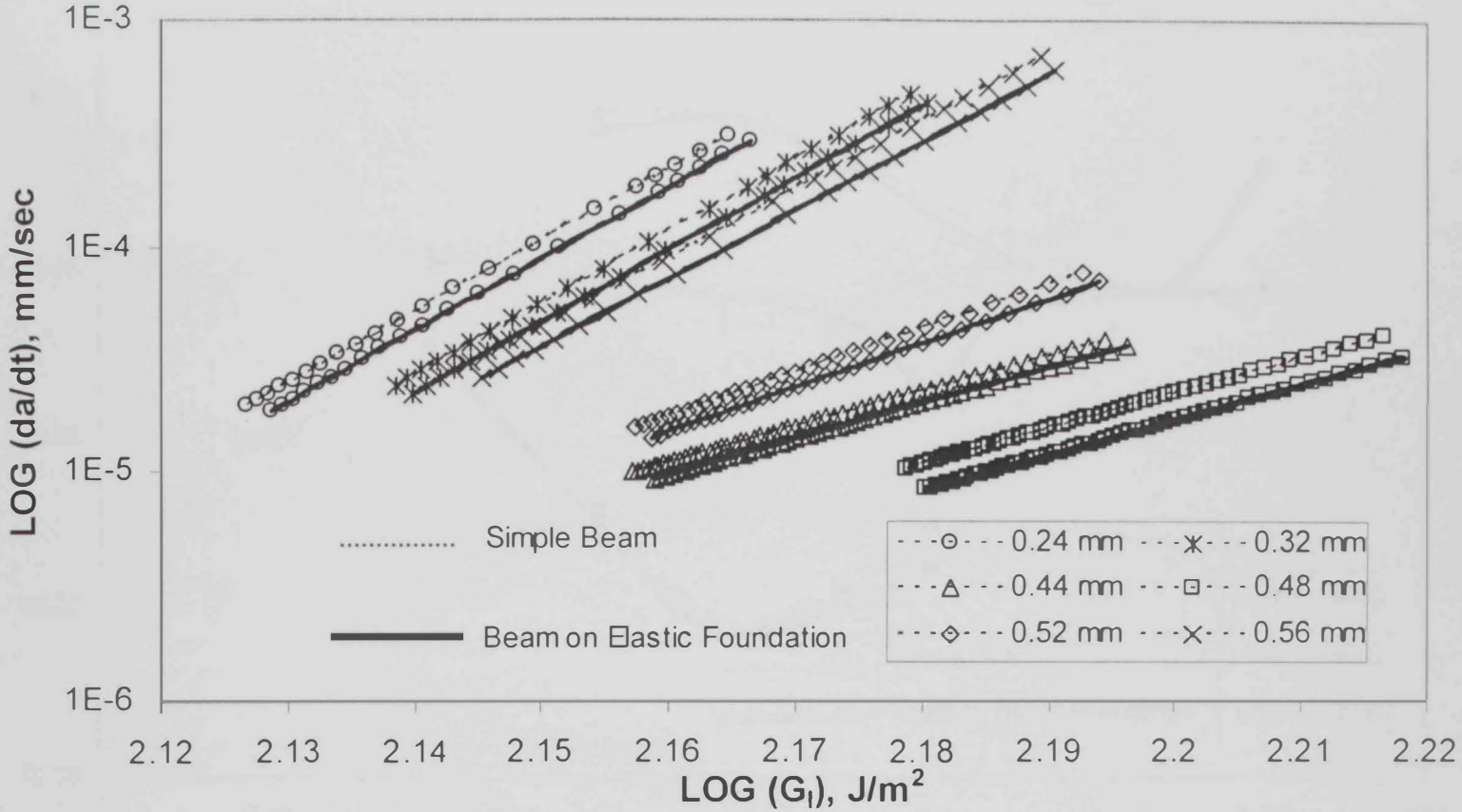

Figure 4.26: Paris plots for crack propagation at 60°C

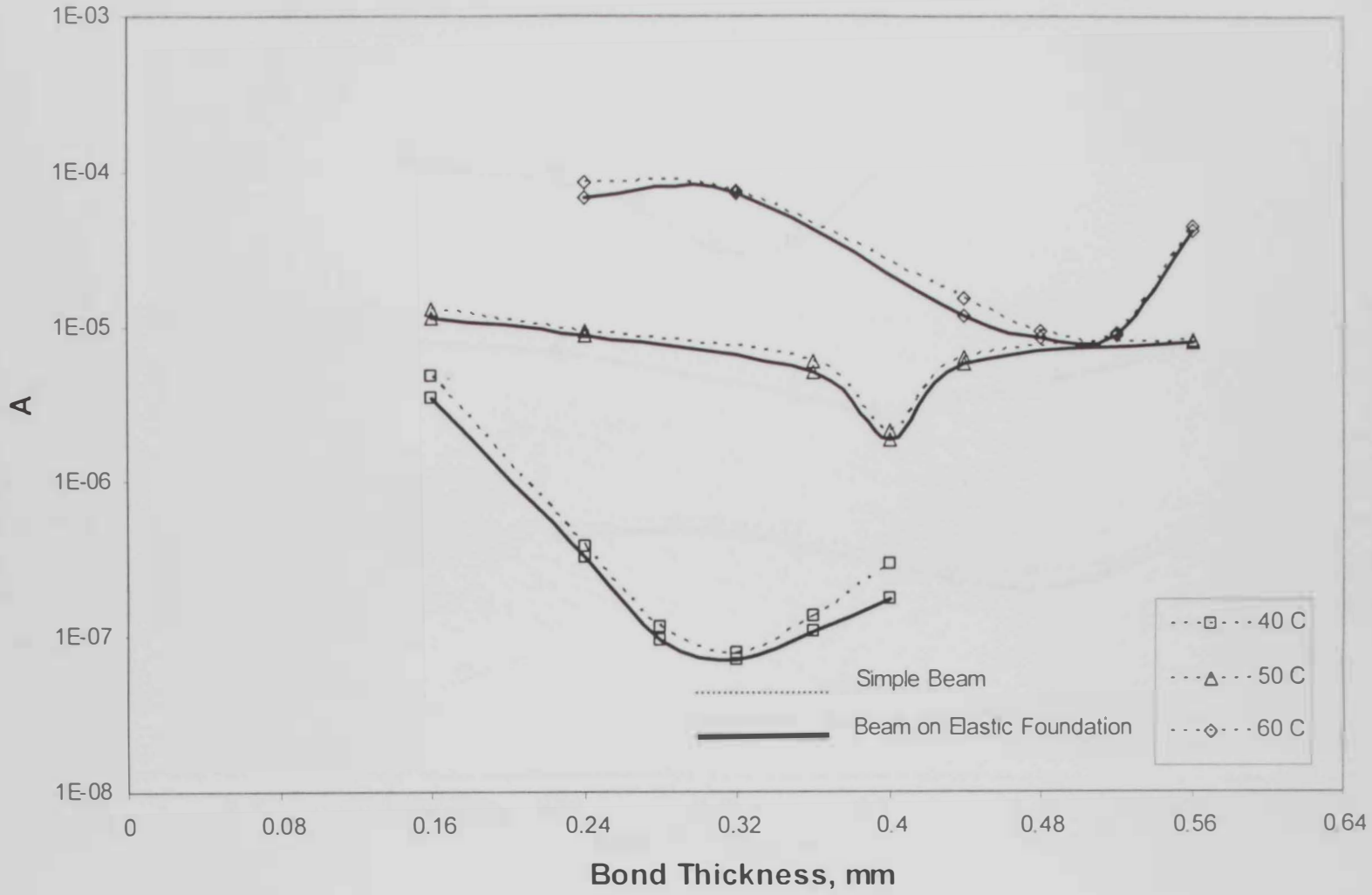

Figure 4.27: Paris kinetic parameter, A, as a function of bond thickness

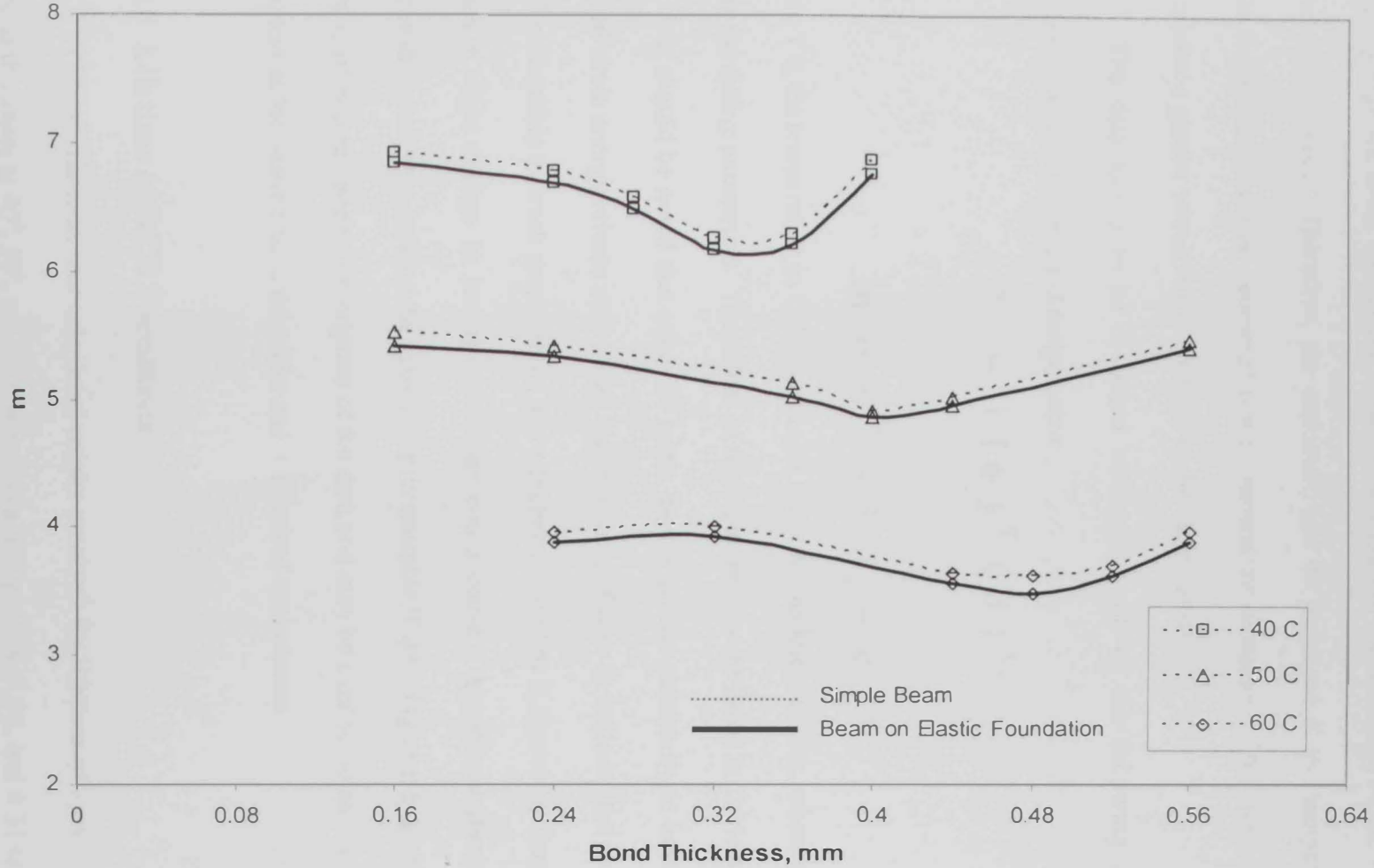

Figure 4.28: Paris kinetic parameter, m, as a function of bond thickness

It should be noted that the values of the exponent, m, for polymeric adhesives are relatively high for lower temperatures, while the values of the intercept, A, are relatively low for lower temperatures. Therefore, the exponent will be increased if the temperature decreases, while the intercept will be decreased if the temperature decreases. This indicates that adhesive joints have a greater sensitivity to changes in the temperature.

The data appear to be described reasonably well by the following expressions as a function of bond thickness and temperature:

$$A = c(a)^{T}(b)^{t_a} \tag{4.6}$$

and

$$m = a'T + b't_a + c' \tag{4.7}$$

where T is the temperature in Celsius and t_a is the bond thickness in mm, where a, b, c, a', b', and c' are the fitting parameters. The values of these parameters are listed in Table 4.3.

It should be noted that adhesive joints have a greater sensitivity to small changes in the applied strain energy release rate. Also, higher values of A or m indicate that an adhesive joint is more susceptible to crack propagation; and a higher value of m is especially dangerous because it means a slight change in testing conditions could cause a significant increase in the crack propagation rate, thus making the system highly unstable if cracking ever begins. Eqs.4.6 and 4.7 seem to offer a reasonable description of the data and may be used to obtain the intercept and the exponent at the desired bond thickness and the desired temperature.

4.2.5 Lifetime of DCB Specimens

The experimental and calculated results obtained for lifetime of specimens as a function of bond thickness at 40°, 50°, and 60°C are shown in Figs.4.29, 4.30, and 4.31 respectively.

Table 4.3: Values of fitting parameters of Eqs.4.6 and 4.7

Fitting Parameters	Simple Beam	Beam on Elastic Foundation
a	1.302	1.326
b	0.0052	0.0305
c	4.497E-11	7.093E-12
a'	-0.135	-0.135
b'	-0.698	-0.728
c'	12.235	12.147

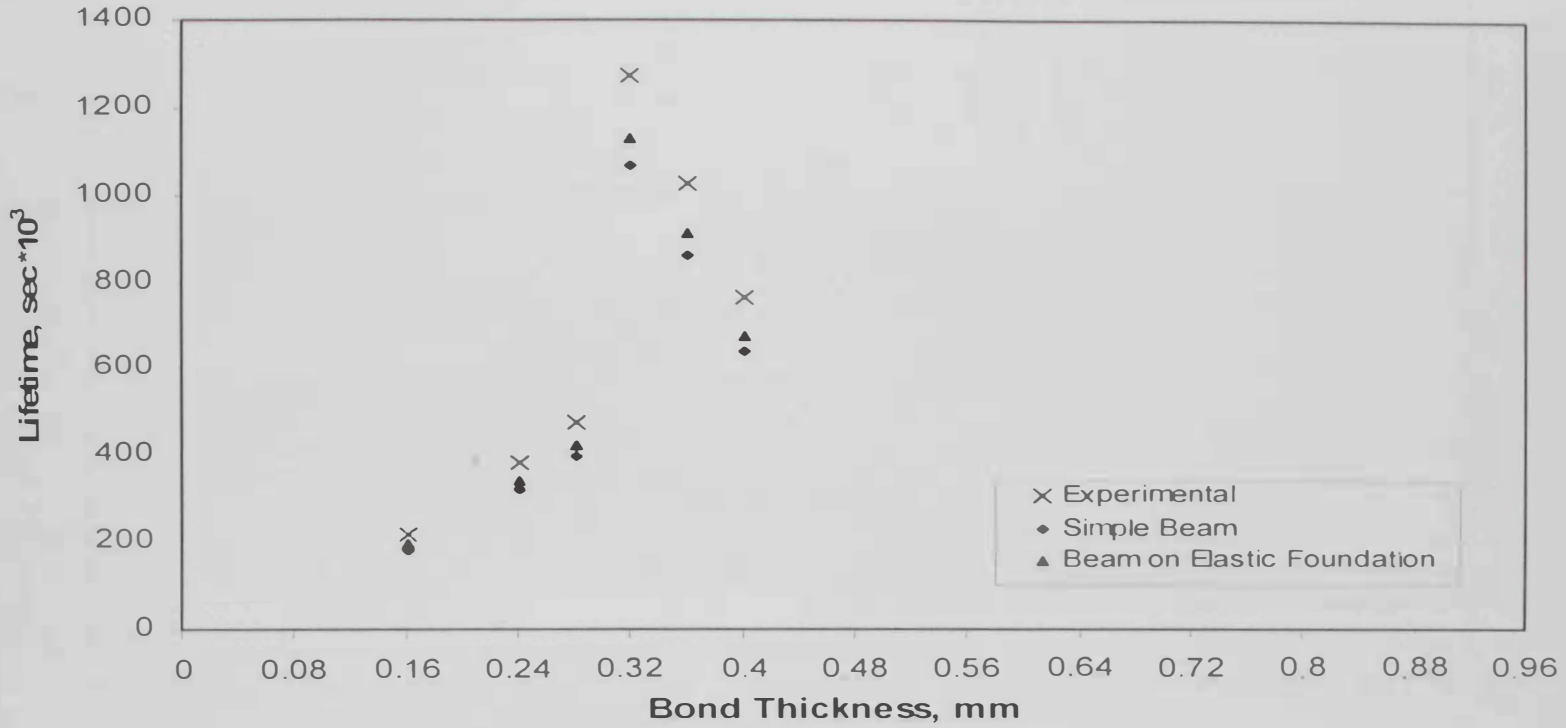

Figure 4.29: Lifetime as a function of bond thickness at 40°C

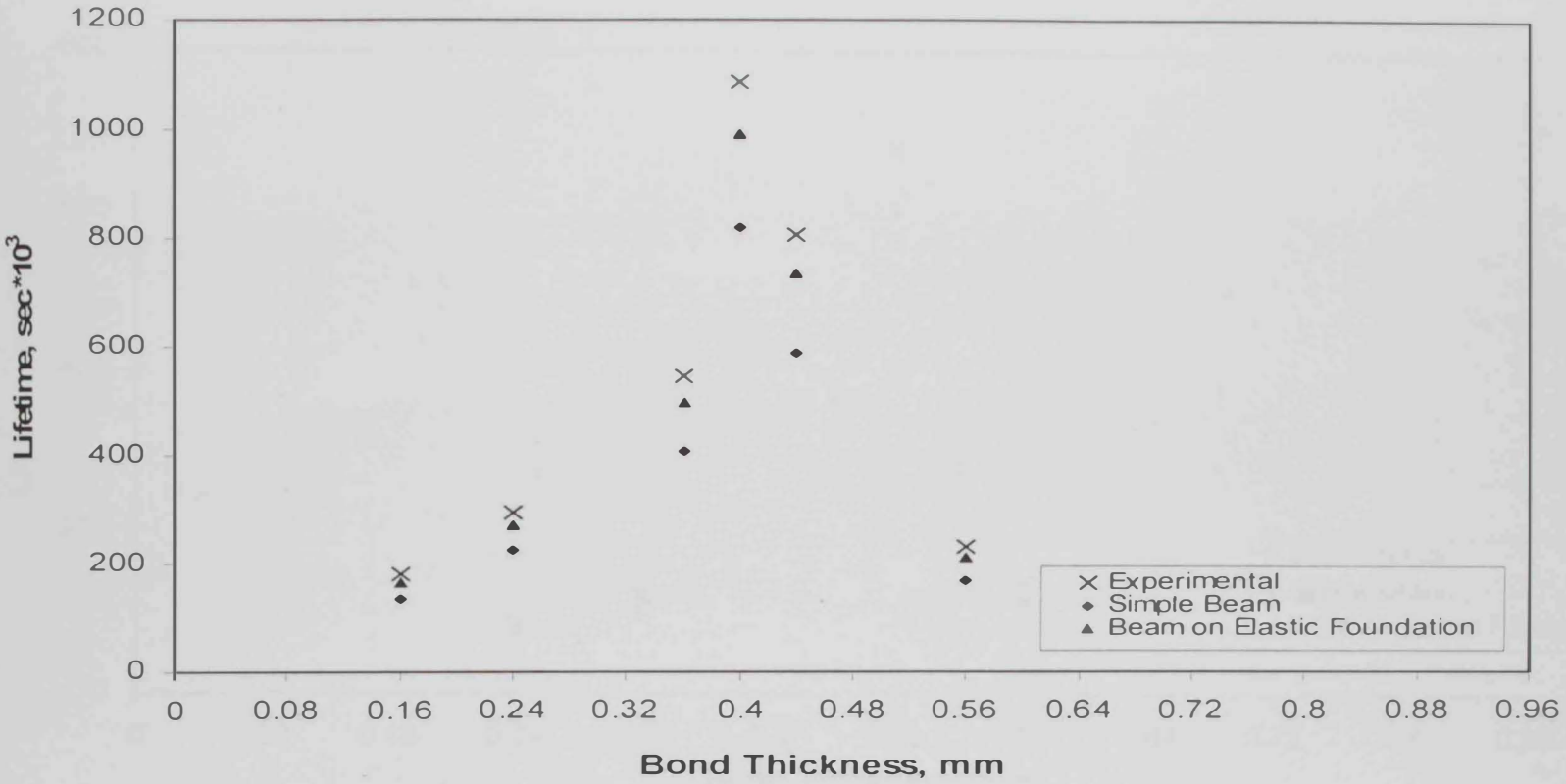

Figure 4.30: Lifetime as a function of bond thickness at 50°C

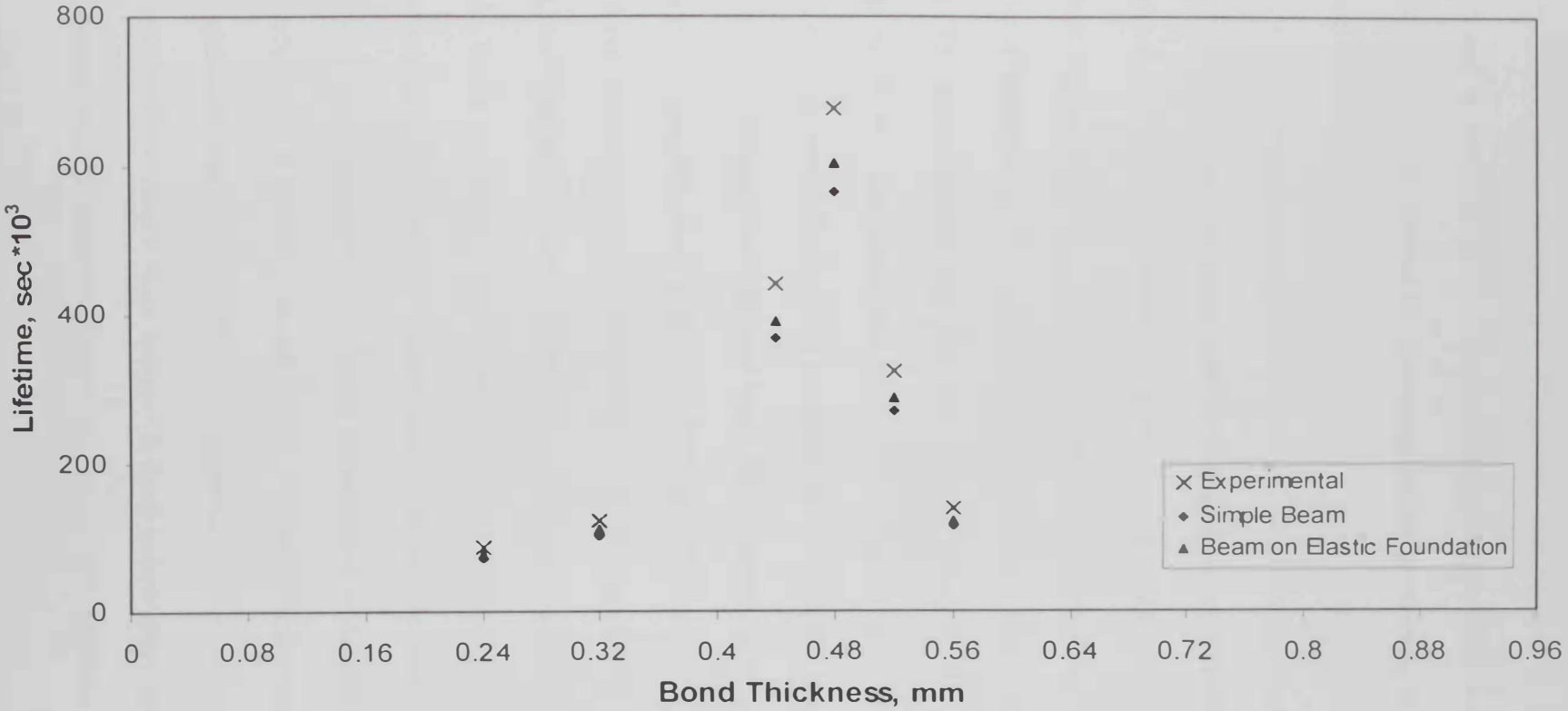

Figure 4.31: Lifetime as a function of bond thickness at 60°C

All curves display the same behavior. They show that lifetime is relatively low at low bond thicknesses and it increases with increasing thickness reaching a maximum and then decreases. A longer lifetime is obtained by decreasing the temperature at an optimum thickness and this optimum thickness differs with changes in temperature. However, the optimum thickness increases if the temperature is increased. Also, both the maximum lifetime and the maximum fracture energy occur at the same optimum thickness for each temperature.

An analytical approach was developed which would enable crack propagation to be modeled and hence lifetime of adhesive joints to be predicted. Therefore, Eqs.4.6 and 4.7 were used to model the variation of the two kinetic parameters of Paris' law with the bond thickness and temperature. This analytical approach was used to predict the lifetime of a typical specimen subjected to the same test conditions but with different bond thickness and at different temperatures. In order to verify the previous relations and to compare the predictions and the experimental results for lifetime, two different bond thicknesses of a typical DCB joint were subjected to the same applying load, each at a different temperature: the first had a bond thickness of 0.20 mm and was tested at room temperature; the second had a bond thickness of 0.28 mm and had tested at 35°C. These two different conditions were not used in describing the analytical model. Table 4.4 compares the lifetimes of the DCB joints determined within the propagation stage experimentally and analytically using both simple beam and beam on elastic foundation analyses. The agreement between the experimental and analytical results in both analyses is relatively good. It should be noted that the lifetime is underestimated by about 11% in the beam on elastic foundation analysis and this underestimation increases in the simple beam analysis to about 16%. Thus, simple beam analysis is more conservative because it neglects the effect of bond thickness in the calculation of the strain energy release rate for DCB specimens.

Table 4.4: Experimental and analytical values of lifetimes of DCB specimens

Temperature (°C)	Bond Thickness (mm)	Lifetime(Sec) (Experiment)	Lifetime(Sec) (Simple Beam)	% Error	Lifetime(Sec) (Beam on Elastic Foundation)	% Error
23±1	0.20	3007362	2512697	16.45	2694371	10.41
35±1	0.28	1958637	1652743	15.62	1743521	10.98

Therefore, it is better to use the beam on elastic foundation analysis in calculating the strain energy release rate and hence for predicting the lifetime of the DCB specimens. At this point, it must be pointed out that the predictions based on the analyses presented above are conservative because these analyses do not account for initiation time, which could be a significant fraction of the total service lifetime. Furthermore, the length of crack propagation that is considered critical to the joint can be determined from Eq.2.14.

4.2.6 Fracture Surface Inspection

Mechanistic observations were obtained by SEM examination of the fracture surfaces after complete separation of the specimen. As previously mentioned, the epoxy polymer exhibits distinct deformation markings in the region of crack initiation [53]. The appearance of the fracture surfaces for the various temperatures showed that no significant differences were noted among the fracture surfaces of different bond thicknesses except that at the lower temperature, the deformation marks were observed in very small regions at the crack initiation. Inspection of fracture surfaces by SEM showed more deformation marks at the crack tip at the higher temperature but no systematic patterns. Figures 4.32, 4.33, and 4.34 showed the fracture surfaces in SEM at 40°, 50°, and 60°C respectively. These figures clearly showed more deformation marks when the temperature is increased. Therefore, the tendency to develop more deformation markings increases with further increase in temperature.

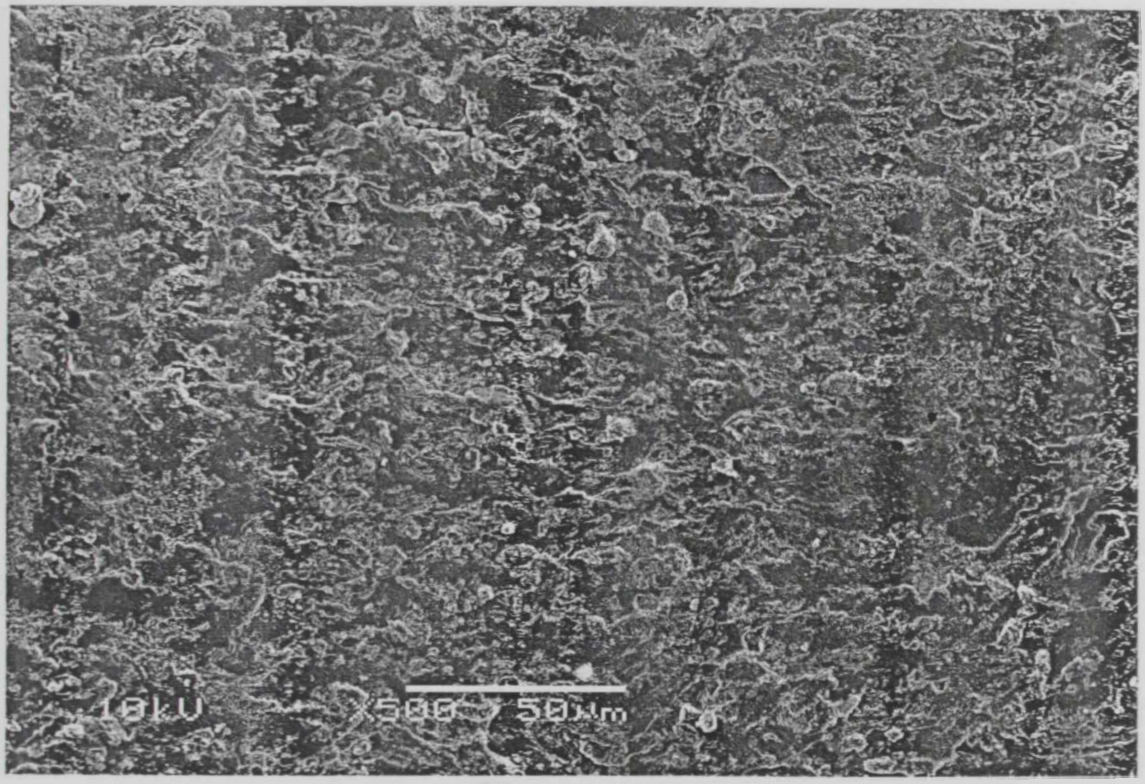

Figure 4.32: SEM picture of fracture surface at 40°C

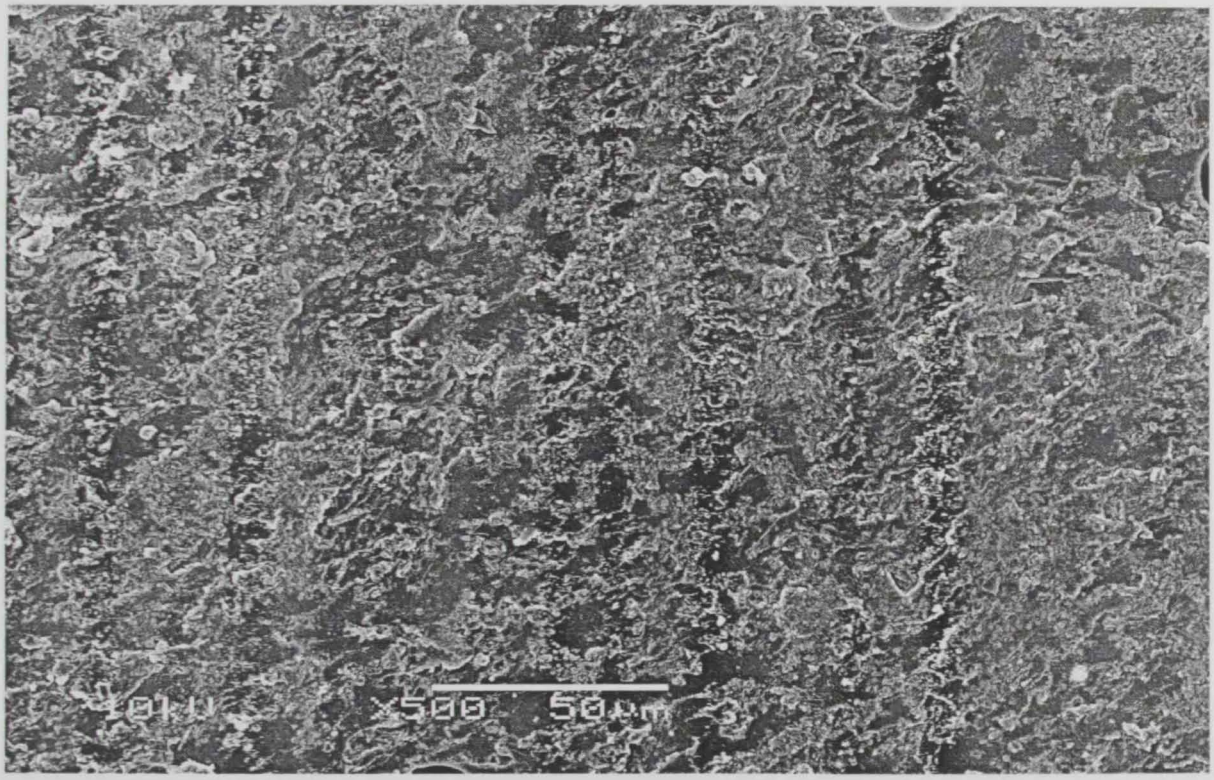

Figure 4.33: SEM picture of fracture surface at 50°C

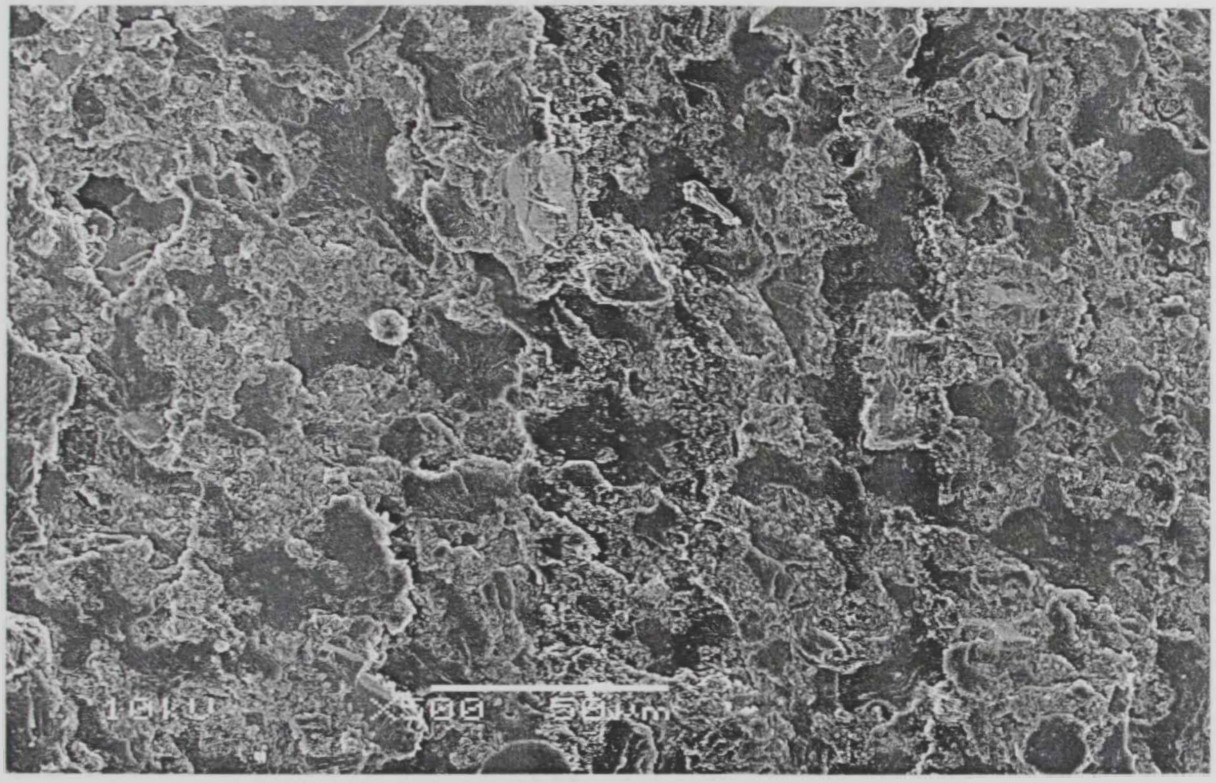

Figure 4.34: SEM picture of fracture surface at 60°C

Results & Discussion

Part III: Different Loads at Constant Temperature

This part will present and discuss the effect of applied constant loads on the lifetime of the DCB specimens at various bond thicknesses. The values of the two kinetic parameters of Paris' law which represent the crack propagation rate will be determined.

4.3.1 Crack Propagation Length

Double cantilever beam (DCB) specimens were tested at three different constant loads (60%, 70%, and 80%) of their static failure loads at 50°C. As previously reported in Parts I and II of this study, the load-point displacement was determined as a function of time for different bond thicknesses for the entire lifetime of the DCB specimens. Then, the crack propagation length was determined as a function of the load-point displacement of both cantilevers using Eq.4.1 in Part I of this study.

4.3.2 Data Analysis

Equation 4.2 in Part I of this study was used to obtain the rate of crack propagation as a function of the crack propagation length. Accordingly, the rate of crack propagation was plotted as a function of strain energy release rate in accordance with Paris' equation (Eq.4.3). The strain energy release rate was determined for DCB specimens by both simple beam and beam on elastic foundation analyses.

4.3.3 Crack Propagation Kinetics

A logarithmic plot of the rates of crack propagation versus the strain energy release rate under the three different loading conditions was plotted in terms of Paris' power law. The two kinetic parameters of Paris' law were determined for different bond thicknesses at each loading condition by both simple beam and beam on elastic foundation analyses. A plot of the intercept, A, as a function of bond thickness for both simple beam and beam on elastic foundation analyses, as shown in Figs. 4.35 and 4.36 respectively, indicates that the intercept at any loading condition is relatively high at low bond thicknesses. It decreases with increasing thickness falling to a minimum and then increases. The minimum value of the intercept is obtained at the optimum thickness and this agrees with the idea that a lower intercept means a longer lifetime. The other kinetic parameter, m, displays the same behavior of the intercept for both simple beam and beam on elastic foundation analyses, as shown in Figs. 4.37 and 4.38 respectively, namely that the minimum value of the exponent is also obtained at the same optimum thickness.

It should be mentioned that the values of the two kinetic parameters of Paris' law obtained by the beam on elastic foundation analysis are lower than those obtained by the simple beam analysis. It should also be noted that the values of the intercept for polymeric adhesives are relatively high for higher loading conditions, which means that the intercept will be increased if the applying loads are increased. The other kinetic parameter, the exponent, displays the same behavior of the intercept. This indicates that adhesive joints have a greater sensitivity to changes in the applying loads.

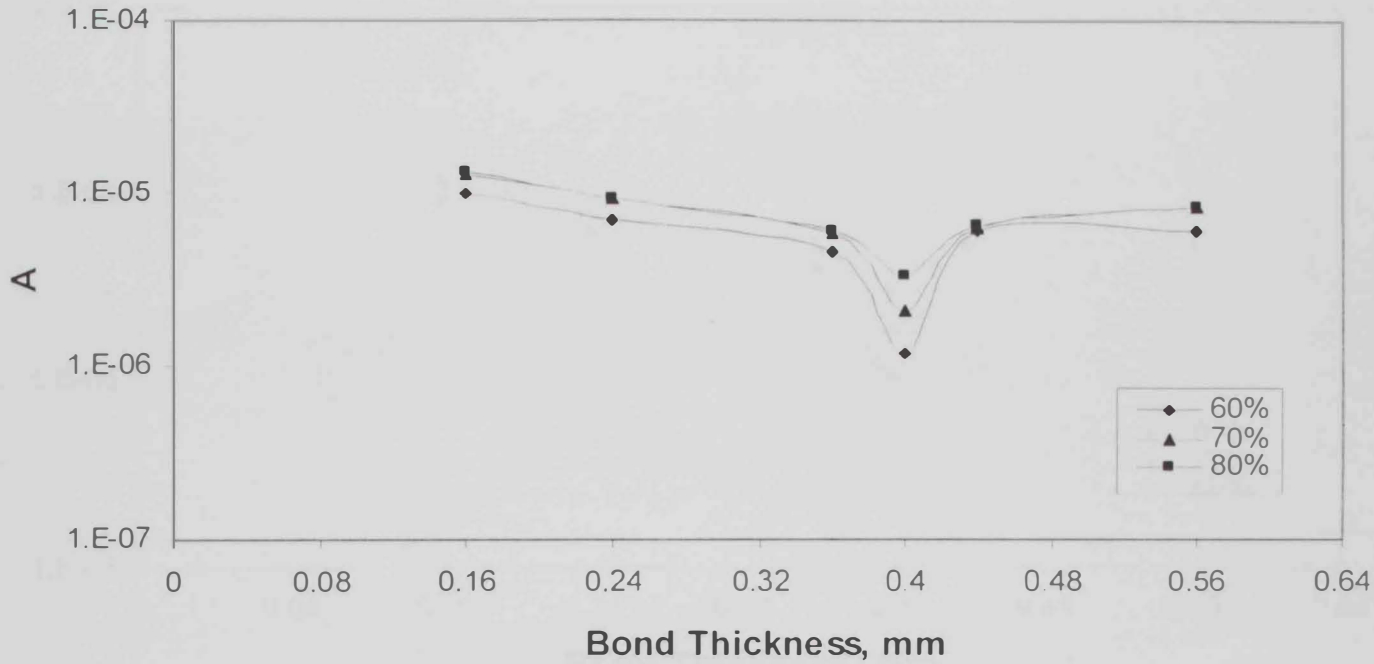

Figure 4.35: Paris kinetic parameter, A, as a function of bond thickness for simple beam analysis

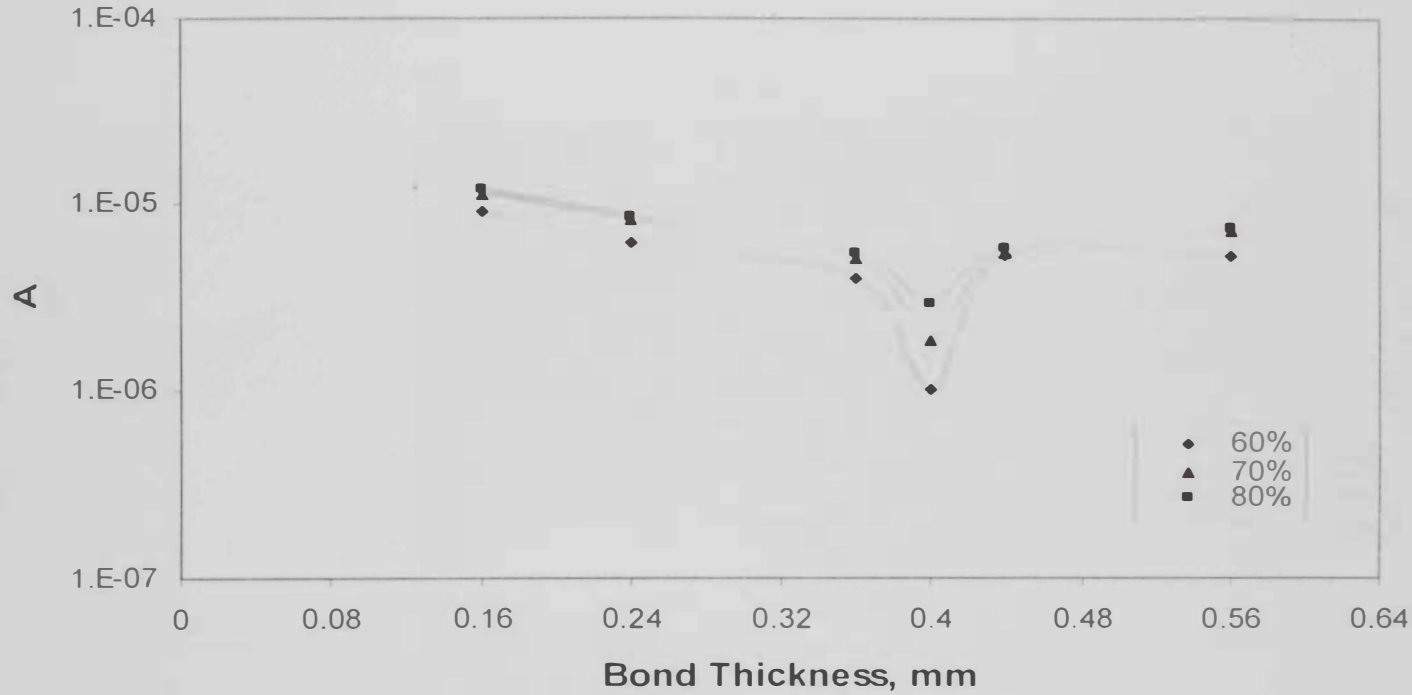

Figure 4.36: Paris kinetic parameter, A, as a function of bond thickness for beam on elastic foundation analysis

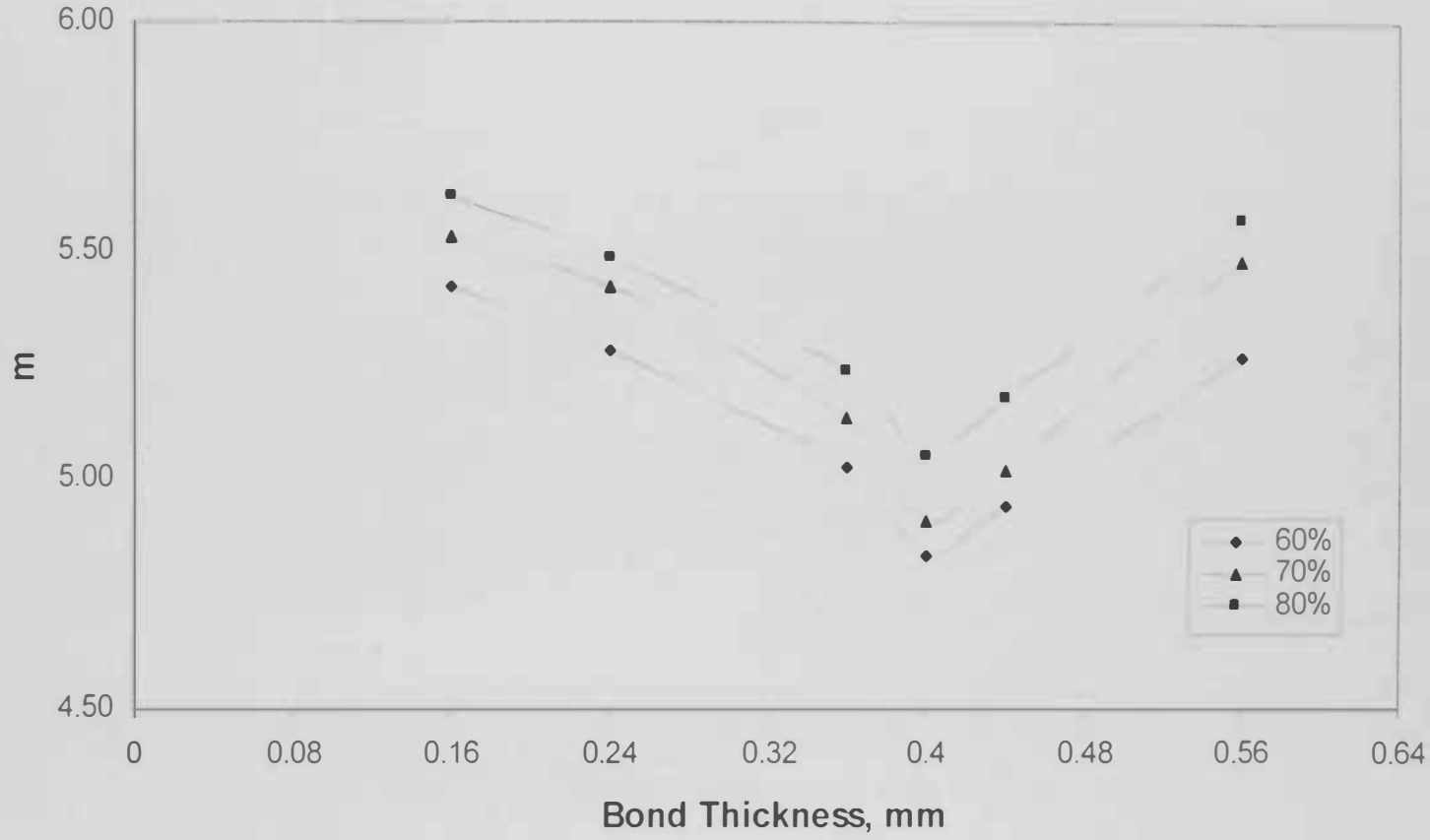

Figure 4.37: Paris kinetic parameter, m, as a function of bond thickness for simple beam analysis

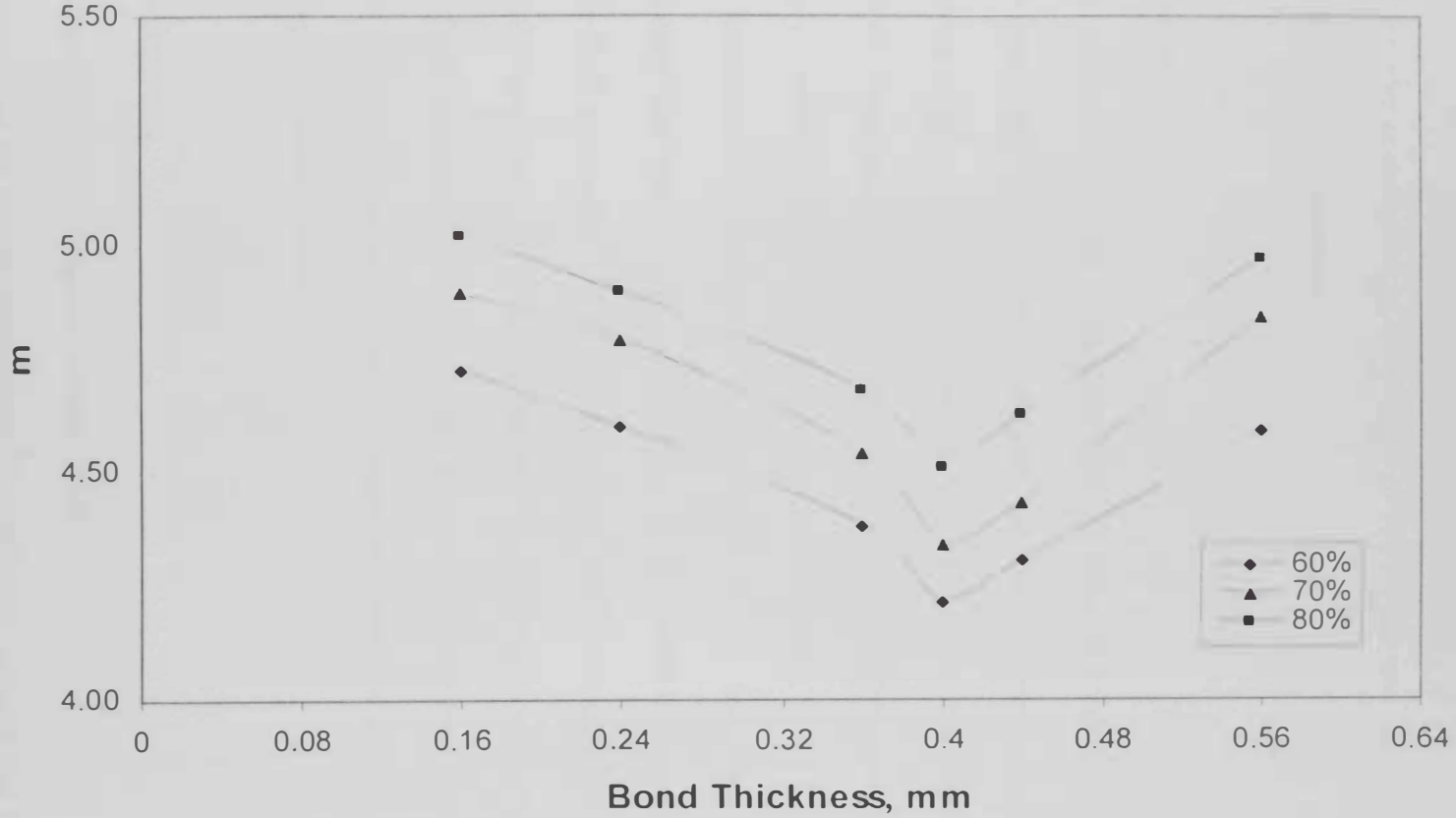

Figure 4.38: Paris kinetic parameter, m, as a function of bond thickness for beam on elastic foundation analysis

5. Summary & Conclusions

This chapter is dedicated to a summary of the results and the main conclusions and suggestions for further investigation.

5.1 Summary

This research was carried out to investigate the effect of bond thickness on the lifetime of adhesive joints under mode I and to evaluate the fracture energy of aluminum-adhesive joints using an epoxy resin as the adhesive material. Double cantilever beam (DCB) specimens were manufactured in a wide range of bond thicknesses and fracture tests were conducted under constant loads over a range of test temperatures.

The lifetime of an adhesive joint was studied using a fracture mechanics analysis. Both simple beam and beam on elastic foundation analyses were used to evaluate the fracture energy of the DCB specimens. Paris' power law was used to describe the crack propagation rate of the DCB specimens. The results obtained were described and an analytical approach was proposed for determining the rate of crack propagation, and hence predicting lifetime of the adhesive joints. It was found that the predictions were in good agreement with the corresponding experimental results.

5.2 Conclusions

In summary, the following conclusions can be drawn:

- The results of the present experimental investigation indicate that bond thickness has an effect on the fracture energy and the lifetime of the DCB specimens.

- As the bond thickness is increased, the constraint at the crack tip is reduced which increases the crack tip plastic zone size; and the fracture energy and the lifetime of the adhesive joint are significantly increased.
- There is a direct relationship between the fracture energy of adhesive joints and the deformation zone formed at the crack tip, which is controlled by the bond thickness.
- The maximum lifetime of the DCB specimens occurs at an optimum bond thickness. The optimum thickness is not a constant at different temperatures.
- The maximum adhesive fracture energy is dependent upon the temperature. As the temperature increases, the optimum bond thickness increases.
- The fracture energy and the lifetime of the DCB specimens showed an increase as the temperature decreased.
- The fracture of the DCB specimens was cohesive, implying adequate surface preparation of the adherends.
- A linear elastic fracture mechanics approach was used for studying the crack propagation behavior of adhesive joints. An analytical approach is proposed for predicting the lifetime of adhesive joints using this approach.
- There is a relation between the crack propagation rate, da/dt, and the strain energy release rate, G. The crack propagation rates could be approximated by Paris' power law as generally found in metals.
- The simple beam analysis is more conservative than the beam on elastic foundation analysis because it neglects the effect of bond thickness in the evaluation of the strain energy release rate of the DCB specimens.

- It is better to use the beam on elastic foundation analysis in calculating the strain energy release rate and predicting the lifetime of the DCB specimens.
- The present analytical approach for lifetime prediction was found to be in a good agreement with the experimental results.
- The problem of designing adhesive joints has been discussed from a fracture mechanics point of view. A procedure has been outlined to develop a design equation from the experimental results. Similar procedures can be applied to different joint configurations and adherend/adhesive material types.
- The behavior of adhesive joints presented in this study should encourage designers and engineers to carefully consider various factors in determining the intended lifetimes of bonded structures.

5.3 Future Work

Several experiments are suggested in this section for future work in the area of predicting the lifetime of adhesive joints. The basic methodology for predicting the lifetime of adhesive joints was assessed in this study but further work is needed to determine improvements to the analytical approach. These improvements can be made by studying more parameters, such as initial crack length, material properties of adhesive and substrates, and bonding geometry to gain an understanding of all the parameters that have an effect on the lifetime of the adhesive joints. Also, studying the service conditions such as temperature and applied loads together rather than individually as well as their effect on the lifetime of adhesive joints will enable the lifetime of adhesive joints to be predicted in a relatively accurate way.

References

1. J. D. Minford, Handbook of Aluminum Bonding Technology and Data. Marcel Dekker, Inc., New York, 1993.
2. R. Houwink and G. Salomon, Adhesion and Adhesives, Vol. 1: Adhesives. Elsevier Publishing Company, Amsterdam, 1965.
3. J. S. Tomblin, C. Yang, and P. Harter, Investigation of Thick Bondline Adhesive Joints, U.S. Department of Transportation Federal Aviation Administration Office of Aviation Research Washington, DC 20591, 2001.
4. B. Duncan and L. Crocker, Review of Tests for Adhesion Strength, UK, 2001.
5. J. S. Tomblin, P. Harter, W. Seneviratne, and C. Yang, Characterization of Bondline Thickness Effects in Adhesive Joints, Journal of Composites Technology and Research, Vol. 24, 2002, pp. 332- 344.
6. K. W. Allen, A review of some basics of adhesion over the past four decades. International Journal of Adhesion and Adhesives, Vol. 23, 2003, pp. 87- 93.
7. D. E. Packham, The mechanical theory of adhesion - a seventy year perspective and its current status, 1st International Congress on Adhesion Science and Technology, 1998, pp. 81-108.
8. A. Baldan, Review: Adhesively-bonded joints and repairs in metallic alloys. polymers and composite materials: Adhesives, adhesion theories and surface pretreatment, Journal of Materials Science, Vol. 39, 2004, pp. 1- 49.
9. B. V. Derjaguin, N. A. Krotova, V. V. Karssev, Y. M. Kirillova, and I. N. Aleinikova, 2nd International Congress Surface Activity, London, 1957.

10. F. M. Fowkes, Journal of Adhesion, Vol. 4, 1972.

11. S. S. Voyutskii and V. L. Vakula, Autohesion and Adhesion of High Polymers, International Science, 1963.

12. J. W. McBain and D. G. Hopkins, J. of Physics and Chemistry, Vol. 29, 1925.

13. J. D. Venables, D. K. McNamara, J. M. Chen, T. S. Sun, and R. L. Hopping, Journal of Applied Surface Science, Vol. 3, 1979.

14. D. M. Brewis, Surface Analysis and Pretreatment of Plastics and Metals, 1982.

15. S. Zhang, R. Panat, and K. J. Hsia, Influence of surface morphology on the adhesive strength of epoxy/aluminum interface, Journal of Adhesion Science and Technology, Vol. 17, 2003, pp. 1685-1711.

16. Y. L. Zhang and G. M. Spinks, Journal of Adhesion Science and Technology, Vol. 11, 1997, pp. 207-223.

17. R. P. Digby and D. E. Packham, Pretreatment of aluminum: surface chemistry and adhesive bond durability, International Journal of Adhesion and Adhesives, Vol.15, 1995, pp. 61-71.

18. G. W. Critchlow and D. M. Brewis, Review of surface pretreatments for aluminum alloys, International J. of Adhesion and Adhesives, Vol. 16, 1996, pp. 255-275.

19. A. J. Kinloch, Interfacial fractures mechanical aspects of adhesive bonded joints, Journal of Adhesion, Vol. 10, 1979, pp. 193-219.

20. O. Lunder, B. Olsen, and K. Nisancioglu, Pre-treatment of AA6060 aluminum alloy for adhesive bonding, International Journal of Adhesion and Adhesives, Vol. 22, 2002, pp. 143-150.

21. R. Houwink and G. Salomon, Adhesion and Adhesives, Vol. 2: Applications, Elsevier Publishing Company, Amsterdam, 1965.

22. A. J. Kinloch, Adhesion and Adhesives-Science and Technology, Chapman and Hall, London, 1987.

23. R. L. Patrick, Treatise on Adhesion and Adhesives, Vol. 5, Marcel Dekker, Inc., New York, 1981.

24. A. P. Parker. Mechanics of Fracture and Fatigue: An Introduction, 1981.

25. D. Broek, Elementary Engineering Fracture Mechanics, Kluwer Academic Publishers, 1982.

26. W. S. Johnson, L. M. Butkus, and R. V. Valentin, Applications of Fracture Mechanics to the Durability of Bonded Composite Joints, U.S. Department of Transportation Federal Aviation Administration Office of Aviation Research, Washington, 1998.

27. L. J. Hart-Smith, Adhesive-Bonded Single-Lap Joints, NASA Report, 1973.

28. G. Fernlund, M. Papini, D. McCammond, and J. K. Spelt, Fracture Load Predictions for Adhesive Joints, Journal of Composite Science and Technology, Vol. 51, 1994, pp. 587-600.

29. M. Papini, G. Fernlund, and J. K. Spelt, The Effect of Geometry on The Fracture of Adhesive Joints, International Journal of Adhesion and Adhesives, Vol. 14, 1994, pp. 5 -13.

30. E. J. Ripling, S. Mostovoy, and R. L. Patrick, Application of Fracture Mechanics to Adhesive Joints, Journal of Adhesion, 1963.

31. J. D. Bardis and K. T. Kedward, Effects of Surface Preparation on Long-Term Durability of Composite Adhesive Bonds, U.S. Department of Transportation Federal Aviation Administration Office of Aviation Research, Washington, 2001.

32. J. D. Bardis and K. T. Kedward, Surface Preparation Effects on Mode-I Testing of Adhesively Bonded Composite Joints, Journal of Composites Technology and Research, Vol. 24, 2002, pp. 30 - 37.

33. W. Brockmann, O. D. Hennemann, H. Kollek, and C. Matz, Adhesion in bonded aluminum joints for aircraft construction, International Journal of Adhesion and Adhesives, Vol. 6, 1986, pp. 115 -143.

34. J. R. Reeder and J. R. Crews, Mixed-Mode Bending Method for Delamination Testing, AIAA Journal, Vol. 28, 1990, pp. 1270-1276.

35. Q. D. Yang, M. D. Thouless, and S. M. Ward, Elastic-Plastic Mode II Fracture of Adhesive Joints, International Journal of Solids and Structures, Vol. 38, 2001, pp. 3251 - 3262.

36. J. R. Reeder and J. H. Crews, Non-Linear Analysis and Redesign of the Mixed-Mode Bending Delamination Test, NASA Technical Memorandum, 1991.

37. B. R. K. Blackman, A. J. Kinloch, M. Paraschi, and W. S. Teo, Measuring the mode I adhesive fracture energy, G_{IC}, of structural adhesive joints: the results of an international round-robin, International Journal of Adhesion and Adhesives, Vol. 23, 2003, pp. 293-305.

38. E. J. Ripling, S. Mostovoy, and R. L. Patrick, Measuring fracture toughness of adhesive joints, Journal of Materials Research and Standards, Vol. 4, 1964, pp. 129-134.

39. E. J. Ripling, C. Bersch, and S. Mostovoy, Environmental Stress Cracking of Epoxy Adhesives, Journal of Corrosion Fatigue, 1972, pp. 702-709.

40. C. Yan, K. Xiao, L. Ye, and Y. W. Mai, Numerical and experimental studies on the fracture behavior of rubber-toughened epoxy in bulk specimen and laminated composites, Journal of Materials Science, Vol. 37, 2002, pp. 921 – 927.

41. Pirondi and G. Nicoletto, Fatigue Crack Growth in bonded DCB specimens, Journal of Engineering Fracture Mechanics. Vol. 71, 2004, pp. 859-871.

42. Pereira and A. B. de Morais, Strength of adhesively bonded stainless steel joints, International Journal of Adhesion and Adhesives, Vol. 23, 2003, pp. 315-322.

43. S. Erpolat, I. A. Ashcroft, A. D. Crocombe, and M. A. Wahab, On the analytical determination of strain energy release rate in bonded DCB joints, Journal of Engineering Fracture Mechanics. Vol. 71, 2004, pp. 1393 -1401.

44. S. Krenk, Energy Release Rate Symmetric Adhesive Joints, Engineering Fracture Mechanics, Vol. 43, 1992, pp. 549 - 559.

45. J. Wang, P. Qiao, and J. F. Davalos, Elastic Foundation Model-Based TDCB Specimen for Mode-I Fracture of Bi-Material Bonded Interfaces, ASCE Engineering Mechanics Conference, Columbia University, New York, 2002.

46. P. Qiao, J. Wang and J. F. Davalos, Tapered beam on elastic foundation model for compliance rate change of TDCB specimen, Journal of Engineering Fracture Mechanics, Vol. 70. 2003, pp. 339 - 353.

47. D. M. Gleich, M. J. L. Van Tooren, and A. Beukers, Analysis and evaluation of bondline thickness effects on failure load in adhesively bonded structures, Journal of Adhesion Science Technology. Vol. 15, 2001, pp. 1091-1101.

48. A. J. Kinloch and S. J. Shaw. The Fracture Resistance of a Toughened Epoxy Adhesive, Journal of Adhesion. Vol. 12, 1981, pp. 59-77.

49. A. J. Kinloch, S. J. Shaw, and D. L. Hunston, Deformation and fracture behavior of a rubber-toughened epoxy: 2. Failure criteria, Journal of Polymer, Vol. 24. 1983. pp. 1355-1363.

50. M. Ben Ouezdou and A. Chudnovsky, Stress and Energy Analysis of Toughness Measurement for Adhesive Bonds. Journal of Engineering Fracture Mechanics. Vol. 29. 1988. pp. 253 - 261.

51. M. Ben Ouezdou, A. Chudnovsky, and A. Moet, Re-evaluation of Adhesive Fracture Energy, Journal of Adhesion, Vol. 25, 1988, pp.169 - 183.

52. W. D. Bascom, R. L. Cottington, R. L. Jones, and P. Peyser, The Fracture of Epoxy and Elastomer-Modified Epoxy Polymers in Bulk and as Adhesives, Journal of Applied Polymer Science, Vol. 19. 1975, pp. 2545-2562.

53. D. L. Hunston, J. L. Bitner, J. L. Rushford, J. Oroshnik, and W. S. Rose, Fracture of Rubber-Toughened Adhesives, J. of Elastomers and Plastics, Vol. 12, 1980.

54. M. M. Abou-Hamda, M. M. Megahed, and M. M. Hammouda, Fatigue Crack Growth in Double Cantilever Beam Specimen with an Adhesive Layer, Journal of Engineering Fracture Mechanics, Vol. 60, 1998, pp. 605 – 614.

55. H. R. Daghyani, L. Ye, and Y. W. Mai, Fracture of Adhesive Joints with Different Bond Thickness, Australian Fracture Group Symposium, Australia, 1994.

56. H. R. Daghyani, L. Ye, and Y. W. Mai, Effect of Bond Thickness on Mode I, Mode II and Mixed Mode Fracture of Adhesive Joints, International Conference on Advanced Materials, Beijing, China. 1996, pp. 651-659.

57. Yan, Y. W. Mai, and L. Ye, Effect of Bond Thickness on Fracture Behavior in Adhesive Joints, Journal of Adhesion, Vol. 75, 2001, pp. 27- 44.

58. Yan, Y. W. Mai, Q. Yuan, L. Ye, and J. Sun, Effect of Substrate Materials on Fracture Toughness Measurement in Adhesive Joints, International Journal of Mechanical Sciences, Vol. 43, 2001, pp. 2091- 2102.

59. S. Krenk, J. Jonsson, and L. P. Hansen, Fatigue analysis and testing of adhesive joints, Journal of Engineering Fracture Mechanics, Vol. 53, 1996, pp. 859 - 872.

60. S. Mall and G. Ramamurthy, Effect of bond thickness on fracture and fatigue strength of adhesively bonded composite joints, International Journal of Adhesion and Adhesives, Vol. 9, 1989, pp. 33 -37.

61. Fatemi and L. Yang, Cumulative fatigue damage and life prediction theories: a survey of the state of the art for homogeneous materials, International Journal of Fatigue, Vol. 20, 1998, pp. 9-34.

62. R. W. Hertzberg, Deformation and Fracture Mechanics of Engineering Materials, John Wiley and Sons Ltd, 1989.

63. H. Ewalds and R. Wanhil, Fracture Mechanics, Edward Arnold, London, 1984.

64. J. A. Harris and P. A. Fay, Fatigue life evaluation of structural adhesives for automotive applications, International Journal of Adhesion and Adhesives, Vol. 12, 1992, pp. 9-18.

65. J. Curley, J. K. Jewtha, A. J. Kinloch, and A. C. Taylor, The fatigue and durability behavior of automotive adhesives. Part III: Predicting the service life, Journal of Adhesion, Vol. 66, 1998, pp. 39-59.

66. J. Curley, H. Hadavinia, A. J. Kinloch, and A. C. Taylor, Predicting the service-life of adhesively-bonded joints, International J. of Fracture, Vol. 103, 2000, pp. 41-69.

67. M. M. Abdel Wahab, I. A. Ashcroft, A. D. Crocombe, and P. A. Smith. Numerical prediction of fatigue crack propagation lifetime in adhesively bonded structures. International Journal of Fatigue, Vol. 24, 2002, pp. 705-709.

68. Lin and K. M. Liechti, Similarity concepts in the fatigue fracture of adhesively bonded joints, Journal of Adhesion, Vol. 21, 1987, pp. 1-24.

69. K. M. Liechti, G. A. Arzoumanidis, and S. J. Park, Fatigue fracture of fully saturated bonded joints, Journal of Adhesion, Vol. 78, 2002, pp. 383-411.

70. X. X. Xu, A. D. Crocombe, and P. A. Smith, Creep crack growth in a filled and toughened adhesive, The 4th European Conference and advanced materials and processes, The Federation of European Materials Societies, Venice, 1995.

71. D. Broek, The Practical Use of Fracture Mechanics, 1998.

72. A. Agrawal and P. Y. Ben Jar, Analysis of specimen thickness effect on interlaminar fracture toughness of fiber composites using finite element models, Journal of Composites Science and Technology, Vol. 63, 2003, pp. 1393-1402.

تأثير سمك اللاصق على عمر الوصلات الملصقة

الملخص

إن الهدف من هذا البحث هو دراسة تأثير سمك اللاصق على طاقة الكسر للوصلات الملصقة وكذلك على عمر هذه الوصلات كما يقدم هذا البحث نموذجا مطورا لتوقع عمر هذه الوصلات وذلك بطريقة تجريبية. وقد استند هذا البحث على علم ميكانيكا الكسر لتقييم عمر وصلة من الالومنيوم / الايبوكسى. وقد أجريت اختبارات هذا البحث باستخدام عينات من كمرة كابولية مزدوجة بأسماك لاصقة مختلفة تحت تأثير أحمال عمودية على الوصلة الملصقة.

تصف هذه الدراسة نظرة للتنبؤ بمعدل نمو الشرخ باستخدام قانون'Paris كما استخدمت هذه الدراسة درجات الحرارة المرتفعة وذلك لتسريع نمو الشرخ تحت تأثير الأحمال الثابتة. وقد اختيرت درجات الحرارة المرتفعة بحيث تقل عن درجة الانتقال الزجاجي للاصق. تهدف الفكرة العامة لهذا البحث إلى التأثير بحمل ثابت على العينات الملصقة وذلك بقيمة أقل من القيمة الحرجة للحمل التي تؤدى إلى الكسر وذلك للسماح لنمو الشرخ نموا بطيئا قابل للقياس. وقد تم تقييم طاقة الكسر للعينات الملصقة باستخدام كلا من تحليل الكمرة البسيط وتحليل الكمرة على أساس مرن. وقد تم اقتراح نموذج مبسط للتنبؤ بمدى اختلاف قيم معاملي قانون'Paris وذلك باختلاف قيم سمك اللاصق. وقد تم تطوير نموذج بحيث يمكن أن تتم محاكاة نمو الشرخ ومن ثم التنبؤ بعمر الوصلات الملصقة.

تأثير سمك اللاصق على عمر الوصلات الملصقة

رسالة مقدمة إلى عمادة الدراسات العليا

بجامعة الإمارات العربية المتحدة

استكمالا لمتطلبات الحصول على درجة

ماجستير العلوم

في

علوم و هندسة المواد

إيهاب محمد السعيد الرفاعى شهاب

2005